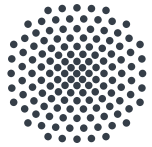

University of Stuttgart
Germany

Quantum Light Interaction with Superatoms

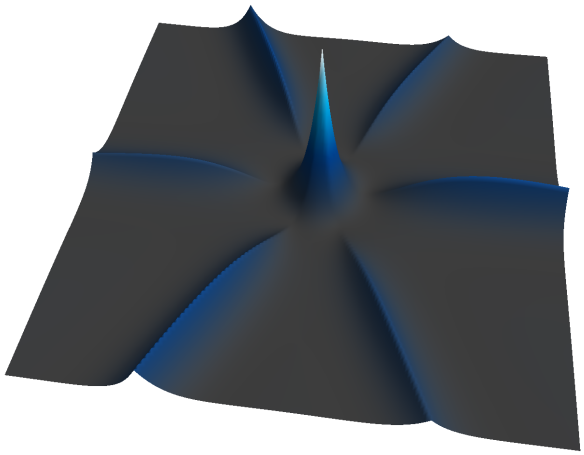

Candidate	Kevin Kleinbeck
Supervisor	Prof. Dr. Hans Peter Büchler
Secondary Corrector	Apl.-Prof. Dr. Jörg Main

III. Institute for Theoretical Physics

14. November 2017

Abstract

Photons inherently interact weakly with other photons and their environment [1]. This fact makes photons excellent qubit candidates, since the weak coupling implies longevity and protection against decoherence [2]. However, the practically missing interaction between the photons themselves tempers our possibilities to control them like any other state of matter. This thesis aims to study mechanisms enabling effective photon-photon interactions and thus providing methods to directly control single photons.

More precisely, we study one-dimensional waveguide systems with broken chirality, i.e., the direction of the traversing photon influences their interaction with the environment. We will show that placing atoms sufficiently close together breaks chirality naturally. In this so-called ***superradiant*** phase, all atoms in the ensemble act as one; they are collectively excited and emit any absorbed photon only in its original direction.

Building upon this, we study the scattering processes at such ***superatoms***. We first discuss some already solved integrable quantum models and provide some necessary simplifications to make following calculations possible. One such model is the Dicke model, consisting of one bosonic mode resembling the waveguide photons, and one single superatom. We will give a derivation of the N-particle Green's function by Yudson [3]. Yet, in this original representation, the Green's function contains so many terms that it is not suitable for further use. We give a transformation to a more applicable form and use it to derive a generating functional for outgoing states.

Having said that, not all chiral waveguide systems are integrable and, for many of them, approximations have to be applied. We primarily focus here on a Markovian method, which neglects retardation effects in the time evolution. While this approximation itself seems to be quite justified at the beginning, we will show that these retardation effects are the primary source of entanglement between the photons and the atoms, and dropping them turns out to be a too harsh assumption for most of the cases.

Lastly, for integrable models, we will study multi-photon effects, such as the creation of spatial correlations between the photons. We will see that even the simplest model is able to correlate incoming photons, at least for suitably chosen initial photonic wave packets. We will find that to make these correlations strong, the initial wave packet must be so wide it cannot traverse the atoms faster than the reciprocal effective decay rate of the superatoms.

Zusammenfassung

Photonen wechselwirken mit der sie umgebenden Materie, aber vor allem auch mit anderen Photonen, nur extrem schwach [1]. Daher wären Photonen perfekte Kandidaten um Qubits zu realisieren [2], denn die Abwesenheit von Wechselwirkungen geht Hand in Hand mit langlebigen, kohärenten Zuständen. Allerdings bedeutet das ebenso, dass wir Photonen und ihre gegenseitige Wechselwirkung kaum kontrollieren können, anders als bei vielen anderen Formen von Materie. Diese Arbeit untersucht Systeme in denen die Photonen eine effektive Wechselwirkung erfahren und somit Zugang zu neuartigen Zuständen gewähren.

Wir betrachten eindimensionale Wellenleitersysteme mit gebrochener Chiralität. Dies bedeutet, dass die Bewegungsrichtung der Photonen innerhalb des Wellenleiters Einfluss auf ihre Wechselwirkung mit dem Wellenleiter selbst hat. Zuerst werden wir zeigen, dass Chiralität für Systeme aus Atomen in hinreichend geringem Abstand zueinander automatisch gebrochen ist. Diese Atome befinden sich dann in einer ***superradianten*** Phase, in welcher sie sich zusammen wie ein einzelnes ***Superatom*** verhalten, dass heißt, Photonen werden kollektiv von allen Atomen absorbiert und können dann nur in die selbe Richtung emittiert werden, aus der sie auch gekommen sind.

Darauf aufbauend untersuchen wir Streuprozesse an solchen Superatomen. Dafür werden wir zuerst einige bereits gelöste, integrable Quantensysteme besprechen. Eines dieser Modelle ist das Dicke-Modell, in dem eine bosonische Mode, welche die Wellenleiterphotonen darstellt, an ein Superatom gekoppelt ist. Für dieses Modell verwenden wir die N-Teilchen Green'sche Funktion von Yudson [3] und werden diese in eine praktischere Form umschreiben, die es uns ermöglicht einige Streuprozesse vollkommen analytisch zu beschreiben.

Jedoch weist nicht jedes chirale Wellenleitersystem analytische Eigenzustände auf, weshalb wir auch die entsprechende Green'sche Funktion nicht exakt bestimmen können. Deshalb müssen Approximationen verwendet werden, um zu einer vereinfachten Beschreibung zu gelangen. Wir konzentrieren uns hier auf Methoden, die auf der Markov-Näherung aufbauen. Dies ist eine Näherung, die Retardierungseffekte in der Zeitentwicklung vernachlässigt. Auf dem ersten Blick scheint dies gerechtfertigt, allerdings wird sich herausstellen, dass sich Ergebnisse, die mit Hilfe der Markov-Näherung hergeleitet wurden, von den exakten Ergebnissen qualitativ unterscheiden. Ursache hierfür ist, dass die Retardierungseffekte die primäre Quelle der Verschränkung zwischen den Wellenleiterphotonen und den Atomen sind. Entsprechend wichtig sind diese Effekte bei Prozessen, die auf solch einer Verschränkung aufbauen.

Zuletzt werden wir die Streuung mehrerer Photonen untersuchen. Insbesondere untersuchen wir hierbei die Entstehung räumlicher Korrelationen zwischen Photonen durch die Wechselwirkung mit Superatomen im Wellenleiter. Wir werden sehen, dass, zumindest für entsprechend ausgewählte Wellenpakete, selbst das einfachste Modell ausreicht,

um einfallende Photonen zu korrelieren. Wir zeigen, dass die Korrelationen zwischen den einzelnen einfallenden Photonen besonders dann groß sind, wenn das einfallende Wellenpaket so breit ist, dass es das System, auf Zeitskalen proportional zur inversen Zerfallsrate, nicht verlassen kann.

Contents

1 Waveguide Quantum Electrodynamics

From all of the four fundamental forces, we possess the most control over electrodynamics. The ability to control the interaction of photons with atoms enabled us to develop unprecedented technologies. We employ strong fields to capture ions in our most precise clocks [4, 5], use cavity modes to build qubits [6] and send out single pairs of entangled photons to measure violations of Bell's inequality [7–9]. However, in all of these examples, the primary interest lies in the interaction of the photons with their surrounding matter. Even in the latter example, where the photons themselves are of interest, they are created in an entangled state and then never feel each other again. The "magic" behind the infamous result lies within the measurement procedure and not within special manipulations of the photon states [10].

It is quite paradoxical that, even though photons are so elementary for many of our experiments, we are barely able to manipulate them in the same way as we can shift around electrons, for example. The reason for this seems obvious. While electrons and protons strongly interact with each other, therefore making it easy to create correlated systems, photons are effectively blind towards other photons. From quantum electrodynamics, we know that there exists a natural appearing photon-photon interaction, which, however, is in lowest order a forth order process $\mathcal{O}(\alpha^4)$ in the fine structure constant α. Consequently, only recently has it been possible to find evidence for the scattering of one photon from another [1].

The lack of control turns out to be a huge problem for modern applications. For instance, universal quantum computation heavily relies upon the perfect control of "flying qubits" and the ability to convert photons into condensed matter excitations and vice versa [11]. Furthermore, due to the weak interaction with their environment, photons themselves are perfect candidates for qubits [2]; coherence times of a couple of seconds are readily achievable [12]. Additionally, by the inability to make photons

interact we are missing out on new physics and novel states of matter, such as photon crystallisation [13] or bound states [14].

Hence, this work aims to deepen our understanding of one way to make photons more controllable: since photons by themselves barely interact, we need to convert them into new, interacting particles and keep them together long enough [2, 13, 15, 16]. After they are converted back to regular photons, the outgoing photons hopefully exist in some non-trivial correlated state [17–19]. For this purpose we will investigate slow-light polaritons; excitations of atomic dipole systems. To be more precisely, in this thesis we consider chiral waveguide dynamics; systems which restrict the photons to one dimension and scattering events are biased towards one direction [3, 20–22].

1.1 Chiral Waveguide Systems

For a didactical approach to this thesis, we start by explaining what we mean when we say that we consider "chiral waveguide systems". Firstly, let us agree upon the convention that we call every setup, in which the dynamics are effectively one-dimensional, a waveguide. This means a photon source, sending off photons into free space with a well-defined wave vector, is as much a waveguide as an optical fibre. Dropping the distinction between these two inherently different systems will be useful for us, since the same set of equations governs their effective dynamics in a specific frequency range.

Now we need something more than just photons, as the absence of direct photon-photon interactions renders their dynamics dull. Hence, we introduce ***emitters***, subsystems which can absorb and re-emit photons from and into the waveguide. For example, a large ensemble of N atoms will show an effect called superradiance [3, 23]; the ensemble will collectively absorb and re-emit photons with an N^2 fold increased rate compared to the single atoms. Furthermore, in this process scattering into any other direction than the incident one is exponentially suppressed.

This brings us to the second concept: ***chirality***. For a one dimensional system, we should consider both forward and backward scattering, or in other words, reflexion and transmission of the photons at the emitters. Even so, it turns out that in some systems, like the superradiant cloud, backward scattering is actively suppressed and can be neglected. There are other ways to achieve chirality, like coating an optical fibre with gold nanoparticles, which breaks the mirror symmetry of the photons by spin-orbit interaction [22]. In order to create a non-linear medium for the photons in the photonic fibre approaches, one either uses a hollow-core fibre and places the emitters inside the fibre [24]. Alternatively, emitters close to the waveguide's surface couple to the photon modes as well [25]. Yet another way to build these chiral waveguides is to use superconducting transmission lines [26, 27].

All of these discussed systems are inherently different, and so are the realisations of the emitters in them. We already discussed that we could employ simple atomic clouds [24], while other implementations rely on driven Rydberg atoms [28]. However, we are not limited to just cold atomic clouds. For the transmission line waveguides, one usually utilises superconducting qubits as artificial atoms [26, 27]. Thus, we want to generalise our definition of emitters, which, from now on, are any subsystems, that effectively interact with the waveguide photons as if they were a single particle. Therefore, we will also use the term "atoms" or, in the two-level case, "spins" for the emitters. For further examples and references of possible implementations see the review of Roy et al. [16], which gives an exhaustive list of examples and explains their corresponding Hamiltonians.

After all of these preliminaries, we now have every definition we need to start building up a generic chiral waveguide Hamiltonian. Apparently, this Hamiltonian consists of three parts

$$H = H_{\mathrm{ph}} + H_{\mathrm{at}} + H_{\mathrm{int}}. \tag{1.1}$$

Here, H_{ph} denotes the photonic part and covers the dispersion of the photons inside the waveguide. Next, the atomic Hamiltonian H_{at} covers the level structure of the emitter and accounts for additional external driving. Lastly, H_{int} describes the interaction between photons and atoms inside the waveguide.

Now, let us start by discussing the photonic Hamiltonian. For free photons inside a one dimension waveguide it reads

$$H_{\mathrm{ph}} = \int \mathrm{d}k\, \hbar\omega(k) b^\dagger(k) b(k), \tag{1.2}$$

where k labels the photons wave vector and $\omega(k)$ is the dispersion relation inside the waveguide. The photonic creation and annihilation operators $b^\dagger$ and b obey the usual commutation relations for bosonic fields. The most intriguing fact about the photonic Hamiltonian is the dispersion relation. While for free photons we have $\omega(k) = c|k|$, it can take multiple forms in different waveguides. Iakoupov [15] computed many of these relations for different realisations. In conclusion, photons can have something resembling the usual linear dispersion or even a quadratic, like free and massive particles.

The dependence of the dispersion relation onto the concrete system presents a hurdle for us, since we are interested in a generic framework which applies to a multitude of systems, without the need of regarding many different dispersion relations. One way to avoid this problem, is to introduce new bosonic field operators as

$$\tilde{b}(\omega) \equiv \frac{b(k^{-1}(\omega))}{\sqrt{\partial\omega/\partial k}},$$

where $k^{-1}(\omega)$ denotes the inverse dispersion relation. Consequently, the new photonic

Hamiltonian becomes

$$\tilde{H}_{\mathrm{ph}} = \int \mathrm{d}\omega\ \hbar\omega \tilde{b}^\dagger(\omega)\tilde{b}(\omega). \tag{1.3}$$

This Hamiltonian equals the one from Equation (1.2) if $\omega(k)$ is invertible.

Going this way is practically as long as we are not interested in interactions between the photons and the emitters. However, the description of the interaction Hamiltonian by the wave vector k is more accessible than by the associated frequencies $\omega(k)$. We will later see, for an fully chiral setup, that we can pull this k dependence into atomic operators, for which we can still use the approach discussed here. But, photon-emitter interactions are central to this work and we will also discuss non-chiral systems. Therefore, we now present an approximative, yet generic way to simplify the dynamics.

Luckily, the waveguide dynamics are usually centred around a central frequency $\omega_0 = \omega(k_0)$. More precisely, we assume the emitters interact only with photons within the range $k_0 + [-\Delta k/2, \Delta k/2] \equiv k_0 + \mathcal{B}$. We call $\mathcal{B}$ the bandwidth of the system. Since photons outside of this range traverse the waveguide without interaction, their dynamics is trivial and we want to restrict our discussion to photons within the non-trivial region. Finally, we assume the dispersion relation to be symmetrical under $k \mapsto -k$, such that there are two interacting wave vector regions. Consequently, we may write for the photonic Hamiltonian, under this restriction,

$$H_{\mathrm{ph}} = \int_{k_0+\mathcal{B}} \mathrm{d}k\ \hbar\omega(k) b^\dagger(k) b(k) + \int_{-k_0+\mathcal{B}} \mathrm{d}k\ \hbar\omega(k) b^\dagger(k) b(k). \tag{1.4}$$

Next, we assume a sufficiently narrow bandwidth, i.e., $\Delta k \ll k_0$ and $\omega(k) \approx \omega_0 \pm v_G(k \mp k_0)$ approximates $\omega(k)$ well within $\pm k_0 + \mathcal{B}$. Here, $v_G = \partial\omega/\partial k|_{k_0}$ denotes the group velocity inside the waveguide at k_0. Now, we replace the dispersion relation in Equation (1.4) by this approximation. While this approximation is only valid for photons within the range $\pm k_0 + \mathcal{B}$, performing the integration over all wave vectors turns out to be convenient for further computations. Increasing the integration domain, however, would break the distinction between photons with positive and negative wave vectors. To remedy this, we introduce the two bosonic fields $b_\pm(k) = b(k \pm k_0)$, representing right and left moving photons respectively. We replace the old bosonic operators in Equation (1.4) with these operators and then lift their definition upon all real values of k, bringing us to

$$H_{\mathrm{ph}} = \int \mathrm{d}k \Big\{ \hbar\big[\omega_0 + v_G k\big] b_+^\dagger(k) b_+(k) + \hbar\big[\omega_0 - v_G k\big] b_-^\dagger(k) b_-(k) \Big\}. \tag{1.5}$$

For now, this is everything we need to know about the photonic Hamiltonian, and we focus our attention to the atomic part. For simplicity, we will work with a single type of emitters at a time, i.e., every atom in our system is described by the same basis states $\{\,|n\rangle\,\}$. Additionally, we label the atomic ground state $|0\rangle$ and associate the energy

$E_0 = 0$. Every other state $|n\rangle$ is an excitation with the energy E_n. To further abbreviate notation, we introduce the "creation" operator $a_n^\dagger = |n\rangle\langle 0|$, which lifts the atom from the ground state to the n-th excited state.

We now have enough to build the atomic Hamiltonian for many systems. However, there are some physical phenomena we are not able to capture yet. For example, imagine a system where Rydberg atoms build our emitters. These have at least a 3-level structure and need external driving between two of these levels. So, to describe driving of the atoms by an external, classical light source, we introduce the Rabi frequencies Ω_{nm}. Altogether, this creates the atomic Hamiltonian

$$H_{\text{at}} = \sum_{\text{i}=1}^{N} \left\{ \sum_n E_n a_{\text{i},n}^\dagger a_{\text{i},n} + \sum_{n<m} \Omega_{nm} a_{\text{i},n}^\dagger a_{\text{i},m} + \Omega_{mn} a_{\text{i},m}^\dagger a_{\text{i},n} \right\}. \tag{1.6}$$

Here, the index i runs over all the N emitters inside the waveguide and $a_{\text{i},n}^\dagger a_{\text{i},m}$ is shorthand notation for

$$a_{\text{i},n}^\dagger a_{\text{i},m} \equiv \left(\bigotimes_{\text{j}=1}^{\text{i}-1} \mathbb{1} \right) \otimes a_n^\dagger a_m \otimes \left(\bigotimes_{\text{j}=\text{i}+1}^{N} \mathbb{1} \right).$$

Lastly, we still need to describe the interaction Hamiltonian. Due to the lack of precise microscopical insight, we will just assume that every emitter has a dipole-like interaction with the photons. Most textbooks on Quantum Mechanics give a derivation for the interaction of the light field with an atom in the dipole approximation, together with the Rotating frame approximation (e.g. [29]). For this reason, we do not want to repeat it here, but directly give the interaction Hamiltonian, which reads

$$H_{\text{int}} = \sum_{\text{i}=1}^{N} \int \mathrm{d}k \sum_{n<m} \left[\sqrt{g_{n,m}(k)} a_{\text{i},n}^\dagger a_{\text{i},m} b^\dagger(k) e^{-ikx_\text{i}} + \sqrt{g_{m,n}(k)} a_{\text{i},m}^\dagger a_{\text{i},n} b(k) e^{ikx_\text{i}} \right], \tag{1.7}$$

where x_i is the position of the i-th atom and $g_{n,m}(k)$ is the coupling strength between the light mode with wave vector k and the atomic transition $n \to m$. Notice, that we assumed that this coupling strength is the same for every emitter and thus it does not depend on the index i.

We now need to recast Equation (1.7) into a more usable form. Firstly, let us again restrict the k integration to $\pm k_0 + \mathcal{B}$. Next, we assume that $g_{n,m}(k)$ is constant over this range of integration. Now we introduce the bosonic fields $b_\pm(k)$ and then expand the integration region back to all k. At last, we demand that the photons can introduce only transitions from the ground state $|0\rangle$ to one excited state $|1\rangle$, and that the coupling for the absorption and emission event is symmetrical, i.e., $g_{0,1}(\pm k_0) = g_{1,0}(\pm k_0) \equiv g_\pm$. Thus, after all of these steps, we arrive at the interaction Hamiltonian

$$H_{\text{int}} = \sum_{\nu=\pm} \sum_{\text{i}=1}^{N} \int \mathrm{d}k \, \sqrt{g_\nu} \left[a_\text{i} b_\nu^\dagger(k) e^{-i(k+\nu k_0)x_\text{i}} + a_\text{i}^\dagger b_\nu e^{i(k+\nu k_0)x_\text{i}} \right]. \tag{1.8}$$

Since, by definition, the transitions happen only between the levels $|0\rangle$ and $|1\rangle$, we dropped the corresponding index in the atomic operators.

Now we need to investigate the Hamiltonian (1.1) in total, as the sum of its three parts. The first fact we notice is that the operator

$$\mathcal{N} = \int \mathrm{d}k \left[b_+^\dagger(k) b_+(k) + b_-^\dagger(k) b_-(k) \right] + \sum_{\mathrm{i}=1}^{N} \sum_n a_{\mathrm{i},n}^\dagger a_{\mathrm{i},n} \tag{1.9}$$

is a symmetry of the Hamiltonian. Clearly, it is "counting" the number of excitations in the system and, consequently, the Hamiltonian dynamics cannot change the number of the excitations in the system. If we restrict our discussion to one of these particle number subsectors, we can simplify the Hamiltonian even further. Notice that H and $H - \kappa\mathcal{N}$ ($\kappa \in \mathbb{R}$) have the same dynamics ***within*** one of these subsectors. Let us choose $\kappa = \hbar\omega_0$. By doing this, the central frequency drops out of the photonic Hamiltonian, and the k_0 term will make it possible for us to switch to real space coordinates. This shift changes the energy term in the atomic Hamiltonian and it becomes $\sum_n (E_n - \hbar\omega_0) a_n^\dagger a_n$, advising us to define the detuning $\delta_n \equiv E_n - \hbar\omega_0$.

Furthermore, we want to study problems in real space. In order to do so, we use the Fourier transformed operators

$$b_\nu(x) = \int \frac{\mathrm{d}k}{\sqrt{2\pi}} b_\nu(k) e^{ikx}.$$

Combining this definition with the discussion from the previous paragraph, we can write the total Hamiltonian as

$$\begin{aligned} H = & \sum_{\nu=\pm} \int \mathrm{d}x b_\nu^\dagger(x)(-i\nu v_G \hbar\partial_x) b_\nu(x) \\ & + \sum_{\mathrm{i}=1}^{N} \left(\sum_n \delta_n a_{\mathrm{i},n}^\dagger a_{\mathrm{i},n} + \sum_{n<m} \Omega_{nm} a_{\mathrm{i},n}^\dagger a_{\mathrm{i},m} + \Omega_{mn} a_{\mathrm{i},m}^\dagger a_{\mathrm{i},n} \right) \\ & + \sum_{\mathrm{i}=1}^{N} \sum_{\nu=\pm} \sqrt{2\pi g_\nu} \left[a_{\mathrm{i}}^\dagger b_\nu(x_{\mathrm{i}}) e^{i\nu k_0 x_{\mathrm{i}}} + a_{\mathrm{i}} b_\nu^\dagger(x_{\mathrm{i}}) e^{-i\nu k_0 x_{\mathrm{i}}} \right]. \end{aligned} \tag{1.10}$$

In the next section, we want to give some concrete examples of physical systems, obeying (1.10). However, before before doing so, we want to discuss the available degrees of freedom. First, let $H \mapsto v_G \hbar H$. This transformation changes the dimension of the Hamiltonian to 1/[Length]. Now, keep in mind that we will later tackle the problem of time-evolving a given initial state. Under the aforementioned transformation, the time evolution operator reads

$$U(t) = e^{-iv_G H t}.$$

We rescale $v_G t \mapsto t$, making the time t a variable of dimension [Length].

If we read the previous procedure as a redefinition of the units of time and mass, then we are free to pick a new length scale as well. Apparently, absorbing k_0 into the definition of x achieves precisely this. However, we will primarily work with chiral systems, for which we can absorb the central frequency k_0 in unobservable quantities anyway. Thus, using it to redefine the length will just jeopardise our attempt to simplify the Hamiltonian. From (1.10) we immediately see that $g/\hbar^2 v_G^2$ has dimension $1/[\text{Length}]$. Since we will always consider cases in which we have photons in the $+$ mode, it is convenient to choose units, in which g_+ is no longer free. Thus, we rescale the bosonic fields $b_\nu(x) \mapsto \sqrt{2\pi g_+} b_\nu(x)$ and use a change of variables $x \mapsto x/2\pi g_+$, $k_0 \mapsto 2\pi g_+ k_0$. To quickly summarise the steps in the last two paragraphs the "physicist's way": From here on we set $\hbar = v_G = 2\pi g_+ = 1$.

After this rescaling, the Hamiltonian in rescaled quantities reads

$$\begin{aligned} H = &\sum_{\nu=\pm} \int \mathrm{d}x b_\nu^\dagger(x)(-i\nu\partial_x) b_\nu(x) \\ &+ \sum_{\mathrm{i}=1}^{N} \left(\sum_n \delta_n a_{\mathrm{i},n}^\dagger a_{\mathrm{i},n} + \sum_{n<m} \Omega_{nm} a_{\mathrm{i},n}^\dagger a_{\mathrm{i},m} + \Omega_{mn} a_{\mathrm{i},m}^\dagger a_{\mathrm{i},n} \right) \\ &+ \sum_{\mathrm{i}=1}^{N} \sum_{\nu=\pm} c_\nu \left[a_{\mathrm{i}}^\dagger b_\nu(x_{\mathrm{i}}) e^{i\nu k_0 x_{\mathrm{i}}} + a_{\mathrm{i}} b_\nu^\dagger(x_{\mathrm{i}}) e^{-i\nu k_0 x_{\mathrm{i}}} \right]. \end{aligned} \tag{1.11}$$

Here we have additionally absorbed every constant factor into the definition of δ_n and Ω_{nm}. The new quantity $c_\nu \equiv (g_\nu/g_+)^{1/2}$ accounts for the chirality of the system. While $c_+ = 1$ by definition c_- is a positive real number and $c_- = 0$ indicates a fully chiral system (no left moving photons), whereas we have $c_- = 1$ for non-chiral systems.

Examples 1.2

1.2.1 Resonant two-level Atoms

Firstly, we imagine the setup where the emitters are two level atoms, which we will call spins. This is the case for superconducting qubit emitters in transmission line systems [26, 27], for example. Also, these systems model the interaction of light with usual atoms under confinement, as due to an optical fibre [24]. For this system, we explicitly consider resonant photons, i.e., $\delta = 0$. Furthermore, we will neglect external

driving setting $\Omega_{01} = \Omega_{10} = 0$. Therefore, the Hamiltonian

$$H = \sum_{\nu=\pm} \int \mathrm{d}x\, b_\nu^\dagger(x)(-i\nu\partial_x)b_\nu(x) + \sum_{\mathrm{i}=1}^{N} \sum_{\nu=\pm} c_\nu \left[a_\mathrm{i}^\dagger b_\nu(x_\mathrm{i}) e^{i\nu k_0 x_\mathrm{i}} + a_\mathrm{i} b_\nu^\dagger(x_\mathrm{i}) e^{-ik_0 x_\mathrm{i}} \right] \tag{1.12}$$

describes the system at hand.

In particular, this thesis focuses on waveguides described by Equation (1.12). In Chapter 3 we will discuss the eigenmodes of this Hamiltonian's various forms and show examples for which we can treat scattering processes analytically. An intriguing physical effect, observable in the non-chiral version of (1.12) is superradiance [23], the effect where a conglomeration of N atoms collectively absorbs and emits photons with an N^2 increased coupling strength. We will derive this effect for an arbitrary number of spins for the single photon subspace in the following chapter.

Atoms in the superradiant phase do not only act like one superatom but also break chirality. The Hamiltonian (1.12) describes such a system in its entirety. In order to study the photon scattering of such a superatom, we set $c_- = 0$ and $N = 1$, bringing us to the ***Dicke*** Hamiltonian

$$H = \int \mathrm{d}x\, b^\dagger(x)(-i\partial_x)b(x) + \left[a^\dagger b_\nu(x_\mathrm{i}) e^{i\nu k_0 x_\mathrm{i}} + a b_\nu^\dagger(x_\mathrm{i}) e^{-ik_0 x_\mathrm{i}} \right]. \tag{1.13}$$

We will study this Hamiltonian in great detail in section 3.1.

1.2.2 Rydberg Emitters

As a minimal model which utilises every part of the general Hamiltonian (1.11), we show the example of a chiral waveguide where each emitter consists of a cloud of Rydberg atoms. An external laser field pumps the excited state $|1\rangle$ into the Rydberg state $|2\rangle$ with the Rabi frequency Ω. The Rydberg blockade prohibits the creation of a second atomic excitation inside the atomic cloud by detuning the excited level $|1\rangle$ if one Rydberg atom is in the Rydberg state. Thus, every cloud effectively acts like one super atom. The Hamiltonian for this type of setups is given by

$$H = \sum_{\nu=\pm} \int \mathrm{d}x b_\nu^\dagger(x)(-i\nu\partial_x)b_\nu(x) + \sum_{\mathrm{i}=1}^{N} \Omega\left(s_\mathrm{i}^\dagger e_\mathrm{i} + e_\mathrm{i}^\dagger s_\mathrm{i}\right) + \sum_{\mathrm{i}=1}^{N} \sum_{\nu=\pm} c_\nu \left[e_\mathrm{i}^\dagger b_\nu(x_\mathrm{i}) e^{i\nu k_0 x_\mathrm{i}} + e_\mathrm{i} b_\nu^\dagger(x_\mathrm{i}) e^{-i\nu k_0 x_\mathrm{i}} \right], \tag{1.14}$$

where $s = |0\rangle\langle 2|$ "destroys" the Rydberg level, and $e = |0\rangle\langle 1|$.

2 Dicke Superradiance

We want to enter the realm of scattering problems in waveguide quantum electrodynamics with a didactical example. In the first chapter we made quite a few references to the phenomenon of Dicke superradiance; the effect when N atoms collectively absorb and re-emit light with an N^2 increased coupling strength. Intriguingly, we find such a superradiant phase transition in one of our models; more precisely, we will work with a variant of the Hamiltonian (1.12). Additionally, this chapter describes the construction of the single excitation sector eigenstates, with which we then compute scattering events of incoming photons.

While, due to backscattering, it is not possible to analytically solve the scattering problem for any number of incoming photons, our work here will give us an insight into how to do calculations in these waveguide systems. For example, we will explicitly derive the single excitation eigenmodes of the Hamiltonian, a task we will skip in Chapter 3, where we cover other models with analytical solutions. For Bethe Ansatz solvable models, we can then construct the excitation spectrum from these single excitation modes.

2.1 Decomposition into Independent Modes

As it shows a superradiant phase transition, we now want to study the non-chiral version of Equation (1.12), i.e., we have $c_- = 1$. While we are only able to solve this model in the single excitation sector, it is of particular interest since it shows a superradiant phase transition for any number of atoms. Figuratively speaking, this phase transition happens when the different atoms are so close, such that single photons cannot distinguish between the individual atoms as the wavelength is much larger than the total atomic separation. Thus, we work in the limit where $k_0(x_N - x_1) \ll 1$, allowing us to approximate $e^{\pm i k_0 x_i} \approx 1$ for atoms centred around $x = 0$.

The most prominent problem when trying to solve (1.12) for its eigenmodes, lies

in the fact that the interaction Hamiltonian couples the two bosonic modes $b_\pm(x)$. Just from looking at the interaction Hamiltonian, we could try to define new modes $\tilde{b}_\pm = b_+(x) \pm b_-(x)$, which decouple the interaction Hamiltonian. However, this would couple the new modes in the photonic Hamiltonian, rendering our attempt futile. Yet, slightly altering the Ansatz to

$$b_R(x) = \frac{b_+(x) + b_-(-x)}{\sqrt{2}}, \qquad b_L(x) = \frac{b_+(x) - b_-(-x)}{\sqrt{2}}, \tag{2.1}$$

prohibits the coupling of the modes in the photonic part.

These new modes cannot decouple the interaction Hamiltonian for any arbitrary atom configuration. So, when are we able to split the entire Hamiltonian into a L and R mode part? It turns out, we need reflection symmetry about the origin to further simplify the Hamiltonian, i.e., if an atom exists at location x_i then there is another atom at $-x_\mathrm{i}$. This is always true for a periodic lattice with the origin at the centre, however more complex distributions are possible as well. Also, a system of two atoms is necessarily symmetric and, in fact, it will be the starting point for our discussion. First, the symmetry condition allows us to relabel the atomic position variables. From now on, x_i will denote the i-th atom with a ***positive*** coordinate and $x_{-\mathrm{i}} = -x_\mathrm{i}$ will label the atoms on the negative side. For an odd number of atoms in the system, we additionally find an atom at $x_0 = 0$. This is a particular case since it naturally only couples to photons in the R mode, and for this atom alone we would end up in the non-chiral Dicke model, which we will discuss in the following chapter.

With this symmetry condition in mind, we can rewrite the interaction-Hamiltonian as

$$\begin{aligned}
&\sum_{\mathrm{i}=1}^{N/2} \big(b_+(x_\mathrm{i}) + b_-(x_\mathrm{i})\big) a_\mathrm{i}^\dagger + \big(b_+(-x_\mathrm{i}) + b_-(-x_\mathrm{i})\big) a_{-\mathrm{i}}^\dagger + \mathrm{H.c.} \\
&\quad = \frac{1}{\sqrt{2}} \sum_{\mathrm{i}=1}^{N/2} \left[b_R(x_\mathrm{i}) + b_R(-x_\mathrm{i}) + b_L(x_\mathrm{i}) - b_L(-x_\mathrm{i})\right] a_\mathrm{i}^\dagger \\
&\qquad\quad + \left[b_R(x_\mathrm{i}) + b_R(-x_\mathrm{i}) - b_L(x_\mathrm{i}) + b_L(-x_\mathrm{i})\right] a_{-\mathrm{i}}^\dagger + \mathrm{H.c.} \\
&\quad = \frac{1}{\sqrt{2}} \sum_{\mathrm{i}=1}^{N/2} \Big[b_R(x_\mathrm{i}) + b_R(-x_\mathrm{i})\Big] \Big[a_\mathrm{i}^\dagger + a_{-\mathrm{i}}^\dagger\Big] \\
&\qquad\quad + \Big[b_L(x_\mathrm{i}) - b_L(-x_\mathrm{i})\Big] \Big[a_\mathrm{i}^\dagger - a_{-\mathrm{i}}^\dagger\Big] + \mathrm{H.c.} \\
&\quad \equiv \sum_{\mathrm{i}=1}^{N/2} \Big[b_R(x_\mathrm{i}) + b_R(-x_\mathrm{i})\Big] a_{R,\mathrm{i}}^\dagger + \Big[b_L(x_\mathrm{i}) - b_L(-x_\mathrm{i})\Big] a_{L,\mathrm{i}}^\dagger + \mathrm{H.c.}
\end{aligned}$$

for an even number of atoms. Here we have defined new bosonic operators

$$a_{R,\mathrm{i}} = \frac{a_\mathrm{i} + a_{-\mathrm{i}}}{\sqrt{2}}, \qquad a_{L,\mathrm{i}} = \frac{a_\mathrm{i} - a_{-\mathrm{i}}}{\sqrt{2}}.$$

They act like lowering operators in the spin-1 algebra, for which we can consider them as ladder operators of three level systems. Additionally, these operators couple at two different locations to the light field. As previously mentioned, for an odd number of atoms there is one exceptional atom at $x_0 = 0$, which solely interacts with the R-mode photons, therefore yielding a term $\sqrt{2}b_R(0)a^\dagger_{R,0} + \text{H.c.}$ to the Hamiltonian. Notice, $a_{R,0} \equiv a_0$, since the above definition is ill-suited for this case.

While we do not consider an atomic Hamiltonian for this system, we will give its concrete form under this transformation for the sake of completeness. The calculation is straightforward and results in

$$\begin{aligned} H_{\text{at}} &= \sum_{\text{i}=1}^{N/2} \delta\Big(a^\dagger_{\text{i}} a_{\text{i}} + a^\dagger_{-\text{i}} a_{-\text{i}}\Big) + \Omega\Big(a^\dagger_{\text{i}} + a^\dagger_{-\text{i}} + a_{\text{i}} + a_{-\text{i}}\Big) \\ &= \sum_{\text{i}=1}^{N/2} \delta\Big(a^\dagger_{R,\text{i}} a_{R,\text{i}} + a^\dagger_{L,\text{i}} a_{L,\text{i}}\Big) + \sqrt{2}\Omega\Big(a^\dagger_{R,\text{i}} + a_{R,\text{i}}\Big). \end{aligned}$$

Interestingly, the detuning stays constant, but only the R-circular atoms experience a Rabi-oscillation, whose frequency is bigger by a factor of $\sqrt{2}$ compared to the old atoms. For an odd number of atoms, the part of the atomic Hamiltonian for the atom at $x_0 = 0$ remains unchanged.

All in all, we have shown that the Hamiltonian (1.12) under our symmetry restrictions splits into two smaller subsystems, namely

$$H = H_R + H_L \tag{2.2}$$

with

$$H_R = \int \mathrm{d}x\, b^\dagger_R(x)(-i\partial_x)b_R(x) + \sum_{\text{i}=1}^{N/2} \Big[b_R(x_{\text{i}}) + b_R(-x_{\text{i}})\Big] a^\dagger_{R,\text{i}} + \Big[b^\dagger_R(x_{\text{i}}) + b^\dagger_R(-x_{\text{i}})\Big] a_{R,\text{i}} \tag{2.3}$$

and

$$H_L = \int \mathrm{d}x\, b^\dagger_L(x)(-i\partial_x)b_L(x) + \sum_{\text{i}=1}^{N/2} \Big[b_L(x_{\text{i}}) - b_L(-x_{\text{i}})\Big] a^\dagger_{L,\text{i}} + \Big[b^\dagger_L(x_{\text{i}}) - b^\dagger_L(-x_{\text{i}})\Big] a_{L,\text{i}} \tag{2.4}$$

for an even number of atoms. The Hamiltonians H_R and H_L differ from the mono-directional one by the fact that each "atom" interacts with the light-field at two separate locations. Additionally, each atom now describes a three level-system, which becomes important considers the multi-excitation subspaces. To clarify, this impedes us from solving the system with the Bethe Ansatz, since now intrinsic three particle interactions emerge. Thus, we have to limit further discussion to the single excitation sector, where no photon-photon interactions are present. However, even under these strong restrictions, interesting phenomena still emerge.

Solutions to the Circular Subspaces 2.2

Unfortunately, the solution of the L- and R-subspaces becomes increasingly involved with a raising number of atoms in the system. This is due to the ambivalent behaviour of the atoms in the L-and R-subspaces: in the picture of the Hamiltonians (2.3) and (2.4) an absorbed photon at x_i can immediately hop back to $-x_\mathrm{i}$. Thus, a single photon can interact with each atom infinitely often. Due to this complication, we will start with the few atom case. In the next chapter, we will solve the problem for a single photon and, owing to the awkward behaviour of the atom at $x_0 = 0$, we want to limit our discussion to an even number of atoms. For now, we are primarily interested in the $N = 2$ case. Nonetheless, we will later discuss $N \in 2\mathbb{N}$.

We start by solving the system for $N = 2$, i.e., each of the L- and R-subspace of the Hamiltonian contain one atom. For both subspaces, we now find the single excitation eigenmodes. Let us commence with H_R, where we make the Ansatz

$$|\lambda\rangle_R = C(\lambda)\left(\int \mathrm{d}x\, e^{i\lambda x} f(x,\lambda) b_R^\dagger(x) + g(x_1,\lambda) a_{R,1}^\dagger\right)|0\rangle\ . \tag{2.5}$$

We demand $H\,|\lambda\rangle = \lambda\,|\lambda\rangle$, and from this, we derive the following differential equation

$$e^{i\lambda x}\partial_x f(x,\lambda) = -ig(x_1,\lambda)\Big(\delta(x-x_1) + \delta(x+x_1)\Big), \tag{2.6}$$

$$\lambda g(x_1,\lambda) = e^{i\lambda x_1} f(x_1,\lambda) + e^{-i\lambda x_1} f(-x_1,\lambda). \tag{2.7}$$

We readily integrate equation (2.6) for f. However, we need to define the behaviour of f at the jump locations $\pm x_1$. The choice

$$f(\pm x_1,\lambda) = \lim_{\delta\to 0^+} \frac{f(\pm x_1+\delta,\lambda) + f(\pm x_1-\delta,\lambda)}{2}$$

is suitable. At each of the regions $x < -x_1$, $-x_1 < x < x_1$ and $x_1 < x$ the function $f(x,\lambda)$ is constant with respect to x and can only depend on λ. This allows us to set $f(x,\lambda) = 1$ for $x < -x_1$ since every λ dependence of this region can be pulled into the normalisation factor $C(\lambda)$. Besides, to keep the notation compact, we will use $f(x\pm,\lambda) \equiv \lim_{\delta\to 0^+} f(x\pm\delta,\lambda)$ from here on out.

For the region $-x_1 < x < x_1$ integration yields

$$f(-x_1+,\lambda) - f(-x_1-,\lambda) = -ie^{ix_1\lambda} g(x_1,\lambda),$$

while for $x_1 < x$ we find

$$f(x_1+,\lambda) - f(x_1-,\lambda) = -ie^{-ix_1\lambda} g(x_1,\lambda).$$

Multiplying with the corresponding exponential factor and adding and subtracting both equations yields

$$e^{-ix_1\lambda}\left(f(-x_1+,\lambda)-f(-x_1-,\lambda)\right)-e^{ix_1\lambda}\left(f(x_1+,\lambda)-f(x_1-,\lambda)\right)=0 \tag{2.8}$$

$$e^{-ix_1\lambda}\left(f(-x_1+,\lambda)-f(-x_1-,\lambda)\right)+e^{ix_1\lambda}\left(f(x_1+,\lambda)-f(x_1-,\lambda)\right)=-2ig(x_1,\lambda). \tag{2.9}$$

We use the first of the two equations to eliminate $f(x_1+,\lambda)$. By using the relation (2.7) for $g(x_1,\lambda)$, we find

$$f(-x_1+,\lambda)-f(-x_1-,\lambda)=-i\lambda^{-1}\left(e^{2ix_1\lambda}f(x_1-,\lambda)+f(-x_1+,\lambda)\right).$$

Remembering that $f(x_1-,\lambda)=f(-x_1+,\lambda)$ and $f(-x_1-,\lambda)=1$ brings us to the equation

$$f(x,\lambda)=\frac{\lambda}{\lambda+i(1+e^{2ix_1\lambda})}$$

in the region $-x_1<x<x_1$. With this relation, we can solve $f(x,\lambda)$ for $x_1<x$, which yields

$$f(x,\lambda)=\frac{\lambda-i(1+e^{-2ix_1\lambda})}{\lambda+i(1+e^{2ix_1\lambda})}.$$

Finally, the term $g(x_1,\lambda)$ results in

$$g(x_1,\lambda)=\frac{2\cos(x_1\lambda)}{\lambda+i(1+e^{2ix_1\lambda})}.$$

To prove that we have all and the correct solutions we will now show that

$$\mathbb{1}_R=\int \mathrm{d}\lambda\ |\lambda\rangle\ \langle\lambda|\ .$$

Each $|\lambda\rangle$ contains one spatial integration, which splits into three different regions. Consequently, we have to integrate nine separate regions as explained in Figure 2.1. We do not need to care about the regions $x,y<-x_1$ and $x,y>x_1$, since here $f^*(x,\lambda)f(y,\lambda)=1$. Additionally, it turns out, that the six regions where x and y definitely differ, group up into three pairs of complex conjugated results. To evaluate these, we need to find the roots of $\lambda+i(1+e^{2ix_1\lambda})$. For now, it is sufficient to know that they lie on the lower half plane; a more rigorous treatment will be performed later when we calculate the time evolution of incident photons. With this, it turns out that these regions, where $x\neq y$, have a vanishing contribution. We are left to compute the region $-x_1<x,y<x_1$. However, it appears that in this region it is not possible to produce the identity. Nevertheless, this is not problematic because we are only interested in the time evolution of wave packets which start well in front of the atoms and are measured behind it.

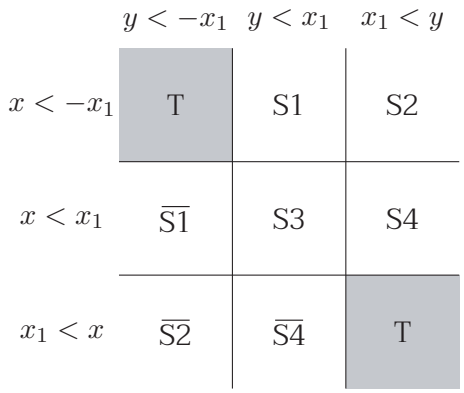

Figure 2.1.
Visual description of the separate regions of integrations. The grey marked areas are trivial to solve, while the three regions on the lower left are just the complex cunjugate of the 3 regions on the upper right corner.

Next, we will repeat the procedure for the L-mode Hamiltonian. Since it is quite similar to the R-mode Hamiltonian the steps are essentially the same, and we find

$$f_L(x,\lambda) = \frac{\lambda}{\lambda + i(1-e^{2ix_1\lambda})} \qquad \text{for } -x_1 < x < x_1,$$
$$f_L(x,\lambda) = \frac{\lambda - i(1-e^{-2ix_1\lambda})}{\lambda + i(1-e^{2ix_1\lambda})} \qquad \text{for } x_1 < x,$$
$$g_L(x_1,\lambda) = \frac{2i\sin(x_1\lambda)}{\lambda + i(1-e^{2ix_1\lambda})},$$

where we made the same Ansatz (2.5) as for the R-mode Hamiltonian. Notice, in all three equations the singularity $\lambda = 0$ is removable. Now, after we have the eigenstates to both Hamiltonians we can efficiently compute the time evolution of arbitrary input states.

2.3 Single Photon Scattering

2.3.1 Scattering at $N = 2$ Atoms

We now ask the question: what is the wave function of a photon after scattering at two atoms at locations $\pm x_1$? For an answer, we determine the single photon Green's function G. Since the Hamiltonian splits into two commuting parts, we know that the time evolution U operator acts independently on the two corresponding subspaces,

$U = U_R \oplus U_L$, respectively. Consequently, the Green's functions splits into a L- and R-part, which we get from

$$|x\rangle_+ \equiv b_+^\dagger(x)\,|0\rangle = \frac{1}{\sqrt{2}}(b_R^\dagger(x) + b_L^\dagger(x))\,|0\rangle \equiv \frac{1}{\sqrt{2}}\left(|x\rangle_R + |x\rangle_L\right).$$

Let us start with the R-mode contribution. Here we have

$$\begin{aligned} G_R(z) &= {}_R\langle y|e^{-iH_R t}|x\rangle_R \\ &= \int \mathrm{d}\lambda\, e^{-i\lambda t}\ {}_R\langle y|\lambda\rangle\langle\lambda|x\rangle_R \\ &\equiv \int \frac{\mathrm{d}\lambda}{2\pi} e^{-i\lambda z}\frac{\lambda - i(1+e^{-2ix_1\lambda})}{\lambda + i(1+e^{2ix_1\lambda})} \\ &= \delta(z) - 4i\int \frac{\mathrm{d}\lambda}{2\pi} e^{-i\lambda z}\frac{\cos^2(x_1\lambda)}{\lambda + i(1+e^{2ix_1\lambda})}, \end{aligned} \tag{2.10}$$

where $z = t+x-y$ and we have assumed $x < -x_1$ and $y > x_1$. We now want to show that the integrand has its singularities on the lower half plane. However, the corresponding transcendental equation does not yield a solution in terms of elementary functions, yet we may express it as

$$\lambda_{\mathrm{i}} = -i\left(1 - \frac{W_{\mathrm{i}}\left(-2x_1 e^{2x_1}\right)}{2x_1}\right),$$

where $W_{\mathrm{i}}(x)$ is the Lambert W function and $\mathrm{i} \in \mathbb{Z}$ labels the countable infinite solutions of the problem.

The Lambert W function gives a somewhat abstract way to label the solutions; therefore we will first determine which kind of solutions are even allowed. Assume λ_0 to be a solution of

$$\lambda + i\left(1 + e^{2ix_1\lambda}\right) = 0. \tag{2.11}$$

Then, $-\overline{\lambda}$ is a solution as well since

$$\begin{aligned} -\overline{\lambda_0} + i\left(1 + e^{-2ix_1\overline{\lambda_0}}\right) &= -\overline{\lambda_0} + i\overline{(1+e^{2ix_1\lambda_0})} \\ &= -\overline{\lambda_0 + i\,(1+e^{2ix_1\lambda_0})} \\ &= 0. \end{aligned}$$

Hence, all possible solutions lie either on the imaginary axis or come in pairs which are reflections about the imaginary axis. A suitable way to label the solution is therefore

- $\lambda_{\mathrm{i}}^{(0)}$ for all solutions on the imaginary axis, where i sorts them in ascending order of their absolute value.

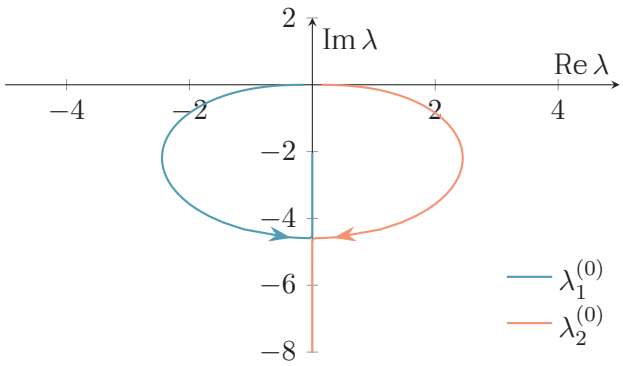

Figure 2.2.
Bifurcation of the singularities for $x_1 \in [10^{-2}, 10]$. One of the imaginary solutions converges to $-2i$, while the other diverges to $-i\infty$. Arrows indicate the direction of ***decreasing*** x_1.

- λ_i^p for all solutions on the right half, where i sorts them in ascending order of the real part. The negative complex conjugate gives the paired solution.

Anyhow, there aren't infinitely many singularities of the first kind but, depending on x_1, there are either no or two singularities with zero real part. We realise that for decreasing x_1 two mirrored singularities walk towards the imaginary axis and at

$$2x_1 e^{2x_1} = e^{-1} \qquad \text{(i.e., } x_1 \approx 0.139\text{)}$$

a bifurcation happens and both singularities start to shift along this axis; one towards $-2i$ and one towards $-i\infty$. This exceptional behaviour is captured in Figure 2.2 and shows the trajectories of those two special singularities for different values of x_1.

Every other singularity increases its distance to the origin for decreasing x_1. In fact, the singularity converging to $-2i$ is the only singularity with finite absolute value for sufficiently small x_1. To prove this, choose an arbitrary $R > 2$ and consider x_1 so small that $1 + e^{2x_1 R} < R$. Then, $|1 + e^{2ix_1\lambda}| < |\lambda|$ on $\partial B(0, R)$ and by the theorem of Rouché the holomorphic functions λ and $\lambda + i(1 + e^{2ix_1\lambda})$ have the same number of zeros in $B(0, R)$, i.e., precisely one. Hence, the singularity converging to $-2i$ has to be the only finite singularity remaining for $x_1 \to 0$.

Now, we want to prove that all singularities have a negative real part. For this, we will disprove the contradiction. Assume $\lambda = a + ib$ is a root of the denominator of Equation (2.10) and $b > 0$. Consequently,

$$\begin{aligned} \operatorname{Im}\left(a + ib + i\left(1 + e^{2ix_1(a+ib)}\right)\right) &= b + 1 + \operatorname{Im}\left(ie^{2ix_1 a}e^{-2x_1 b}\right) \\ &= b + 1 + \cos(2x_1 a)e^{-2x_1 b} \\ &> 0 \end{aligned}$$

since $e^{-2x_1 b} < 1$. Therefore, there are no singularities with a positive imaginary part, which restricts the photons to the causal region $y < x + t$.

We go back to our initial task, the computation of the transition amplitude (2.10). In the last paragraphs we discussed that only the $\lambda \approx -2i$ singularity remains significant in the $x_1 \to 0$ limit. A good approximation in this limit is given by

$$G_R(z) = \langle y | e^{-iH_R t} | x \rangle = \delta(z) + 4\Theta(z) \frac{\cosh^2(2x_1)}{1 - 2x_1} e^{-2z}, \tag{2.12}$$

where $z = t + x - y$, as above. This Green's function consists of a delta-distribution, corresponding to free propagation of the incoming photons, as well as an exponentially decaying tail. A Heaviside function $\Theta(z)$ is superimposed, ensuring causality. As we will see in the next chapter, this is exactly the Green's function for a system of one chiral atom with an effective interaction constant $N^2 g$ with $N = 2$. Intuitively, one would expect to see oscillations in this system, when the incident photon gets backscattered, or, in the picture of the R-mode Hamiltonian, the at x_1 absorbed photon reappears later at $-x_1$. However, it is not only that decay and oscillation processes have different time scales, but even stronger, oscillations are bifurcationally suppressed, and their absence is symmetry protected.

Now we need to solve the L-part of the scattering process and add it to our result. Again, all calculations are quite the same and skipping over them should suffice. A similar analysis shows the same pairing behaviour as in the R-mode case. Contrariwise, for the L-mode photons no two singularities ever meet at the imaginary axis to build a bifurcation pair. We again use Rouché's theorem once again to show that the denominator of the L-mode decomposition, $\lambda + i(1 - e^{2ix_1\lambda})$, has exactly one finite zero at $\lambda = 0$ for $x_1 \to 0$. However, the $\lambda = 0$ singularity is removed by its numerator. Consequently, the L mode equivalent of equation (2.10) possess only the $\delta(z)$-part in the $x_1 \to 0$ limit, i.e., the L-photons propagate freely.

2.3.2 Scattering at Multiple Atoms

We focused on the $N = 2$ case for various reasons. Here we gave an integral representation for the transition amplitude for the scattering of a single photon, managed to derive an analytic expression for the singularities of its integrand and precisely describe the superradiant limit, which yielded a symmetry protected suppression of oscillations and an effective spontaneous emission rate of $2 = N$. Albeit exhaustive, the treatment of the last section lacked generality. Additionally, the purpose of this chapter is to study the scattering of a photon at an atomic cloud. Consequently, considering merely two atoms does not do this idea justice. In this section, we want to discuss the system with multiple atoms. We will keep the number of emitters even for the same reasons as before, and show that the bifurcation is still existent.

For this system, the Ansatz (2.5) yields the coupled set of equations

$$e^{i\lambda x}\partial_x f(x,\lambda) = -i\sum_{\mathrm{i}=1}^{N/2} g(x_\mathrm{i},\lambda)\Big(\delta(x-x_\mathrm{i})+\delta(x+x_\mathrm{i})\Big), \tag{2.13}$$

$$\lambda\sum_{\mathrm{i}=1}^{N/2} g(x_\mathrm{i},\lambda) = \sum_{\mathrm{i}=1}^{N/2} e^{i\lambda x_\mathrm{i}} f(x_\mathrm{i},\lambda) + e^{-i\lambda x_\mathrm{i}} f(-x_\mathrm{i},\lambda). \tag{2.14}$$

Firstly, we assume

$$\lambda g(x_\mathrm{i},\lambda) = e^{i\lambda x_\mathrm{i}} f(x_\mathrm{i},\lambda) + e^{-i\lambda x_\mathrm{i}} f(-x_\mathrm{i},\lambda),$$

which will be justified by the solution. The major hurdles come from the delta functions in (2.13), more precisely from the definition $f(x,\lambda) = (f(x+,\lambda)+f(x-,\lambda))/2$ at the points of discontinuity and the fact that g depends both on the value of f at x_i and $-x_\mathrm{i}$. These two facts imply that wave function at $x > x_\mathrm{i}$ depends on itself at three different locations, namely $x_\mathrm{i}-$, $-x_\mathrm{i}+$ and $-x_\mathrm{i}-$. This means one has to solve N equations "inward to outward" since $f(x_{N/2},\lambda)$ can only be solved if f is known for every other position.

However, our Ansatz for $g(x_\mathrm{i},\lambda)$ allows us to make two very useful rearrangements

$$\begin{aligned} f(x_\mathrm{i}-,\lambda) &= e^{-2ix_\mathrm{i}\lambda}\left[(i\lambda-1)f(-x_\mathrm{i}+,\lambda) - i\lambda f(-x_\mathrm{i}-,\lambda)\right], \\ f(x_\mathrm{i}+,\lambda) &= e^{-2ix_\mathrm{i}\lambda}\left[i\lambda f(-x_\mathrm{i}+,\lambda) - (1+i\lambda) f(-x_\mathrm{i}-,\lambda)\right], \end{aligned}$$

where we expressed the amplitude f for positive arguments by itself for negative values. Next, we begin by solving the equations which contain terms with x_1. This is where our Ansatz starts to shine since we find

$$f(x_1+,\lambda) = \frac{\lambda - i(1+e^{-2ix_1\lambda})}{\lambda + i(1+e^{2ix_1\lambda})} f(-x_1-,\lambda) \equiv \frac{\overline{P_1(\bar\lambda)}}{P_1(\lambda)} f(-x_1-,\lambda).$$

If our system included only two atoms, i.e., just one emitter in the R and L subspaces, we could set $f(-x_1-,\lambda)=1$ and would recover our previous solution. But this result reveals that the wave function at $x_\mathrm{i}+$ can only depend on its value at $-x_\mathrm{i}-$ times some complex function in λ on the unit circle. Solving now for $f(x_2+,\lambda)$ yields

$$f(x_2+,\lambda) = \frac{\lambda\overline{P_1(\bar\lambda)} - i(\overline{P_1(\bar\lambda)} + P_1(\lambda)e^{-2ix_2\lambda})}{\lambda P_1(\lambda) + i(P_1(\lambda) + \overline{P_1(\bar\lambda)}e^{2ix_2\lambda})} f(-x_2-,\lambda) \equiv \frac{\overline{P_2(\bar\lambda)}}{P_2(\lambda)} f(-x_2-,\lambda).$$

Through this, we receive the wave function in the case of 4 atoms. By simple induction, we can show that

$$\begin{aligned} f(x_N+,\lambda) &= \frac{\overline{P_N(\bar\lambda)}}{P_N(\lambda)} f(-x_N-,\lambda) \\ &\equiv \frac{\lambda\overline{P_{N-1}(\bar\lambda)} - i(\overline{P_{N-1}(\bar\lambda)} + P_{N-1}(\lambda)e^{-2ix_N\lambda})}{\lambda P_{N-1}(\lambda) + i(P_{N-1}(\lambda) + \overline{P_{N-1}(\bar\lambda)}e^{2ix_N\lambda})} f(-x_N-,\lambda). \end{aligned} \tag{2.15}$$

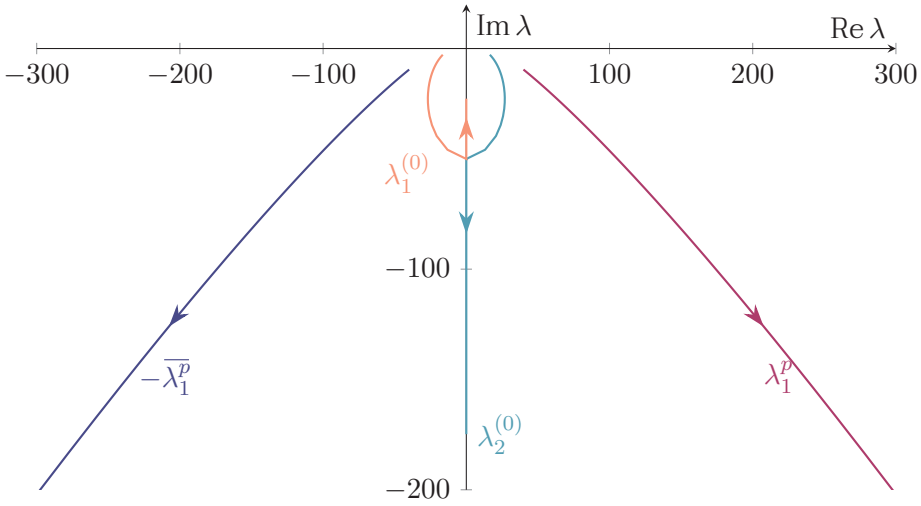

Figure 2.3.
Bifurcating singularities and the first two trivial ones for $a \in [10^{-3}, 10^{-2}]$. Again, one of the imaginary solutions converges, while the other diverges to $-i\infty$. The trivial singularities lose their importance with decreasing x_1, since their imaginary part is always below that of the bifurcating singularities. Arrows indicate the direction of decreasing a.

This recursion formula allows us to give the value of wave function for any number of atoms in the spatial region $x > x_N$, where we want to measure our transition amplitude anyway. It also shows why we have bad luck with every attempt to get a closed form solution of the Green's function G, for which we have to compute the singularities of (2.15).

$P_N(\lambda)$ will consist of products of powers of λ up to N as well as exponential functions $e^{2ix_i\lambda}$. The singularities are already no longer expressible by analytic functions for $N = 2$, and we have to rely on numerics to compute the S Matrix elements for arbitrary x_i. Nevertheless, the solutions of $P_N(\lambda) = 0$ behave quite similar to the ones of $P_1(\lambda) = 0$. For example, we can generalise our previous propositions by induction, i.e., if λ is a solution of $P_N(\lambda) = 0$ then so is $-\bar{\lambda}$, and for every solution λ we have $\mathrm{Im}(\lambda) < 0$.

Before we go on and explain our numerical results we will make a practical restriction. We emphasise once more that our results hold for any atom distribution as long as it is symmetric about the origin. Each of the $N/2$ non-trivial coordinates is an additional degree of freedom which we have to consider. However, having the ability to freely place every atom pair wherever we want overcomplicates the underlying problem. We now reduce our discussion on atoms on a lattice with the lattice parameter a. As a result, the coordinates are given by $x_{i+1} - x_i = a$ and $x_1 = a/2$. This decreases the number of degrees of freedom down to one, simplifying the upcoming example.

Next, we can show numerically that a bifurcation is still happening. For that, we deter-

mined the first four singularities in a system of 22 atoms and followed their "trajectories" along decreasing values of a. Figure 2.3 pictures these curves. We find two important features. Firstly, the two innermost singularities approach the imaginary axis similar to the $N = 2$ case and branch off at roughly $\lambda = -50i$, one singularity diverging, the other converging to some finite imaginary value ($(N + 1)i$ for N atoms). The other two singularities maintain a non-zero real part and increase their distance to the real axis throughout this process. Their imaginary part always stays below that of the bifurcating singularities, rendering them unimportant in the $x_1 \to 0$ limit, as they correspond to infinitely fast decaying solutions.

We made another important numerical observation, concerning the critical value of a for which the bifurcation happens. While for two atoms we found a bifurcation at $a \approx 0.28$ (we had $x_1 \approx 0.14$ and thus $a = 2x_1$), in the upper example of $N = 22$ the bifurcation occurs at much smaller values, namely at $a \approx 0.0018$. We tested every system from two atoms up to 30 and found that the point of bifurcation monotonically decreases. At $N = 30$ we reach a critical value of $a < 10^{-3}$ for the first time. Beyond $N = 30$ computation becomes increasingly expensive. Therefore we have to limit our knowledge to these values. A simple fit of the critical separations against the number of atoms N revealed neither an algebraic nor an exponential dependence.

3 Integrable Waveguide Models

Generic one-dimensional waveguide systems are usually not analytically solvable. This stems from the fact that the effective interaction between the waveguide photons takes a non-trivial form, which can involve up to all waveguide photons at the same time. However, in the fully chiral case, the N-particle scattering matrix decomposes into a product of 2-particle scattering matrices, or, in an equivalent picture, the time evolution operator obeys the Yang-Baxter equation. Both facts imply that the underlying model is integrable; the algebraic Bethe Ansatz yields the scattering states of the waveguide Hamiltonian [30, 31].

These scattering states will serve as the foundation for this thesis. For example, in Chapter 4, where we will investigate approximative ways of solving the scattering problem, we need some entirely analytical results to derive statements about the failures and successes of those schemes. Beyond this, we will find that the exact treatment gives raise to universal many body bound states, as we will see in Chapter 5.

For now, we will start with the simplest waveguide model, the Dicke Model, consisting of a single superatom. The Dicke Model will help us understand more complex systems, for which it has both didactic importance and is a relevant physical system by its own. For the Dicke model, we will derive the Green's function by the method of Yudson and then cast on into a more practical form, especially applicable for multi-particle problems. Then we will discuss a related model, a system consisting of multiple superatoms with irregular spacing. While, for the chiral case, it again is fully integrable (i.e., we can find its complete eigenbasis), we cannot derive a closed form N-particle Green's function. However, we will show a simplified form, suitable for the few photon and few atom limit.

The Dicke Model
3.1

The Dicke Model consists of only a single emitter, without loss of generality, at the centre of the setup at $x = 0$. For now, consider an arbitrary degree of chirality c_-, such that the Dicke Hamiltonian reads

$$H = \sum_{\nu=\pm} \int \mathrm{d}x\, b_\nu^\dagger(x)(-i\nu\partial_x)b_\nu(x) + \sqrt{2\pi g_\nu}\big(b_\nu(0)a^\dagger + b_\nu^\dagger(0)a\big). \tag{3.1}$$

Since the emitter sits at $x = 0$, the phase influence due to the central frequency vanishes. Notice, here we did not set $2\pi g_+ = 1$, because this will help us in the following discussion.

Obviously, the left and right moving photons are coupled by the emitter; a right moving photon can be absorbed by the emitter and re-emitted into the left moving mode and vice versa. However, for the fully non-chiral case $g_+ = g_- = g$, we can find new bosonic modes, which are not coupled to another and are therefore an excellent choice for describing the system. To be precise, the substitutions

$$\begin{aligned} b_R(x) &= (b_+(x) + b_-(-x))/\sqrt{2}, \\ b_L(x) &= (b_+(x) - b_-(-x))/\sqrt{2} \end{aligned} \tag{3.2}$$

do the trick. The Hamiltonian then splits into an L and R part, which are

$$H_R = \int \mathrm{d}x\, b_R^\dagger(x)(-\partial_x)b_R(x) + 2\sqrt{2\pi g}\big(b_R(0)a^\dagger + b_R^\dagger(0)a\big), \tag{3.3}$$

$$H_L = \int \mathrm{d}x\, b_L^\dagger(x)(-\partial_x)b_L(x). \tag{3.4}$$

Apparently, the L mode photons obey a free propagation, while the R mode bosons have a chiral Dicke model Hamiltonian with an interaction constant $4g$, four times the original one. Thus, from here on, we will only investigate the chiral part of the system.

3.1.1 Scattering States and String Solutions

Given an initial many-body state $|\Psi\rangle$ at $t = 0$, how does it evolve in time under the influence of the Hamiltonian H defined in (3.1)? Usually, this question is best answered in the eigenbasis of the corresponding Hamiltonian: Let $B = \{\,|\lambda\rangle\,\}$ be a complete set, such that $H\,|\lambda\rangle = E_\lambda\,|\lambda\rangle$ for all $|\lambda\rangle \in B$, where λ is a parameter from some measurable set Λ_B. Then

$$e^{-iHt}\,|\Psi\rangle = \int_{\Lambda_B} \mathrm{d}\lambda\, e^{-iHt}\,|\lambda\rangle\langle\lambda|\Psi\rangle = \int_{\Lambda_B} \mathrm{d}\lambda\, e^{-iE_\lambda t}\,\langle\lambda|\Psi\rangle|\lambda\rangle\,. \tag{3.5}$$

While it is easy to write down this identity, the basis B and its parameter space Λ_B obviously depend on the Hamiltonian of consideration. Luckily for us, the Dicke Model is readily solved by the Bethe Ansatz; its n-particle eigenmodes are [3]

$$|\lambda\rangle = C(\lambda) \int \mathrm{d}^n y \prod_{\mathrm{i}<\mathrm{j}} \left(1 - \frac{i \operatorname{sgn}(y_\mathrm{i} - y_\mathrm{j})}{\lambda_\mathrm{i} - \lambda_\mathrm{j}}\right) \prod_{\mathrm{i}=1}^{n} f(y_\mathrm{i}, \lambda_\mathrm{i}) e^{i\lambda_\mathrm{i} y_\mathrm{i}} r^\dagger(y_\mathrm{i}, \lambda_\mathrm{i}) \, |0\rangle \ , \tag{3.6}$$

where

$$f(y, \lambda) = \frac{\lambda - i/2 \operatorname{sgn} y}{\lambda + i/2},$$
$$r^\dagger(y, \lambda) = b^\dagger(y) + \frac{1}{\lambda} \delta(x) a^\dagger,$$

$\lambda = (\lambda_1, \ldots, \lambda_n)$ and $C(\lambda)$ is a "string dependant" normalisation; more on strings in the following paragraphs. These eigenmodes are best derived by constructing the single excitation and then finding the solutions in the other particle number sectors by the Bethe Ansatz. However, to just prove that Equation (3.6) describes the eigenmodes of the Hamiltonian (3.1) one only needs to compute $H \, |\lambda\rangle$, which leads to

$$H \, |\lambda\rangle = E_\lambda \, |\lambda\rangle = \sum_{\mathrm{i}=1}^{n} \lambda_\mathrm{i} \, |\lambda\rangle \ , \tag{3.7}$$

a linear dispersion relation.

We still need to discuss the parameter space Λ_B of the parameters λ_i of the eigenmode $|\lambda_1, \ldots, \lambda_n\rangle$. The similarity of these modes to plane waves as well as the dispersion relation (3.7) suggests that $\Lambda_B = \mathbb{R}^n$, yet one then finds

$$\int_{\mathbb{R}^n} \mathrm{d}^n \lambda \, |\lambda\rangle\langle\lambda| \neq \mathbb{1}$$

for all choices of $C(\lambda)$. Are we missing out on some eigenmodes of the Hamiltonian? As it turns out, no, we were just too restrictive. Since H is a Hermitian operator, its eigenvalues E_λ have to be real numbers; yet this can also be accomplished by complex λ_i, as long as the sum over all parameters is still real.

Thus, we now relax the condition of real parameters λ and introduce the weaker condition that the amplitude of the eigenmodes (3.6) is bounded for all y. This turns out to be possible, when we group individual parameters λ_i such that they have the same real part and their imaginary part differs by exactly 1, or, in the old units, by the coupling constant g. We will call such a configuration a "string". Figure 3.1 illustrates the possible strings for the 3-excitation subspace. It is evident that we increased the parameter space

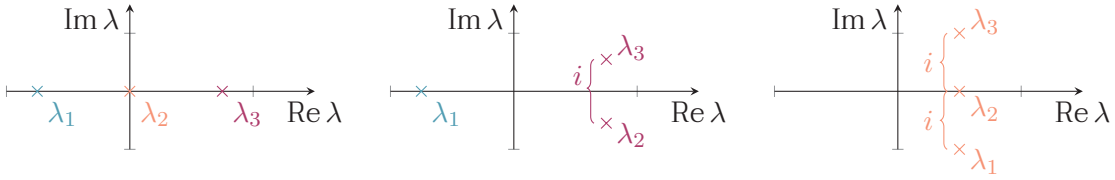

Figure 3.1.
Illustration of all possible string configurations in the three excitation subspace. In the first case we have three real rapidities, corresponding to free particles. Next, there is the configuration with two rapidities lying symmetrically about the real axis with a distance of 1. This corresponds to two bonded excitations. Lastly, all three rapidities share the same real value, while their imaginary parts still differ by 1 and are arranged symmetrically around the real axis.

Λ_B over just $\mathbb{R}^n$. Now, summing over all the possible string configuration allows us to prove

$$\int_{\Lambda_B} \mathrm{d}^n\lambda \, |\lambda\rangle\langle\lambda| = \sum_{\text{strings}} \int \mathrm{d}^n\lambda \, |\lambda\rangle\langle\lambda| = \mathbb{1}.$$

Thus we found the full eigenbasis.

As a final remark, the similarity of λ to the momentum k of the plane waves temps us to give λ the same interpretation, for which we will call the λ_i 's rapidities henceforth. Since in a string solution multiple excitations share the same real part of a rapidity (i.e., its physical momenta) we will identify string solutions with bound states. A string with two coupled rapidities corresponds to two bounded particles and so forth.

3.1.2 Yudson's Approach for the Eigenmode Decomposition

The discussion in the last section brought us a step closer to our intermediate goal — to analytically describe scattering processes in the Dicke model. We have seen that the basis states of given excitation number decompose into strings of rapidities, which are, in principle, known. These strings, however, impede the decomposition of an arbitrary wave function into the eigenmodes. The number of string configurations in the N excitation subspace equals part(N), the number of partitions of N into positive integers. For this, the decompositions should become unfeasible for just four or more photons. As another lucky fact, there is a way to avoid the pesky summation over string configurations.

As first shown by Yudson in 1985 [3], for spatial basis states $|\Psi\rangle = \prod_{\mathrm{i}=1}^{N} b^\dagger(x_\mathrm{i}) \, |0\rangle$, one can introduce an auxiliary state $|\lambda\rangle_A$ and a complex contour $\Gamma : \mathbb{R}^n \to \mathbb{C}^n$ such that the eigenmode decomposition (3.5) no longer needs the cumbersome string summation, but only a single contour integration along Γ. Furthermore, this fixes the normalisation

in (3.6) to

$$C(\lambda) = \frac{1}{\sqrt{N!}(2\pi)^{N/2}} \prod_{i<j} \frac{\lambda_i - \lambda_j}{\lambda_i - \lambda_j + i}.$$

Yet, $\mathrm{Img}(\Gamma) \not\subset \Lambda$ and thus one needs to analytically continue $|\lambda\rangle$ onto $\lambda \in \mathbb{C}^N$, up to a set of simple singularities. This statement is so important that we will formally prove it and phrase it as:

1 Theorem

Let $|\Psi\rangle = |x_1, \ldots, x_N\rangle = \prod_{i=1}^N b^\dagger(x_i)\,|0\rangle$ and, without loss of generality, let $x_1 \geq \cdots \geq x_k > 0 > x_{k+1} \geq \cdots \geq x_N$. Define

$$|\lambda\rangle_A = \frac{\sqrt{N!}}{(2\pi)^{N/2}} \int \mathrm{d}^n y \Theta(y_1 \geq \cdots \geq y_N) \prod_{i=1}^N f(y_i, \lambda_i) e^{i\lambda_i y_i} r^\dagger(y_i, \lambda_i)\,|0\rangle\,,$$

Then for any complex contour $\Gamma : \gamma_1 \otimes \cdots \otimes \gamma_N$, $\gamma_i : \mathbb{R} \to \mathbb{C}$, with $\mathrm{Im}\,\gamma_{i+1} - \mathrm{Im}\,\gamma_i > 1$ and $\mathrm{Im}\,\gamma_i < 1/2$ for $i \leq k$ or $\mathrm{Im}\,\gamma_i > -1/2$ for $i > k$,

$$|\Psi(t)\rangle = \int_\Lambda \mathrm{d}\lambda e^{-iHt}\,|\lambda\rangle\langle\lambda|\Psi\rangle = \int_\Gamma \mathrm{d}\lambda e^{-iE_\lambda t}\,{}_A\langle\lambda|\Psi\rangle|\lambda\rangle\,. \tag{3.8}$$

Proof First, consider $t = 0$ before treating the time dependent case.

1. Step For $|x_1, \ldots, x_n\rangle$ as defined as in the theorem we have

$${}_A\langle\lambda|x_1, \ldots, x_N\rangle = \frac{\sqrt{N!}}{(2\pi)^{N/2}} \prod_{i=1}^N \overline{f(x_i.\overline{\lambda_i})} e^{-i\lambda_i x_i}.,$$

Thus we find

$$\begin{aligned}\int_\Gamma \mathrm{d}\lambda\,{}_A\langle\lambda|x_1, \ldots, x_N\rangle|\lambda\rangle = \frac{1}{(2\pi)^N} \int_\Gamma \mathrm{d}\lambda \int \mathrm{d}^n y \prod_{i<j} \frac{\lambda_i - \lambda_j + i\,\mathrm{sgn}(y_i - y_j)}{\lambda_i - \lambda_j + i} \\ \times \prod_{i=1}^N \frac{\lambda_i - i/2\,\mathrm{sgn}\,y_i}{\lambda_i + i/2} \frac{\lambda_i + i/2\,\mathrm{sgn}\,x_i}{\lambda_i - i/2} e^{i\lambda_i(y_i - x_i)} r^\dagger(y_i, \lambda_i)\,|0\rangle\,.\end{aligned} \tag{3.P1}$$

2. Step We now show that the wave function defined by (3.P1) has its support on $y_i \geq x_i$. For this assume $y_1 < x_1$. Since $\mathrm{Im}\,\gamma_{i+1} - \mathrm{Im}\,\gamma_i > 1$ the only singularity of λ_1 in the lower half plane is the $\lambda_1 + i/2$ denominator. However, since $y_1 < x_1$, this singularity

is cancelled by the numerators, either because if $x_1 > 0$ then $\lambda_1 + i/2 \operatorname{sgn} x_1 = \lambda_1 + i/2$ or if $x_1 < 0$ then $\lambda_1 - i/2 \operatorname{sgn} y_1 = \lambda_1 + i/2$. Thus, we can close the γ_1 contour below such that it does not wind around any singularity and therefore, by the Residue theorem, the integral vanishes. Consequently, the wave function has its support in the $y_1 \geq x_1$ section.

Now consider $y_2 < x_2$. λ_2 again has the singularity $-i/2$ in the lower half plane, but also the singularity $\lambda_1 - \lambda_2 + i$. From the previous paragraph and the current assumption we know that $y_1 \geq x_1 > x_2 > y_2$. Ergo $\lambda_1 - \lambda_2 + i \operatorname{sgn}(y_1 - y_2) = \lambda_1 - \lambda_2 + i$ and thus cancels the singularity of the same form. Therefore, the only relevant singularity, which remains in the lower half plane, is $\lambda_2 + i/2$ and, by the same arguments as in the previous paragraph, it is cancelled by one of the numerators. Hence, we can close the γ_2 contour below without encircling any singularity, which again leads to a support of $y_2 \geq x_2$. These arguments are now inductively repeated up to x_k.

For x_{k+1} both the singularities $\lambda_{k+1} - i/2$ and $\lambda_{k+1} + i/2$ could be relevant, while the singularities from the first product are cancelled yet again in the same fashion as before. From $0 > x_{k+1}$ we find $0 > y_{k+1}$ and thus both numerators in the second product take the right form to cancel their respective denominators. Hence, we are able to close γ_{k+1} below and the integral vanishes by the Residue theorem. This argumentation is now continued up to x_N.

3. Step Now, complementary to step 2, we show that the support of (3.P1) lies within the $y_\mathrm{i} \leq x_\mathrm{i}$ sector. Here, we start from the other end, i.e., consider $y_N < x_N$. Due to $\operatorname{Im} \gamma_N > -1/2$ and $\operatorname{Im} \gamma_{\mathrm{i}+1} - \operatorname{Im} \gamma_\mathrm{i} > 1$ the λ_N part has a single singularity at $\lambda_N = i/2$ in the upper half plane. But, from $x_N < y_N$ we realise that one of the numerators removes this singularity again. Thus we close γ_N above, find no encircled singularity, and therefore the γ_N integration vanishes. Consequently, $y_N \leq x_N$ must be the non-trivial region of the wave function. In the same manner as in the second step, the argumentation continues for all other γ_i's down to $\mathrm{i} = k + 1$.

For $\mathrm{i} \leq k$ we are in the same situation as in step 2, where there were two possible singularities. However, with the assumption $x_\mathrm{i} < y_\mathrm{i}$ these singularities again vanish due to their corresponding numerators. Thus we can show that the λ_k integration yields zero for $y_k > x_k$ and this argument can be extended for all $\mathrm{i} < k$, which brings us to $y_\mathrm{i} \leq x_\mathrm{i}$, as stated.

4. Step In the second step we found $y_\mathrm{i} \geq x_\mathrm{i}$ for the support of the wave function and in the latest step we found $y_\mathrm{i} \leq x_\mathrm{i}$. Both conditions are only met for $y_\mathrm{i} = x_\mathrm{i}$. Since both variables are equal we can exchange them at will, and we will do so everywhere, but in the exponential function. Using the ordering convention $x_\mathrm{i} \geq \cdots \geq x_N$ and $x_\mathrm{i} \neq 0$ for

all i brings us to

$$\int_\Gamma \mathrm{d}\lambda \; {}_A\langle\lambda|x_1,\ldots,x_N\rangle|\lambda\rangle \;=\; \frac{1}{(2\pi)^N}\int_\Gamma \mathrm{d}\lambda \int \mathrm{d}^n y \prod_{\mathrm{i}=1}^{N} e^{i\lambda_\mathrm{i}(y_\mathrm{i}-x_\mathrm{i})} b^\dagger(x_\mathrm{i})\;|0\rangle \;.$$

This is an entire function in λ_i and hence we are allowed to shift the contours such that $\gamma_\mathrm{i}(t) = t$. The remaining λ_i integration is the well known identity for the delta function $\delta(x_\mathrm{i} - y_\mathrm{i})$ and thus we end up in

$$\int_\Gamma \mathrm{d}\lambda \; {}_A\langle\lambda|x_1,\ldots,x_N\rangle|\lambda\rangle \;=\; \int \mathrm{d}^n y \prod_{\mathrm{i}=1}^{N} \delta(x_\mathrm{i}-y_\mathrm{i}) b^\dagger(x_\mathrm{i})\;|0\rangle \;=\; \prod_{\mathrm{i}=1}^{N} b^\dagger(x_\mathrm{i})\;|0\rangle \;=\; |x_1,\ldots,x_N\rangle \;.$$

This completes the proof for the special case $t = 0$ and $|\Psi\rangle = |x_1,\ldots,x_N\rangle$.

Final Step Now consider the general case of $t \in \mathbb{R}$. Here

$$\begin{aligned} |\Psi(t)\rangle \;&= e^{-iHt}\;|x_1,\ldots,x_N\rangle \\ &= \int_\Gamma \mathrm{d}\lambda\, e^{-iHt}\; {}_A\langle\lambda|x_1,\ldots,x_N\rangle|\lambda\rangle \\ &= \int_\Gamma \mathrm{d}\lambda\, e^{-iE_\lambda t}\; {}_A\langle\lambda|x_1,\ldots,x_N\rangle|\lambda\rangle \;, \end{aligned}$$

which was to be proven. ■

For completeness, one should have considered an atomic excitation as well. However, there the argumentation is precisely the same, but one only needs to takes care of the particular case of $y = 0$, which was not of importance here and thus shortened our argumentation. We now continue, knowing that the more general version with an initially excited atom still holds.

3.1.3 Green's Function

Why did we go through so much trouble performing a two-page long proof? As it turns out, the quantity

$$e^{-iHt}\;|x_1,\ldots,x_N\rangle \;=\; \int_\Gamma \mathrm{d}\lambda\, e^{-iE_\lambda t}\; {}_A\langle\lambda|x_1,\ldots,x_N\rangle|\lambda\rangle$$

has an analytical solution, or, more precisely, can be cast into the form

$$\begin{aligned} \int_\Gamma \mathrm{d}\lambda\, e^{-iE_\lambda t}\; {}_A\langle\lambda|x_1,\ldots,x_N\rangle|\lambda\rangle \;\equiv\; &\int_{\mathbb{R}^N} \mathrm{d}^N y\, G(x-y) \prod_{\mathrm{i}=1}^{N} b^\dagger(y_\mathrm{i})\;|0\rangle \\ &+ \int_{\mathbb{R}^{N-1}} \mathrm{d}^{N-1} y\, G_1(x-y) a^\dagger \prod_{\mathrm{i}=1}^{N-1} b^\dagger(y_\mathrm{i})\;|0\rangle \qquad (3.9) \end{aligned}$$

of a N particle wave function, such that the Green's functions G and G_1 is exactly known. It is evident that (3.9) has indeed these two parts, characterised by the atomic excitation. We only focus on the photon contribution, defined by $G(x-y)$, since, for $t \to \infty$, spontaneous emission will have removed all atomic excitations, i.e., $G_1(x-y) \to 0$ for $t \to \infty$. A quick calculation readily verifies this. However, let us now compute $G(x-y)$.

Inserting the exact expressions for $|\lambda\rangle$ and $|\lambda\rangle_A$ into (3.9) yields

$$G(x-y) = \int_\Gamma \frac{\mathrm{d}^N\lambda}{(2\pi)^N} \prod_{\mathrm{i}<\mathrm{j}} \frac{\lambda_\mathrm{i} - \lambda_\mathrm{j} + i\,\mathrm{sgn}(y_\mathrm{i} - y_\mathrm{j})}{\lambda_\mathrm{i} - \lambda_\mathrm{j} + i} \prod_{\mathrm{i}=1}^{N} \frac{\lambda_\mathrm{i} - i/2}{\lambda_\mathrm{i} + i/2} e^{i\lambda_\mathrm{i}(y_\mathrm{i} - t - x_\mathrm{i})}. \tag{3.10}$$

This integral by itself probably refuses any analytical treatment. However, we may not forget that $G(x-y)$ displays a wave function. Hence, we are only interested in its fully symmetric part. First and foremost, due to the contours from above, $G(x-y)$ builds its support only in the causal region $y_\mathrm{i} \leq x_\mathrm{i} + t$. Next, it turns out that the wave function is totally antisymmetric everywhere but in the region $y_N \leq x_N + t \leq \cdots \leq y_1 \leq x_1 + t$. A full proof of this statement appears to be too cumbersome, for which we will only show the general idea in the special case of $N = 2$ and then give a physical explanation, why this must be.

For $N = 2$ the symmetrised Green's function reads

$$\begin{aligned} G_\mathrm{sym}(z-y) = \int_\Gamma \frac{\mathrm{d}^2\lambda}{(2\pi)^2} \Bigg(& \frac{\lambda_1 - \lambda_2 + i\,\mathrm{sgn}(y_1 - y_2)}{\lambda_1 - \lambda_2 + i} e^{i\lambda_1(y_1 - z_1) + i\lambda_2(y_2 - z_2)} \\ & + \frac{\lambda_1 - \lambda_2 - i\,\mathrm{sgn}(y_1 - y_2)}{\lambda_1 - \lambda_2 + i} e^{i\lambda_1(y_2 - z_1) + i\lambda_2(y_1 - z_2)} \Bigg) \prod_{i=1}^{2} \frac{\lambda_i - i/2}{\lambda_i + i/2}, \end{aligned}$$

where we introduced the retarded coordinate $z_\mathrm{i} = x_\mathrm{i} + t$. We already know that $y_\mathrm{i} \leq z_\mathrm{i}$, so that $y_\mathrm{i} \leq z_1$ for all i. This allows closing the γ_1 contour below. Additionally, since this is the symmetric form of G, we may assume $y_1 \geq y_2$ without loss of generality. The last two statements together bring us to

$$\begin{aligned} G_\mathrm{sym}(z-y) &= \int_{\gamma_2} \frac{\mathrm{d}\lambda_2}{2\pi} \left(\frac{\lambda_2 - i/2}{\lambda_2 + i/2} e^{(y_1 - z_1)/2 + i\lambda_2(y_2 - z_2)} \right. \\ &\quad \left. + \left(1 + \frac{i}{\lambda_2 + i/2}\right) e^{(y_2 - z_1)/2 + i\lambda_2(y_1 - z_2)} \right) \\ &= e^{(y_1 - z_1)/2 + (y_2 - z_2)/2} + \delta(y_1 - z_2) e^{(y_2 - z_1)/2} - e^{(y_2 - z_1)/2 + (y_1 - z_2)/2} \\ &= 0. \end{aligned}$$

The delta distribution vanishes due to the assumption $y_1, y_2 < z_2$. We conclude that $G(z-y)$ is totally antisymmetric in the region $y_1, y_2 < z_2$. Hence, when we limit the discussion to the sector $y_1 \geq y_2$, we find the support $z_1 \geq y_1 \geq z_2 \geq y_2$.

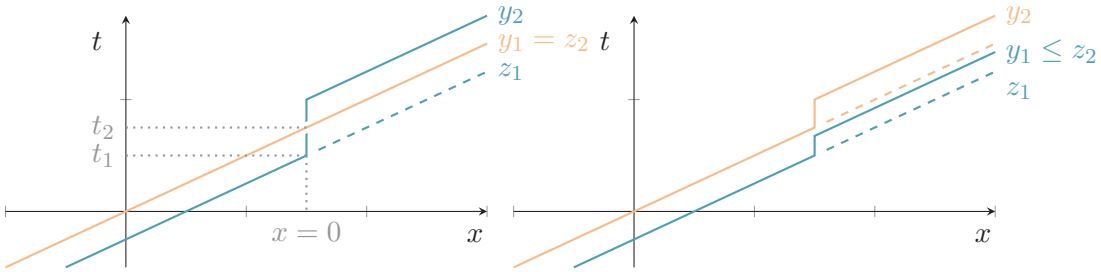

Figure 3.2.
Classical explanation of the support of the wave function. If the first photon is absorbed by the emitter and stays an excitation long enough, then the second photon has to pass the emitter without retardation. Then the first photon is measured at z_2. If the first photon gets absorbed and re-emitted before the second arrives, we again find a photon in the region $z_2 \leq y_1 \leq z_1$.

As already said, we do not want to generalise this for multiple photons. However, we can give a physical interpretation for why this symmetry restriction holds for any number of incoming photons. Imagine two photons, initially at x_1, x_2 with $x_1 > x_2$. At time t_1 the first photon arrives at the emitter. Now the wave function consists of two parts: firstly, both photons are still free, i.e., the first has passed the atom, and secondly, the first photon got absorbed and the atom is excited. Apparently, for the first part of the wave function, $y_1 = z_1$. Therefore, only the second part is non-trivial. Now, at time t_2, the second photon arrives at the emitter. If the atomic excitation has not decayed yet, the second photon can pass the atom without interaction or induce a stimulated emission. Either way, we definitely measure the first photon at z_2 or earlier. If the second photon arrives at an unexcited atom, then a spontaneous emission event must have occurred, for which we trivially have $z_2 \leq y_1 \leq z_1$. Figure 3.2 pictures these different processes. The argument over the photon trajectories is readily generalised for multiple photons.

We now turn back our attention towards the computation of the Green's function. We figured out that $y_N \leq z_N \leq \cdots \leq y_1 \leq z_1$. What is the implication? At first, this means that for the symmetrisation we do not need to care about all $N!$ permutations, but only permutations of the reduced set $S'_N \equiv \{\sigma \in S_N | \sigma_\mathrm{j} \geq \mathrm{j} - 1\}$. Secondly, assume we have a permutation for which $\sigma_N = N - 1$. Then

$$\prod_{\mathrm{i}=1}^{N-1} \frac{\lambda_\mathrm{i} - \lambda_N + i\,\mathrm{sgn}(y_{\sigma_\mathrm{i}} - y_{N-1})}{\lambda_\mathrm{i} - \lambda_N + i}$$

differs from 1 only on a set of measure zero. On the other hand, this expression is trivially equal to 1 for any permutation with $\sigma_N = N$. Continuing the argumentation for all i allows us to exchange the first product in (3.10) with the identity. The remaining integral

is now trivially evaluated with the Residue theorem:

$$\begin{aligned} G(z-y) &= \int_\Gamma \frac{\mathrm{d}^N\lambda}{(2\pi)^N} \prod_{\mathrm{i}=1}^{N} \frac{\lambda_\mathrm{i} - i/2}{\lambda_\mathrm{i} + i/2} e^{i\lambda_\mathrm{i}(y_\mathrm{i}-z_\mathrm{i})} \\ &= \prod_{\mathrm{i}=1}^{N} \big(\delta(z_\mathrm{i}-y_\mathrm{i}) + \Theta(z_\mathrm{i}-y_\mathrm{i})\big) e^{-(z_\mathrm{i}-y_\mathrm{i})/2}. \end{aligned}$$

Remember, this is not the fully symmetrical Green's function and secondly, this representation is only valid in the region $y_N \leq z_N \leq \cdots \leq y_1 \leq z_1$. Thus, we identify

$$G(z,y) = \Theta(y_N \leq z_N \leq \cdots \leq y_1 \leq z_1) \sum_{\sigma\in S'_N} \prod_{\mathrm{i}=1}^{N} \big(\delta(z_\mathrm{i}-y_{\sigma_\mathrm{i}}) + \Theta(z_\mathrm{i}-y_{\sigma_\mathrm{i}})\big) e^{-(z_\mathrm{i}-y_{\sigma_\mathrm{i}})/2} \tag{3.11}$$

as the correct Green's function, where S'_N was the reduced set of permutations with $\sigma_\mathrm{j} \geq \mathrm{j}-1$ for $\sigma \in S'_N$.

Let us summarise what we have achieved so far. For a general number N of initial excitations in the system, we managed to avoid the string problem, where we needed to sum over part(N) different configurations, by replacing the summation with an aptly chosen contour. Then, we managed to write down the integral equation (3.10) for the Green's function and showed that it is totally antisymmetric for most choices of arguments. This, in turn, allowed us to avoid many of the $N!$ possible permutations, which enabled us to perform the last integrals and finally arrive at the exact expression (3.11).

Yet, even this representation of the Green's function is not suitable for practical applications. While the convolution with the Green's function is simpler than the integral over all strings, the — albeit reduced — set of permutations creates more terms than feasible for most practical applications. There is a neat trick to avoid the permutations altogether, namely, by replacing them with simple derivatives. We will show how in the next section.

3.1.4 Generating Functional for Outgoing States

The following theorem will help us to get rid of the pesky summation over the reduced set of permutations. We will first state it, before we demonstrate its usage in a concrete example.

2 Theorem

Define $\lim_{z\to-\infty}\Theta(x-z)\equiv 1$ and $\lim_{z\to-\infty}\delta(x-z)\equiv 0$ and let $S'_N=\{\sigma\in S_N\mid \sigma_\mathrm{j}\geq \mathrm{j}-1\}$, then

$$\begin{aligned}&\Theta(y_N\leq z_N\leq\cdots\leq y_1\leq z_1)\sum_{\sigma\in S'}\prod_{\mathrm{i}=1}^{N}\{\delta(z_\mathrm{i}-y_{\sigma_\mathrm{i}})-\chi\Theta(z_\mathrm{i}-y_{\sigma_\mathrm{i}})\}\\&=\lim_{z_{N+1}\to-\infty}\prod_{\mathrm{i}=1}^{N}\partial_{\alpha_\mathrm{i}}e^{-\chi\alpha_\mathrm{i}}\Theta(z_\mathrm{i}+\alpha_\mathrm{i}-y_\mathrm{i})\Theta(y_\mathrm{i}+\alpha_\mathrm{i}-z_{\mathrm{i}+1})\Big|_{\alpha_\mathrm{i}=0}\end{aligned}\tag{3.12}$$

almost everywhere (i.e., everywhere except on a set of measure zero).

While this theorem carries vital importance for the following parts, its proof carries no didactical purpose whatsoever for which we shift it into Appendix A. For the proof, one uses induction in N and utilises that S' allows only two kinds of permutations for the N-th index. Instead of performing these calculations here, we now rather put our attention to some examples.

Our representation of the Dicke model's Green's function mainly reduces the effort when computing output states. Yudson's result had a summation over permutations, which bloats every attempt of an exact treatment and, for example, makes it hard to compute expectation values, due to the appearing double summation. We, instead, replaced these summation with derivatives. The final result is obviously the same, however the derivatives can always be computed last, making every intermediate step easier than before. Furthermore, some of the z_i variables in Yudson's solution appeared in up to three Heaviside functions, for which expressing integration boundaries becomes tedious. In our representation, every z_i variable for $\mathrm{i}\geq 2$ has two corresponding Heaviside functions, and thus integration boundaries are trivially determined.

To further motivate our result and to give a practical intermediate result for our forthcoming computations let us consider a Fock state in which N photons are initially in the same wave function $E_\mathrm{in}(x)$. We utilise our Green's function representation to determine the outgoing photonic wave function $\Psi_\mathrm{out}(y_1,\ldots,y_N)$, which is

$$\Psi_\mathrm{out}(y_1,\ldots,y_n)=\int_{\mathbb{R}^N}\mathrm{d}^N z\,G(z-y)\prod_{\mathrm{i}=1}^{N}E_\mathrm{in}(z_\mathrm{i}),\tag{3.13}$$

where y denotes the retarded coordinate, i.e., it is the actual spatial coordinate shifted

by the time t. Equation (3.13) mostly consists of terms like

$$\begin{aligned}
&\int_{y_\mathrm{i}-\alpha_\mathrm{i}}^{y_{\mathrm{i}-1}+\alpha_{\mathrm{i}-1}} \mathrm{d}z_\mathrm{i}\, e^{-(z_\mathrm{i}-y_\mathrm{i})/2} E_\mathrm{in}(z_\mathrm{i}) \\
&\quad = \int_{y_\mathrm{i}-\alpha_\mathrm{i}}^{\infty} \mathrm{d}z_\mathrm{i}\, e^{-(z_\mathrm{i}-y_\mathrm{i})/2} E_\mathrm{in}(z_\mathrm{i}) - \int_{y_{\mathrm{i}-1}+\alpha_{\mathrm{i}-1}}^{\infty} \mathrm{d}z_\mathrm{i}\, e^{-(z_\mathrm{i}-y_\mathrm{i})/2} E_\mathrm{in}(z_\mathrm{i}) \\
&\quad = e^{\alpha_\mathrm{i}/2} \int_0^\infty \mathrm{d}z_\mathrm{i}\, e^{-z_\mathrm{i}/2} E_\mathrm{in}(z_\mathrm{i} + y_\mathrm{i} - \alpha_\mathrm{i}) \\
&\qquad - e^{(y_\mathrm{i}-y_{\mathrm{i}-1}-\alpha_{\mathrm{i}-1})/2} \int_0^\infty \mathrm{d}z_\mathrm{i}\, e^{-z_\mathrm{i}/2} E_\mathrm{in}(z_\mathrm{i} + y_{\mathrm{i}-1} + \alpha_{\mathrm{i}-1}) \\
&\quad \equiv e^{\alpha_\mathrm{i}/2} \Big\{ E_\mathrm{out}(y_\mathrm{i} - \alpha_\mathrm{i}) - e^{(y_\mathrm{i}-y_{\mathrm{i}-1})/2} e^{-(\alpha_\mathrm{i}+\alpha_{\mathrm{i}-1})/2} E_\mathrm{out}(y_{\mathrm{i}-1} + \alpha_{\mathrm{i}-1}) \Big\}
\end{aligned} \tag{3.14}$$

Here we defined $E_\mathrm{out}(y) = \int_0^\infty \mathrm{d}z \exp(-z/2) E_\mathrm{in}(z+y)$, which is the key building block of the outgoing wave function, hence the name.

Now we have enough to solve our particular problem. We insert the Green's function (3.12) into (3.13), plug in (3.14) for every integral and get the outgoing wave function

$$\begin{aligned}
\Psi(y_1, \ldots, y_N) =& \partial_{\alpha_1} \ldots \partial_{\alpha_N} e^{-(\alpha_1+\cdots+\alpha_N)/2} E_\mathrm{out}(y_1 - \alpha_1)\Big|_{\alpha_1=0} \\
&\times \prod_{\mathrm{i}=2}^{N} \Big\{ E_\mathrm{out}(y_\mathrm{i} - \alpha_\mathrm{i}) - e^{(y_\mathrm{i}-y_{\mathrm{i}-1})/2} e^{-(\alpha_\mathrm{i}+\alpha_{\mathrm{i}-1})/2} E_\mathrm{out}(y_{\mathrm{i}-1} + \alpha_{\mathrm{i}-1}) \Big\}\Big|_{\alpha_\mathrm{i}=0}.
\end{aligned} \tag{3.15}$$

Remember, due to the structure of the Green's function, this is the outgoing wave function in the $y_1 \geq \cdots \geq y_N$ sector. Nevertheless, it is readily extended onto $\mathbb{R}^N$ by symmetrisation, and we will do so later for many examples.

3.2 Multiple Scatterer

After the exhaustive discussion of the Dicke model, it is time to consider the first generalisations to it. For this, we will add additional atoms to our Hamiltonian. Hence, it now reads

$$H = \sum_{\nu=\pm} \int \mathrm{d}x\, b_\nu^\dagger(x)(-i\nu\partial_x) b_\nu(x) + \sum_{\mathrm{i}=1}^{M} c_\nu \big(e^{-i\nu k_0 x_\mathrm{i}} b_\nu(x_\mathrm{i}) a_\mathrm{i}^\dagger + e^{i\nu k_0 x_\mathrm{i}} b_\nu^\dagger(x_\mathrm{i}) a_\mathrm{i} \big). \tag{3.16}$$

For $c_- = 1$ and $k_0 x_\mathrm{i} \ll 1$ this represents the Hamiltonian discussed in chapter 2. There, we already discussed why we are only able to treat the single excitation subspace analytically. Here, on the other hand, we want to consider the fully chiral system, for which we can derive the full eigenbasis of the Hamiltonian.

Thus, as in the Dicke model before, we will set $c_- = 0$, i.e., we neglect back scattering. Therefore, we will only consider right moving photons. The absence of left moving modes allows us to perform the unitary transformation $a_\mathrm{i} \mapsto e^{-i\nu k_0 x_\mathrm{i}} a_\mathrm{i}$, under which the central frequency drops out. However, the minuscule role of the central frequency does not come as a surprise, since, without backscattering, every incoming photon passes each atom exactly once. Therefore, relative phase shifts have to stay constant under the evolution. All in all, the Hamiltonian becomes

$$H = \int \mathrm{d}x\, b^\dagger(x)(-i\partial_x)b(x) + \sum_{\mathrm{i}=1}^{M} \big(b(x_\mathrm{i})a_\mathrm{i}^\dagger + b^\dagger(x_\mathrm{i})a_\mathrm{i}\big). \tag{3.17}$$

The following steps are the same as for the Dicke model. First, note that both the eigenmodes, as well as the dispersion relation, have the same forms (3.6) and (3.7) as in the single atom case, except for

$$f(y,\lambda) = \prod_{\mathrm{i}=1}^{M} \frac{\lambda - i/2\,\mathrm{sgn}(y - x_\mathrm{i})}{\lambda + i/2}.$$

Consequently, the eigenmodes do not span the Hilbert space for real λ and we have to consider string solutions again. Next, we can avoid the string summation problem again by introducing a suitable complex contour Γ and performing the λ integration alongside it. In our current case, we are even able to pinpoint Γ such that it does not depend on the initial state $|\Psi\rangle$, making (3.8) exact for every arbitrary initial state [3].

It turns out that this is the most practical way of computing general scattering events. We could, analogously to the previous section, try to derive the Green's function of the system. To this end, take the initial state $|x_1, \ldots, x_N\rangle$ with $x_1 \geq \cdots \geq x_N$ and compute its time evolution. Similarly to before, we would end up with a (photonic) Green's function of the form

$$G(x-y) = \int_\Gamma \frac{\mathrm{d}^N\lambda}{(2\pi)^N} \prod_{\mathrm{i}<\mathrm{j}} \frac{\lambda_\mathrm{i} - \lambda_\mathrm{j} + i\,\mathrm{sgn}(y_\mathrm{i} - y_\mathrm{j})}{\lambda_\mathrm{i} - \lambda_\mathrm{j} + i} \prod_{\mathrm{i}=1}^{N} \left(\frac{\lambda_\mathrm{i} - i/2}{\lambda_\mathrm{i} + i/2}\right)^{M_\mathrm{i}} e^{i\lambda_\mathrm{i}(y_\mathrm{i} - t - x_\mathrm{i})}. \tag{3.18}$$

Here M_i denotes the number of atoms to the right of the position x_i. From this, problems are emerging. When we simplified the Green's function the last time, we took advantage of the fact that there is exactly one photon in each interval $[z_{\mathrm{i}+1}, z_\mathrm{i}]$, where $z_\mathrm{i} = x_\mathrm{i} + t$. This no longer holds — just imagine two incident photons arriving at a system of at least two emitters. These photons could, in principle, be stored as atomic excitations indefinitely. We can still solve the integrals in (3.18) for given N. However, this procedure becomes increasingly tedious for growing N and, for arbitrary N, it were not possible to find a close form solution. Consequently, we will limit the oncoming discussions to the single excitation sector.

We now derive the single photon Green's function for M emitters. In fact, this is the only scattering process, which we can fully understand analytically for an arbitrary number of atoms. The discussion here would be the foundation for two and N photon scattering, which we will, however, not cover in the coming discussions. Lastly, the results derived here will be significant on their own, since, in the next chapter, we will analyse approximative schemes to describe scattering processes, where we will use the results from this section to benchmark the numerical results.

So, let us compute the Green's function (3.18) for $N = 1$. For this, we need

$$\begin{aligned}
\operatorname{Res}\left(\left[\frac{\lambda - i/2}{\lambda + i/2}\right]^M e^{-i\lambda z}, -i/2\right) &= \frac{1}{(M-1)!}\lim_{\lambda\to -i/2}\frac{\mathrm{d}^{M-1}}{\mathrm{d}\lambda^{M-1}}(\lambda - i/2)^M e^{-i\lambda z} \\
&= \frac{1}{(M-1)!}\lim_{\lambda\to -i/2}\sum_{m=0}^{M-1}\binom{M-1}{m}\left[\frac{\mathrm{d}^{M-m-1}}{\mathrm{d}\lambda^{M-m-1}}(\lambda - i/2)^M\right](-iz)^m e^{-i\lambda z} \\
&= \frac{1}{(M-1)!}\sum_{m=0}^{M-1}\binom{M-1}{m}\frac{M!}{(m+1)!}(-i)^{m+1}(-iz)^m e^{-z/2} \\
&= -iL_{M-1}^{(1)}(z)e^{-z/2}, \qquad (3.19)
\end{aligned}$$

where $L_M^{(\alpha)}(x)$ is the M-th order generalised Laguerre polynomial. Now, since $(\lambda - i/2)/(\lambda + i/2) \to 1$ as $|\lambda| \to \infty$, we cannot close the Γ contour in (3.18) due to lacking convergence of the integrand on the added sector. Naturally, we first need to extract the singular part, and doing so yields

$$\begin{aligned}
G(z) &= \int_{-\infty}^{\infty}\frac{\mathrm{d}\lambda}{2\pi}\left(\frac{\lambda - i/2}{\lambda + i/2}\right)^M e^{-i\lambda z} \\
&= \int_{-\infty}^{\infty}\frac{\mathrm{d}\lambda}{2\pi}e^{-i\lambda z} + \left[\left(\frac{\lambda - i/2}{\lambda + i/2}\right)^M - 1\right]e^{-i\lambda z} \\
&= \delta(z) + i\Theta(z)\operatorname{Res}\left\{\left[\left(\frac{\lambda - i/2}{\lambda + i/2}\right)^M - 1\right]e^{-i\lambda z}, -i/2\right\} \\
&= \delta(z) + \Theta(z)L_{M-1}^{(1)}(z)e^{-z/2}. \qquad (3.20)
\end{aligned}$$

Here we introduced the retarded coordinate $z = x_i + t - y_i$.

The single photon greens function for multiple atoms (3.20) is quite similar to the one for just a single atom (3.11), since it consists of a free propagation part and a non-trivial, exponentially decaying tail. However, on this tail, an oscillation due to the Laguerre polynomials is superimposed. Furthermore, for $M = 1$ we have $L_0^{(\alpha)}(x) = 1$, yielding the exact result from the previous section. Figure 3.3 pictures the non-trivial parts for different numbers of atoms M. With increasing M three effects emerge; namely, the

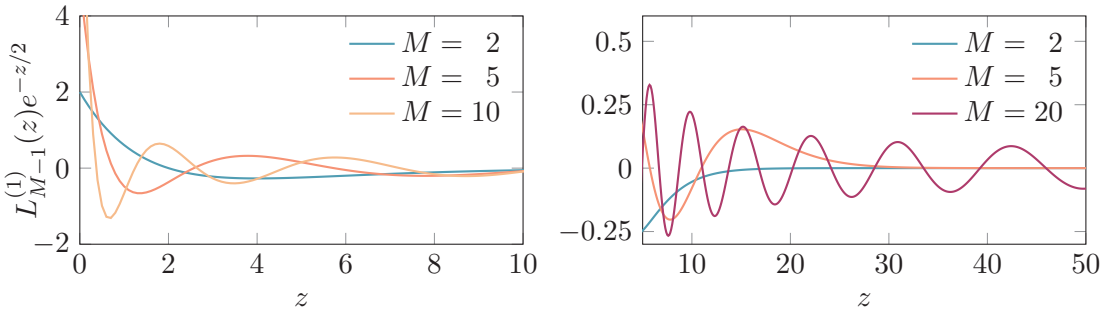

Figure 3.3.
Exponential tail of the single photon Green's function. The different lines correspond to the number n of atoms in the system. Each distribution starts with a generic delta peak at $y - x - ct = 0$. From these graphs it is evident that the atoms delay the transition of the photons, as well as broaden their distribution.

oscillations frequency close to $z = 0$ increases, as well as the number of oscillations, given by the roots of the Laguerre polynomial. Lastly, the amplitude decays much slower.

4 Approximative Methods

The previous two chapter showed us that we work right at the edge of what is analytically computable. While quantum simulators posses the ability to probe the waveguide dynamics accurately [32], we are still far from a universal quantum computer. Therefore, for the most systems, one must employ approximative or numerical schemes to describe the dynamics inside waveguide systems. For example, Pichler et al. [33, 34] applied matrix product state techniques to study the influence of retardation effects in photonic waveguides. Yet another group utilised a real-time path integral method to determine the non-Markovian contributions of spin-boson models [35].

Even so, the aforementioned methods lack in generality. In the quest for an adaptive framework, the realm of Quantum Optics provides good answers. As a frequently used technique, one considers the photonic degrees of freedom as an effective thermodynamic bath which is coupled with the waveguide emitters. One then integrates out the bath modes and ends up with an effective description for the atoms [16, 19, 36–38]. These methods rely on the Born-Markov approximation; basically, they neglect retardation effects, which is assumed to be valid if the spacing of the atoms is sufficiently small compared to the wavelength.

Which quantities can we compute under this effective approach? The *quantum regression theorem* provides the answer. We are always able to determine equal time correlation functions; however, unequal time correlation functions only obey the effective dynamics iff the photons and atoms do not become correlated. While the theorem itself is rigorous, its applicability for most systems is up to debate. In principle, one would need to analytically solve for all correlation functions of a given system to validate the conditions of the regression theorem, in which case one would no longer need it. Therefore, many authors just apply it without special care about the regimes in which it does not work.

Both in the Markovian and Non-Markovian regime, results based on the regression theorem may strongly differ from their exact form [39]. Problems emerge when considering unequal time correlation functions of order two and higher. The purpose of this chapter is to give an overview of regression theorem based approaches to waveguide QED. Then, we will compare some analytical calculations with their corresponding results stemming from these effective theories. Lastly, we will provide a short proof, which shows that the regression theorem is not applicable for most of the chiral waveguide systems, if not all, and conclude that these effective theories are therefore limited in their scope.

4.1 Quantum Regression Theorem and effective Hamiltonian

For the beginning, imagine a bipartite quantum system, consisting of an environment $\mathcal{E}$ and system $\mathcal{S}$. Suppose, at time $t = 0$ the density matrix $\varrho_{\mathcal{SE}}(0)$ of system and environment splits into a direct product

$$\varrho_{\mathcal{SE}}(0) = \varrho_{\mathcal{S}}(0) \otimes \varrho_{\mathcal{E}}(0), \tag{4.1}$$

i.e., there are no initial correlations between system and environment. Under this assumption, one can prove [40] the existence of a completely positive and trace-preserving map $\Lambda(t)$ such that

$$\varrho_{\mathcal{S}}(t) = \mathrm{Tr}_{\mathcal{E}}\left\{e^{-i\int_0^t \mathrm{d}t' H}\varrho_{\mathcal{SE}}(0)e^{i\int_0^t \mathrm{d}t' H}\right\} = \Lambda(t)[\varrho_{\mathcal{S}}(0)]. \tag{4.2}$$

Basically, this implies that we are able to study the dynamics of the system $\mathcal{S}$ without the need to consider the entire environment $\mathcal{E}$. As a consequence, we can compute operator expectation values of ***system*** observables by the same fashion. To verify this statement, we consider an operator of the form $A = A_{\mathcal{S}} \otimes \mathbb{1}_{\mathcal{E}}$. It's expectation value at time t reads

$$\langle A(t)\rangle = \mathrm{Tr}_{\mathcal{S}}\left[A_{\mathcal{S}}\,\mathrm{Tr}_{\mathcal{E}}\left\{e^{-i\int_0^t \mathrm{d}t' H}\varrho_{\mathcal{SE}}(0)e^{i\int_0^t \mathrm{d}t' H}\right\}\right] = \mathrm{Tr}_{\mathcal{S}}\left[A_{\mathcal{S}}\Lambda(t)[\varrho_{\mathcal{S}}(0)]\right].$$

The quantum regression theorem now makes a statement about unequal time correlation functions of order two or higher. Again, start with an initially uncorrelated system of the form (4.1) and consider two operators $A = A_{\mathcal{S}} \otimes \mathbb{1}_{\mathcal{E}}$ and $B = B_{\mathcal{S}} \otimes \mathbb{1}_{\mathcal{E}}$, only acting on the system. Then

$$\langle B(t_2)A(t_1)\rangle = \mathrm{Tr}_{\mathcal{S}}\left[B_{\mathcal{S}}\,\mathrm{Tr}_{\mathcal{E}}\left\{e^{-i\int_{t_1}^{t_2} \mathrm{d}t\, H}(A_{\mathcal{S}} \otimes \mathbb{1}_{\mathcal{E}})\varrho_{\mathcal{SE}}(t_1)e^{i\int_{t_1}^{t_2} \mathrm{d}t\, H}\right\}\right] \tag{4.3}$$

Now, assume that the central part of (4.3), the operator $(A_{\mathcal{S}} \otimes \mathbb{1}_{\mathcal{E}})\varrho_{\mathcal{SE}}(t_1)$, again is a density matrix, which obeys the same positive and trace-preserving map $\Lambda(t)$ as the

initial state (4.1). This is exactly the case iff $\varrho_{\mathcal{SE}}(t_1) = \varrho_{\mathcal{S}}(t_1) \otimes \varrho_{\mathcal{E}}(t_1)$. Consequently, we here assumed that under the time evolution of $\varrho_{\mathcal{SE}}(0)$ ***no correlations*** between system and environment are built up. This is the central assumption of the quantum regression theorem.

With this additional restriction, we find

3 Theorem (Quantum Regression Theorem [39, 41])

If $\varrho_{\mathcal{SE}}(t_1) = \varrho_{\mathcal{S}}(t_1) \otimes \varrho_{\mathcal{E}}(t_1)$ for all $t_1 \geq 0$, $A_\mathrm{i} = A_{\mathcal{S},\mathrm{i}} \otimes \mathbb{1}_{\mathcal{E}}$ and $\varrho_{\mathcal{S}}(t_1) = \Lambda(t_1)[\varrho_{\mathcal{S}}(0)]$ then

$$\langle A_2(t_2)A_1(t_1)\rangle_{\mathrm{qrt}} = \mathrm{Tr}_{\mathcal{S}}\left[A_{\mathcal{S},2}\Lambda(t_2,t_1)[A_{\mathcal{S},1}\varrho_{\mathcal{S}}(t_1)]\right].$$

Here the index qrt denotes, that this is the second order correlation function based on the quantum regression theorem.

We can formulate the quantum regression theorem in terms of differential equations. For us, this will be more convenient than the form of Theorem 3 when we later show that the chiral waveguide systems do not meet the conditions of the regression theorem. For this, let $\{E_\mathrm{i}\}$ be a set of operators onto the system $\mathcal{S}$ and assume their expectation values obey

$$\partial_t\langle E_\mathrm{i}(t)\rangle = \sum_\mathrm{j} G_\mathrm{ij}(t)\langle E_\mathrm{j}\rangle, \tag{4.4}$$

then

$$\partial_\tau\langle E_\mathrm{i}(t+\tau)E_\mathrm{k}(t)\rangle = \sum_\mathrm{j} G_\mathrm{ij}(\tau)\langle E_\mathrm{j}(t)E_\mathrm{k}(t)\rangle, \tag{4.5}$$

i.e., the second order correlation functions are described by the same set of equations as the first order correlation functions.

Now that we have stated the regression theorem, let us put it to use. As explained above, we want to derive an effective method to describe the emitter dynamic for Hamiltonian systems in the form of (1.11). A detailed description is given in Ref. [36] and [37]; we will just state the necessary steps. First, one solves the Heisenberg equations for the photonic operators, i.e., formally integrate

$$\partial_t b_\nu(x,t) = i[H, b_\nu(x,t)].$$

Next, one does the same for the atomic operators a_i. There, retarded atomic operators $a_\mathrm{i}(t-|x_\mathrm{i}-x_\mathrm{j}|)$ emerge, for which we employ the Markov approximation

$$a_\mathrm{i}(t-|x_\mathrm{i}-x_\mathrm{j}|) \approx a_\mathrm{i}(t)e^{ik_0|x_\mathrm{i}-x_\mathrm{j}|}. \tag{4.6}$$

This in turn, allows one to define the effective Hamiltonian

$$H_\mathrm{eff} = H_\mathrm{at} - \frac{i}{2}\sum_{\mathrm{i,j}} a_\mathrm{i}^\dagger a_\mathrm{j} e^{ik_0|x_\mathrm{i}-x_\mathrm{j}|} \tag{4.7}$$

for the emitters. Notice, the fully chiral case restricts the latter sum to i $\geq$ j.

At this point, the quantum regression theorem comes into play for the first time. Quantities like $\langle a_{\mathrm{i}}(t)a_{\mathrm{j}}(t)\rangle$ can be computed exactly (in the Markov sense) by the effective Hamiltonian (4.7). However, unequal time correlators like $\langle a_{\mathrm{i}}(t_2)a_{\mathrm{j}}(t_1)\rangle$ are only exact under evolution with H_{eff}, if the quantum regression theorem applies. However, these unequal time correlators are of great importance, since they enable us to compute the Green's function

$$G(t_1,\ldots,t_N,t_1',\ldots,t_N') \equiv \langle 0|\, b_+(x_M,t_1)\ldots b_+(x_M,t_N)b_+^\dagger(x_1,t_1')\ldots b_+^\dagger(x_1,t_N')\,|0\rangle\ , \tag{4.8}$$

where x_1 and x_M are the coordinates of the left- and rightmost atoms, respectively. Notice, for $\tau > 0$ we have $b(x_M,t) = b(x_M+\tau,t+\tau)$ and $b(x_1,t) = b(x_1-\tau,t-\tau)$, due to the free propagation of the photons in the regions $x > x_M$ and $x < x_1$. By this, we can rewrite (4.8) in the conventional form

$$\begin{aligned} G(y_1,\ldots,y_N,y_1',\ldots,y_N') &\equiv \langle 0|\, b_+(y_1,t_2)\ldots b_+(y_N,t_2)b_+^\dagger(y_1',t_1)\ldots b_+^\dagger(y_N',t_1)\,|0\rangle \\ &= \big\langle y_1\ldots y_N\big|U(t_2,t_1)\big|y_1'\ldots y_N'\big\rangle\ , \end{aligned} \tag{4.9}$$

with $y_i \geq x_M$ and $y_i' \leq x_1$.

In the effective dynamic, mediated by the effective Hamiltonian (4.7), we only have access to the atomic operators a_{i}. However, the photonic creation and annihilation operators are related to the atomic ones by the relation

$$\begin{aligned} b_\nu(x,t) &= b_\nu(x-\nu t) - i\sum_{\mathrm{i}=1}^{M}\Theta(\nu(x-x_{\mathrm{i}}))a_{\mathrm{i}}(t-\nu(x-x_{\mathrm{i}})) \\ &\approx b_\nu(x-\nu t) - i\sum_{\mathrm{i}=1}^{M}\Theta(\nu(x-x_{\mathrm{i}}))a_{\mathrm{i}}(t)e^{i\nu k_0(x-x_{\mathrm{i}})} \end{aligned} \tag{4.10}$$

for $x > x_M$ as shown by Caneva et al. [37]. Through this replacement formula and the quantum regression theorem, we can eliminate the photonic operators from Equation (4.8) and get the important result

$$\begin{aligned} G^+_{\mathrm{qrt}}(t_1,\ldots,t_N,t_1',\ldots,t_N') =& \mathcal{T}\ \langle 0|\, a(t_1)\ldots a(t_N)a^\dagger(t_1')\ldots a^\dagger(t_N')\,|0\rangle \\ &+ \mathcal{O}\Big(\Big[b_+(x_M-t_{\mathrm{i}}),b_+^\dagger(x_1-t_{\mathrm{j}}')\Big]\Big). \end{aligned} \tag{4.11}$$

where we introduced the time ordering operator $\mathcal{T}$ and defined the collective operator

$$a(t) = \sum_{\mathrm{i}=1}^{M} a_{\mathrm{i}}(t)e^{i\nu k_0(x-x_{\mathrm{i}})}.$$

The index qrt again stems from the fact that we perform each time propagation in Equation (4.11) with the effective time evolution operator $\exp(-iH_{\text{eff}}t)$. We emphasise, this is exact only if no correlations between the photons and atoms are created under the full time evolution. Obviously, there are terms, which stem from the $[b_\nu(x_M, t_\text{i}), b^\dagger_\nu(x_1, t'_\text{j})]$ commutator. However, for compactness, we did not explicitly write them down here, but we will keep them in later examples.

Comparison with Exact Results 4.2

The result (4.11) provides a method for exact computations, while it also enables to perform efficient and exact numerics — within the realm of the Markov approximation and the applicability of the regression theorem. For example, if we consider an initial state of N excitations, the total dimension of all relevant sectors in the atomic Hilbert space is

$$\sum_{\text{n}=1}^{N} \binom{M}{n},$$

where M is the number of atoms. This grows as $\mathcal{O}(M^N)$, allowing us to deal with a few hundred atoms in the single excitation sector.

No matter how nice this may seem, we first need to benchmark results based on (4.11) against exact computations, since it is already known, that results based on the regression theorem can wildly vary from their exact counterparts [39]. Nevertheless, for the Dicke model, Cirac et al. [36] proved that the results obtained by Equation (4.11) equal the exact results we obtained in Section 3.1. Therefore, we turn our attention to the next more complicated model, the one with multiple scatterers, discussed in Section 3.2.

We start in the single photon case but consider an arbitrary number of atoms M. Assume that at time $t = 0$ the photon arrives at $x = x_1$, the first atom. We compute the transition amplitude to find the photon after a time t at $x = x_M$, right after the last atom. This equals the Green's function (3.20) for $z = x_1 + t - x_M$. Now, let us perform the computation under the approximations mentioned above. We start with the Green's function (4.8) and use the identity (4.10)

$$\begin{aligned} G_{\text{qrt}}(t) &= \left\langle 0 \middle| b_+(x_M, t) b^\dagger_+(x_1) \middle| 0 \right\rangle \\ &= \left\langle 0 \middle| \left(b_+(x_M - t) - ia(t)\right) b^\dagger_+(x_1) \middle| 0 \right\rangle \\ &= \delta(z) - i \left\langle 0 \middle| a(t) \left(b^\dagger_+(x_M, x_M - x_1) + ia^\dagger(\underbrace{x_M - x_1}_{\equiv t'}) \right) \middle| 0 \right\rangle \\ &= \delta(z) + \mathcal{T} \left\langle 0 \middle| a(t) a^\dagger(t') \middle| 0 \right\rangle . \end{aligned} \tag{4.12}$$

Here, we used relation (4.10) twice, first to express the outgoing photon operator by the atomic operators and then to map the incoming photon onto the outgoing operators. For $t < x_M - x_1$ it is clear that the photon cannot have left the atomic system for which $a(t)$ trivially commutes with the operator to the right, while for $t > x_M - x_1$ the introduced creation operator $b_+^\dagger(x_M, x_M - x_1)$ commutes with $a(t)$ [37]. Lastly, we defined $t' = x_M - x_1$ to shorten the notation.

4.2.1 Superradiance in the Non-Chiral System

Our first example will be the scattering of a single photon at M non-chiral atoms. Since we mainly take an interest in how this compares to the results we found in Chapter 2, we initially consider $k_0 x_\mathrm{i} \approx 0$ for all i. With this, we compute the single photon Green's function (4.12)

$$\begin{aligned}
\sum_{\mathrm{ij}} \langle 0|\, a_\mathrm{i}(t) a_\mathrm{j}^\dagger(t')\, |0\rangle &= \sum_{\mathrm{ij}} \langle 0|\, a_\mathrm{i} e^{-iH_\mathrm{eff}(t-t')} a_\mathrm{j}^\dagger\, |0\rangle \\
&= \sum_{n=0}^{\infty} \frac{(-(t-t'))^n}{n!} \sum_{\mathrm{ij}} \langle 0|\, a_\mathrm{i} \left(\sum_{kl} a_k^\dagger a_l \right)^n a_\mathrm{j}^\dagger\, |0\rangle \\
&= \sum_{n=0}^{\infty} \frac{(-(t-t'))^n}{n!} \sum_{\mathrm{ij}} \left(\prod_{m=1}^{n} \sum_{k_m l_m} \right) \langle 0|\, (a_\mathrm{i} a_{k_1}^\dagger)(a_{l_1} a_{k_2}^\dagger) \dots (a_{l_n} a_\mathrm{j}^\dagger)\, |0\rangle \\
&= \sum_{n=0}^{\infty} \frac{(-(t-t'))^n}{n!} \sum_{\mathrm{ij}} \left(\prod_{m=1}^{n} \sum_{k_m l_m} \right) \langle 0|\, (a_{k_1}^\dagger a_\mathrm{i} + \delta_{\mathrm{i},k_1}) \dots (a_\mathrm{j}^\dagger a_{l_n} + \delta_{l_n,\mathrm{j}})\, |0\rangle \\
&= M \sum_{n=0}^{\infty} \frac{(-M(t-t'))^n}{n} \\
&= M \exp\left(-M(t-t')\right). \qquad (4.13)
\end{aligned}$$

Remembering that $z = x_M + t - x_1 = t - t'$ we find exactly the superradiance effect discussed in Chapter 2, giving hope that the approximative schemes from the Markov approach fit the theory quite well. However, as we have seen with the earlier result (2.12), the exact Green's function in the $k_0 x_\mathrm{i} \approx 0$ limit still depends on the atomic position due to the photon field, while the upper result under the same approximation is independent of x_i.

For this fact, let us have a closer look at the underlying non-chiral dynamics mediated by the effective Hamiltonian (4.7). Other than in the exact calculations we can even compute the Green's function for $k_0 x_\mathrm{i} \neq 0$. This task will still be a little cumbersome, so we again restrict us to just two emitters, which, also allows us to better compare the result with the previous one (2.12). For the non-trivial part of the Green's function, we find

$$
\begin{aligned}
G_{\mathrm{qrt}}(z) - \delta(z) &= \langle 0| \sum_{\mathrm{ij}} a_{\mathrm{i}}(t) a_{\mathrm{j}}^{\dagger}(t') e^{ik_0 x_0(\mathrm{i}-\mathrm{j})} |0\rangle \\
&= \langle 0| \sum_{\mathrm{ij}} a_{\mathrm{i}} e^{-iH_{\mathrm{eff}} z} a_{\mathrm{j}}^{\dagger} e^{ik_0 x_0(\mathrm{i}-\mathrm{j})} |0\rangle \\
&= \sum_{n=0}^{\infty} \frac{(-z/2)^n}{n!} \sum_{\mathrm{ij}} e^{ik_0 x_0(\mathrm{i}-\mathrm{j})} \langle 0| a_{\mathrm{i}} \left(a_{-1}^{\dagger} a_{-1} + e^{ik_0 x_0} (a_{-1}^{\dagger} a_1 + a_1^{\dagger} a_{-1}) + a_1^{\dagger} a_1 \right)^n a_{\mathrm{j}}^{\dagger} |0\rangle \\
&\equiv \sum_{n=0}^{\infty} \frac{(-z/2)^n}{n!} \sum_{ij} e^{ik_0 x_0(\mathrm{i}-\mathrm{j})} P_{\mathrm{ij}}^{(n)}. \qquad (4.14)
\end{aligned}
$$

We used $x_{\mathrm{i}} \equiv x_0 \cdot \mathrm{i}$, $\mathrm{i} \in \{\pm 1\}$. Thus, to determine the Green's function for this two atom model, we need to find an exact representation for the series of matrices P_{ij}^n. The next two Lemmas will help us with this.

1 Lemma

$P_{\mathrm{i,j}}^{(n)}$ has the recurrence relation

$$P_{\mathrm{i,j}}^{(n)} = P_{\mathrm{i,-j}}^{(n-1)} e^{ik_0 x_0} + P_{\mathrm{i,j}}^{(n-1)}$$

with the initial value $P_{\mathrm{i,j}}^0 = \delta_{\mathrm{i,j}}$.

Proof

$$
\begin{aligned}
P_{\mathrm{i,j}}^{(n)} &= \langle 0| a_{\mathrm{i}} \left(a_{-1}^{\dagger} a_{-1} + a_{-1}^{\dagger} a_1 e^{ik_0 x_0} + a_1^{\dagger} a_{-1} e^{ik_0 x_0} + a_1^{\dagger} a_1 \right)^n a_{\mathrm{j}}^{\dagger} |0\rangle \\
&= \langle 0| a_{\mathrm{i}} \left(a_{-1}^{\dagger} a_{-1} + a_{-1}^{\dagger} a_1 e^{ik_0 x_0} + a_1^{\dagger} a_{-1} e^{ik_0 x_0} + a_1^{\dagger} a_1 \right)^{n-1} (a_{-\mathrm{j}}^{\dagger} e^{ik_0 x_0} + a_{\mathrm{j}}^{\dagger}) |0\rangle \\
&= P_{\mathrm{i,-j}}^{(n-1)} e^{ik_0 x_0} + P_{\mathrm{i,j}}^{(n-1)}.
\end{aligned}
$$

For $n = 0$ we have $\langle 0| a_i a_j^{\dagger} |0\rangle = \langle 0| (a_{\mathrm{j}}^{\dagger} a_{\mathrm{i}} + \delta_{\mathrm{i,j}}) |0\rangle = \delta_{\mathrm{i,j}}$, by invoking the spin-1/2 algebra of the atomic operators. ■

2 Lemma

The closed-form representation of $P_{\mathrm{i,j}}^{(n)}$ reads

$$P_{\mathrm{i,j}}^{(n)} = \sum_{m=0}^{n} \binom{n}{m} e^{ik_0 x_0 m} \delta_{\mathrm{i},(-\mathrm{j})^m},$$

where $(-\mathrm{j})^k = \mathrm{j}$ for k even and $(-\mathrm{j})^k = -\mathrm{j}$ for an odd k.

Proof We will prove by induction. Notice that the induction start was already done in Lemma 1. Now, assuming Lemma 2 holds for one n we have

$$\begin{aligned}
P_{\mathrm{i,j}}^{(n+1)} &\overset{\text{Lem.1}}{=} P_{\mathrm{i},-\mathrm{j}}^{(n)} e^{ik_0x_0} + P_{\mathrm{i,j}}^{(n)} \\
&= \sum_{m=0}^{n} \binom{n}{m} e^{ik_0x_0(m+1)} \delta_{\mathrm{i},(-\mathrm{j})^{m+1}} + \sum_{m=0}^{n} \binom{n}{m} e^{ik_0x_0m} \delta_{\mathrm{i},(-\mathrm{j})^m} \\
&= \sum_{m=1}^{n+1} \binom{n}{m-1} e^{ik_0x_0m} \delta_{\mathrm{i},(-\mathrm{j})^m} + \sum_{m=0}^{n} \binom{n}{m} e^{ik_0x_0m} \delta_{\mathrm{i},(-\mathrm{j})^m} \\
&= e^{ik_0x_0(n+1)} \delta_{\mathrm{i},(-\mathrm{j})^{n+1}} + \delta_{\mathrm{i,j}} + \sum_{m=1}^{n} \left[\binom{n}{m-1} + \binom{n}{m} \right] e^{ik_0x_0m} \delta_{\mathrm{i},(-\mathrm{j})^m} \\
&= e^{ik_0x_0(n+1)} \delta_{\mathrm{i},(-\mathrm{j})^{n+1}} + \delta_{\mathrm{i,j}} + \sum_{m=1}^{n} \binom{n+1}{m} e^{ik_0x_0m} \delta_{\mathrm{i},(-\mathrm{j})^m} \\
&= \sum_{m=0}^{n+1} \binom{n+1}{m} e^{ik_0x_0m} \delta_{\mathrm{i},(-\mathrm{j})^m}.
\end{aligned}$$

This concludes the proof. ■

Now we are left to evaluate the Green's function $G_{\mathrm{qrt}}(z)$ by the expression (4.14). We perform the i, j summation and first treat the two cases of $\mathrm{i} = \mathrm{j}$. Here we have $\delta_{\mathrm{i},(-\mathrm{j})^m} = (1 + (-1)^m)/2$, which brings us to

$$\begin{aligned}
\frac{1}{2} \sum_{n=1}^{\infty} \frac{(-z)^n}{n!} \sum_{m=0}^{n} \binom{n}{m} e^{ik_0x_0m} (1 + (-1)^m) &= \frac{1}{2} \sum_{n=0}^{\infty} \frac{(-z)^n}{n!} \left[(1 + e^{ik_0x_0})^n + (1 - e^{ik_0x_0})^n \right] \\
&= \frac{1}{2} \left[e^{-z(1+e^{ik_0x_0})} + e^{-z(1-e^{ik_0x_0})} \right]. \qquad (4.15)
\end{aligned}$$

Equivalently, we find for the $\mathrm{i} \neq \mathrm{j}$ part

$$\frac{1}{2} \sum_{n=1}^{\infty} \frac{(-z)^n}{n!} \sum_{m=0}^{n} \binom{n}{m} e^{ik_0x_0m} (1 - (-1)^m) = \frac{1}{2} \left[e^{-z(1+e^{ik_0x_0})} - e^{-z(1-e^{ik_0x_0})} \right]. \qquad (4.16)$$

Together, this yields the Green's function

$$G_{\mathrm{qrt}}(z) = \delta(z) + (1 + \cos k_0x_0) e^{-z(1+e^{ik_0x_0})} + (1 - \cos k_0x_0) e^{-z(1-e^{ik_0x_0})}. \qquad (4.17)$$

The result (4.17) allows us to compare the approximative method with the analytical results (2.12) from Chapter 2. Firstly, we notice that in the regression theorem based scheme the Green's function $G_{\mathrm{qrt}}(z)$ splits into two parts, namely the one with the

$1 + \cos k_0 x_0$ coefficient and the one with $1 - \cos k_0 x_0$ in front. The latter vanishes in the limit $x_0 \to 0$, in which we discussed all results. Therefore we link it to the L mode part of the Hamiltonian and drop it in the further discussion. Thus, at $x_0 \to 0$, we end up with

$$G_{\mathrm{qrt}}(z) = \delta(z) + 2e^{-2z},$$

which makes it identical in behaviour to our previous result (2.12), as we have already discussed at the beginning of this section.

Therefore, we now want to discuss $x_0 \ll 1$, but with $x_0 \neq 0$. This is the part where the two results start to drift apart. Most noticeably, splitting the $e^{ik_0 x_0}$ term in the exponent into its real and complex part yields a decay rate of $1 + \cos k_0 x_0$ and an oscillation frequency of $\sin k_0 x_0 \lesssim k_0 x_0$. Hence, the decay rate in the numerical approximation is at most 2, but always bounded from above, while, in the exact results, the decay rate decreases from much larger values to its exact limit of 2. Next, we always have a finite oscillation frequency in the approximative approach, no matter how small x_0 becomes, which distinguishes itself the most from our exact result, where oscillations are suppressed by symmetry.

4.2.2 The fully Chiral Case

Now, after we have discussed the non-chiral case, let us investigate a system of M non-chiral emitter. Surprisingly, even though this system is obviously more restrictive, its discussion is far more complicated. Furthermore, here we will see the regression theorem based approach fails at large scales. As previously discussed, if the regression theorem applies to these systems, we may evolve (4.12) with the effective Hamiltonian (4.7). Now, remember, we had

$$a(t) = \sum_{\mathrm{i}=1}^{M} a_{\mathrm{i}}(t)$$

in the chiral case. Thus, we determine the expectation value in (4.12) to

$$\begin{aligned}
\sum_{\mathrm{ij}} \langle 0|\, a_{\mathrm{i}}(t) a_{\mathrm{j}}^\dagger(t')\, |0\rangle &= \sum_{\mathrm{ij}} \langle 0|\, a_{\mathrm{i}} e^{-iH_{\mathrm{eff}} z} a_{\mathrm{j}}^\dagger\, |0\rangle \\
&= \sum_{n=0}^{\infty} \frac{(-z/2)^n}{n!} \sum_{\mathrm{ij}} \langle 0|\, a_{\mathrm{i}} \left(\sum_{\mathrm{k} \geq m} a_{\mathrm{k}}^\dagger a_m \right)^n a_{\mathrm{j}}^\dagger\, |0\rangle \\
&\equiv \sum_{n=0}^{\infty} \frac{(-z/2)^n}{n!} \sum_{\mathrm{ij}} P_{\mathrm{i,j}}^{(n)},
\end{aligned} \tag{4.18}$$

where we used the earlier defined $z = x_M + t - x_1 = t - t'$. Similarly to Equation (4.14), we introduced the matrix $P_{\mathrm{ij}}^{(n)}$. However, it differs from this previous definition since the (k, m)-summation here is restricted to $k \geq m$.

Apparently, the first hurdle will be the computation of the expectation value

$$P_{\mathrm{i,j}}^{(n)} = \langle 0|\, a_{\mathrm{i}} \left(\sum_{\mathrm{k} \geq m} a_{\mathrm{k}}^{\dagger} a_m \right)^n a_{\mathrm{j}}^{\dagger}\, |0\rangle \ . \tag{4.19}$$

First and foremost, $P_{\mathrm{i,j}}^{(n)} = 0$ for $\mathrm{i} < \mathrm{j}$, since the action of the Hamiltonian transports atomic excitations only towards x_M, i.e., in increasing directions in the indices. Additionally, $P_{\mathrm{i,j}}^{(n)}$ does not depend on i and j independently, but only on $\Delta \equiv \mathrm{i} - \mathrm{j}$. This again is due to the chirality; since the Hamiltonian does not contain terms which can bring an excitation from the positive to the negative side in position space, it is completely irrelevant if there is any atom in front of the i-th or behind the j-th one. The only atoms, which contribute to the dynamics, are therefore the ones in between the j-th and i-th. We thus rewrite

$$\sum_{\mathrm{ij}} P_{\mathrm{i,j}}^{(n)} = \sum_{\Delta=0}^{M} (M - \Delta) P_{n,\Delta}, \tag{4.20}$$

where $(M - \Delta)$ is the number of different (i, j) configurations with $\Delta = \mathrm{i} - \mathrm{j}$.

Now, we need to think up ways to evaluate $P_{n,\Delta}$. For this, we recast the problem onto a path counting problem, which will turn out to be both an elegant and practical abstraction of the initial problem. Imagine a state like

$$\sum_m a_{\mathrm{k}}^{\dagger} a_m a_{\mathrm{j}}^{\dagger}\, |0\rangle = \sum_m \delta_{m\mathrm{j}} a_{\mathrm{k}}^{\dagger}\, |0\rangle = a_{\mathrm{k}}^{\dagger}\, |0\rangle \ .$$

We can say that, under the action of the operator $\sum_m a_{\mathrm{k}}^{\dagger} a_m$, the excitation jumped from $a_{\mathrm{j}}^{\dagger}\, |0\rangle$ to $a_{\mathrm{k}}^{\dagger}\, |0\rangle$. In (4.19) there are n such jump operators. Since we sum over all possible outcomes of these jumps we are actually counting the number of paths from $a_{\mathrm{j}}^{\dagger}\, |0\rangle$ to $a_{\mathrm{i}}^{\dagger}\, |0\rangle$ within n steps and without dropping in "height".

We illustrated the path counting problem in Figure 4.1. Here, every orange line pictures a possible segment of one of the overall paths. From this graphical representation, the useful recurrence relation

$$P_{n,\Delta} = \sum_{\Delta'=0}^{\Delta} P_{n-1,\Delta'} \tag{4.21}$$

immediately follows, which is readily proven by the exact expression (4.19). In a second we will argue how $P_{n,\Delta}$ has to look like and then prove this claim by showing that it obeys (4.21).

Notice, within each jump, j may change by any number between 0 and Δ, which presents the major hurdle for this problem. If j may only increase by 1 per layer, then the problem is trivial: We need to distribute Δ climbing events in n total events, yielding

$$\tilde{P}_{n,\Delta} = \binom{n}{\Delta}.$$

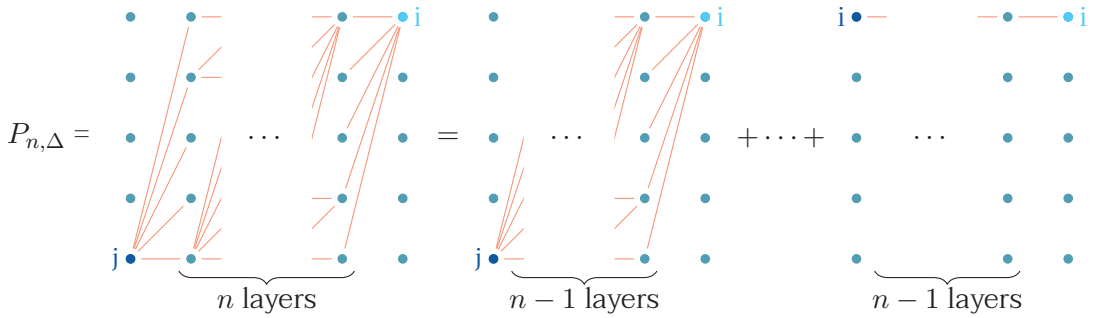

Figure 4.1.
Illustration of the path counting problem. For $P_{n,\Delta}$ we need to count every path connecting j to i, which never drops in height, here marked in violet. Furthermore, the idea behind the recurrence relation (4.21) immediately follows just from visual inspection: all paths from j to i through n layers can be put together by cutting off the first layer and considering every contribution by its own.

Here, the tilde indicates that we are only allowing paths which climb at most one lattice site at a time.

Yet, our graphs may climb multiple lattice sites per step. However, we can imagine the processes in which an excitation jumps over m atomic positions as m single jumps after introducing $m-1$ additional, virtual layers. For a general network with n intermediate layers and a height of Δ we consequently need to introduce $\Delta-1$ hidden layers to flatten out the paths. This is illustrated for the example $n=1$ and $\Delta=2$ in Figure 4.2. If this claim is valid, we have

$$P_{n,\Delta} = \tilde{P}_{n+\Delta,\Delta} = \binom{n+\Delta}{\Delta}. \tag{4.22}$$

Notice, at $\tilde{P}$ we wrote $n+\Delta$ instead of $n+\Delta-1$, since, per definition, $\tilde{P}$ also counts the final layer, whereas $P_{n,\Delta}$ only considered the n inner layers.

The hypothesis (4.22) still has to be proven. For this, just verify that it solves the recurrence relation (4.21). Since this is a linear equation, we are free to rescale any solution with an arbitrary multiplier. However, we can readily verify that (4.22) already yields the correct boundary values $P_{0,\Delta}=1$. Thus, we have found the proper solution to Equation (4.21).

Next, we need to compute the expectation value $\sum_{\mathrm{ij}} P^{(n)}_{\mathrm{i,j}}$ from (4.20). A quick evalua-

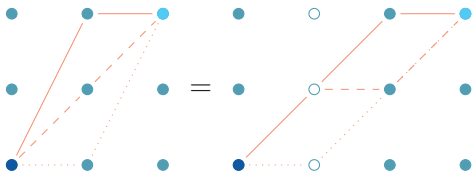

Figure 4.2.
The introduction of hidden layers allows us to fix the jump height to 1. Here we pictured the example $n = 1$ and $\Delta = 2$ and marked all allowed paths in the original problem and after the introduction of one hidden layer, marked by empty circles. Both path problems have a matching number of solutions, however, just from this graphical representation, it is not obviously true that this holds for all pairs (n, Δ).

tion with Mathematica reveals

$$\sum_{\mathrm{ij}} P^{(n)}_{\mathrm{i,j}} = \binom{M+n+1}{M-1}. \tag{4.23}$$

Finally, we are able to calculate the non-trivial part (4.13) of the Green's function (4.12). The solution takes the form of the hypergeometric function of the first kind, which again, can be expressed as a generalized Laguerre polynomial times an exponential function

$$G_{\mathrm{qrt}}(z) = \delta(z) + \Theta(z) L^{(2)}_{M-1}(z/2) e^{-z/2}. \tag{4.24}$$

This result, obtained through the Markov approximation and the application of the quantum regression theorem looks tolerably close to the exact result (3.20). However, it fails at two points. Firstly, the parameter α of the generalized polynomial happens to be 2 instead of the correct $\alpha = 1$. Next and more importantly, the argument of the Laguerre polynomial scales with a factor of $1/2$, making the Green's function decaying too fast compared to the exact results. Only for $M = 1$, where $L^{(\alpha)}_0(z) = 1$ is both independent of α and z the regression theorem yields the correct result, as already proven in full generality by Shi et al. [36]. Otherwise, both solutions differ qualitatively quite a lot, as Figure 4.3 reveals.

4.3 Invalidity of the Regression Hypothesis

Lastly, we show in full generality that the regression theorem does not apply to generic chiral waveguide systems. For this purpose, we use the differential form (4.5) and show that such a decomposition is generally not possible. We want to restrict the proof to

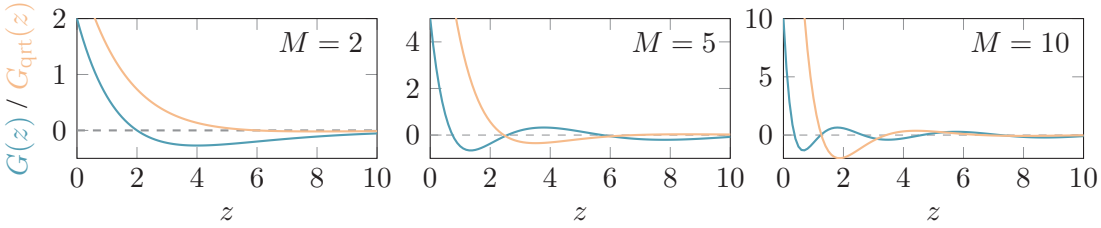

Figure 4.3.
Exact Green's function (3.20) versus the approximative Green's function (4.24) for different number of atoms. The approximative results have much larger amplitudes for small values z, while they decay faster for increasing z.

quantities of physical interests to us, i.e., we will only study photonic Green's functions

$$G(\tau) = \langle 0|\, b_+(x_M) e^{iH\tau} b_+^\dagger(x_1)\, |0\rangle \,. \tag{4.25}$$

In fact, we computed this quantity both for the chiral and non-chiral case in the last section and thus, in principle, disproved the applicability of the regression theorem for all cases. Yet, the upcoming general treatment will directly reveal the underlying problem that prohibits the use of the regression theorem.

The Green's function (4.25) obviously vanishes for $\tau < x_M - x_1$, and thus we consider only $\tau > x_M - x_1$. We demand a strict inequality to avoid pesky, but otherwise unimportant boundary terms. Now, start to evaluate Equation (4.5) for the choice of operators (4.25)

$$\begin{aligned}\partial_\tau \langle 0|\, b_+(x_M,\tau) b_+^\dagger(x_1)\, |0\rangle &= \partial_\tau \langle 0| \left(b_+(x_M - \tau) - i \sum_{\mathrm{i}=1}^{M} a_i(\tau - x_M + x_{\mathrm{i}}) \right) b_+^\dagger(x_1)\, |0\rangle \\ &= -i \sum_{\mathrm{i}=1}^{M} \partial_\tau \langle 0|\, a_i(\tau - x_M + x_{\mathrm{i}}) b_+^\dagger(x_1)\, |0\rangle \,. \end{aligned} \tag{4.26}$$

Here, we used the relation (4.10) to express the time evolved photonic annihilation operator by a time-independent one and atomic operators. Since $\tau > x_M - x_1$ we can just commute the remaining photonic operators. Next, we need the identity

$$\dot{a}_{\mathrm{i}}(t) = -i \sum_{\nu=\pm} b_\nu(t - \nu x_{\mathrm{i}}) - \sum_{\mathrm{j}=1}^{M} a_{\mathrm{j}}(t - |x_{\mathrm{i}} - x_{\mathrm{j}}|), \tag{4.27}$$

derived in [37].

This relation allows us to perform the time derivative in (4.26). Notice, the emerging photonic terms trivially vanish, due to the restriction $\tau > x_M - x_1$ and since the $b_+^\dagger$ and b_- operators commute anyway. We end up with

$$\partial_\tau \langle 0|\, b_+(x_M,\tau) b_+^\dagger(x_1)\, |0\rangle = i \sum_{\mathrm{ij}} \langle 0|\, a_{\mathrm{j}}(\tau - x_M + x_{\mathrm{i}} - |x_{\mathrm{i}} - x_{\mathrm{j}}|) b_+^\dagger(x_1)\, |0\rangle \ . \tag{4.28}$$

Next, we again use Equation (4.10) to get

$$b_+^\dagger(x_1) = b_+^\dagger(x_M, x_M - x_1) - i \sum_{m=1}^{M} a_m^\dagger(x_m - x_1). \tag{4.29}$$

Combining the last two equations finally yields

$$\partial_\tau \langle 0|\, b_+(x_M,\tau) b_+^\dagger(x_1)\, |0\rangle = \sum_{\mathrm{ij}m} \langle 0|\, a_{\mathrm{j}}(\tau - x_M + x_{\mathrm{i}} - |x_{\mathrm{i}} - x_{\mathrm{j}}|) a_m^\dagger(x_m - x_1)\, |0\rangle \ . \tag{4.30}$$

In contrary to Equation (4.5), we did not find a relation of the form $\langle 0|\, a_{\mathrm{j}}(\tau) a_m^\dagger\, |0\rangle$. However, we now see the reasons why the regression theorem does not apply.

By employing the Markov approximation (4.6) we find

$$\partial_\tau \langle 0|\, b_+(x_M,\tau) b_+^\dagger(x_1)\, |0\rangle = \sum_{\mathrm{j}m} G_{\mathrm{j}m} \langle 0|\, a_{\mathrm{j}}(\tau) a_m^\dagger\, |0\rangle \ , \tag{4.31}$$

where we defined

$$G_{\mathrm{j}m} = \sum_{\mathrm{i}=1}^{M} \exp\Big(- ik_0 \big[x_M - x_1 - x_{\mathrm{i}} + x_m + |x_{\mathrm{i}} - x_{\mathrm{j}}| \big] \Big). \tag{4.32}$$

Surprisingly, after using the Markov approximation, the quantum regression theorem starts to apply. Therefore, the only reason why we failed in the first place, was due to the missing the retardation effects. These are the sole cause of the correlations between the spins and the photon bath. Neglecting retardations thus removes a large part of possible physical effects.

5 Multiple Photon Interactions

So far, we primarily studied single photon processes. However, the most intriguing effects emerge when investigating the effective interaction between photons, mediated by the emitters in a chiral waveguide system. We need to understand these multiphoton effects, for they give rise to novel phenomena, like pure quantum information by light [42]. This chapter will solely deal with those correlated photons in the few particle limit. To be precise, we will consider the scattering of two and three photons at a single atom.

We need to quantify the interaction between the photons. For this, we will rely on the N-th order correlation functions, which indicate whether the photons tend to "stick together". Furthermore, as discussed in Chapter 3, we can classify the eigenmodes of the Hamiltonian into free states and n-particle bound states. Thus, we can project the incoming and outgoing wave packets onto these subspaces, which gives a direct measure of how tightly the photons are bonded. Most intriguingly, we will find that for the Dicke model, those bound states have a universal form, where only the centre of mass degree of freedom is influenced by the initial conditions.

Before we now start with the derivations of all of these quantities, let us agree upon a physical picture. Imagine a photon source which spawns coherent photon pulses in the few photon regime. Then, at some later time, the pulse arrives at the superatom and the photons within the pulse interact. In the end, the photons are measured behind the emitter setup. Incidents, in which we measure N photons are then linked to the N-particle wave function. For a complete lossless dynamic this assumption is justified.

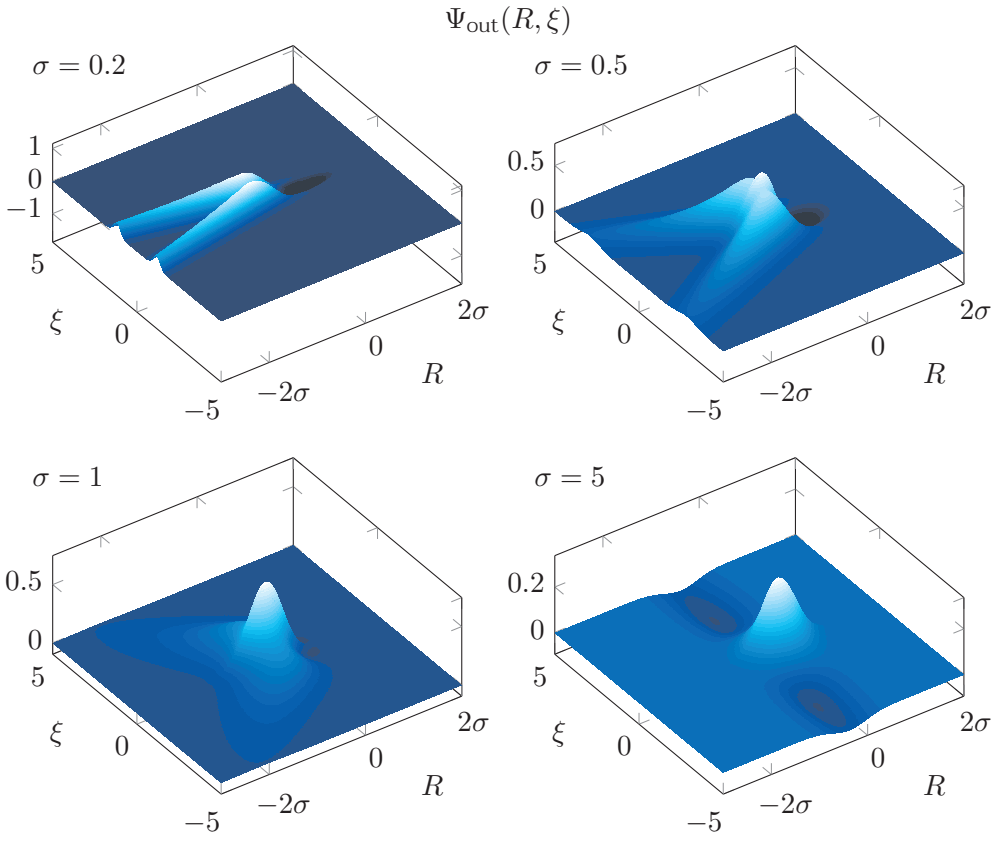

Figure 5.1.
Outgoing wave function for an initial Gaussian pulse of width σ in centre-of-mass and relative coordinates. For small widths σ the pulse shape gets quite distorted and the wave function amplitude peaks for $\xi \neq 0$, since the initial wave packet is so small that absorption with subsequent stimulated emission is unlikely. The bigger the wave packet, the likelier stimulated emission becomes, bringing the photons closely together. This is captured by the fact that the width of the outgoing wave packet in ξ direction is roughly independent from the width of the initial wave packet.

5.1 Two-Photon Scattering

Our work towards understanding multiphoton effects will start with the scattering of two photons by a single emitter. On the one hand, we need to understand the two excitation sector before we start discussing more complex systems. The methods and conclusions derived here will follow us throughout the rest of this chapter. On the other hand, the following discussions are meaningful by themselves since even the two-photon interaction is not a trivial phenomenon.

In Chapter 3, we have derived a general solution for the scattering problem of such wave functions. While we are able to perform every computation analytically, the outgoing wave function, derived with the generating functional (3.15), contains too many terms to reasonably discuss them. Thus, we shift the solution for the exact outgoing wave function into the Appendix B. Keep in mind that every result in this chapter stems from the analytical results (B.1).

For the beginning let us discuss the wave function itself. Figure 5.1 displays the outgoing wave functions of the scattered Gaussian wave packet for different widths in centre-of-mass and relative coordinates, i.e.,

$$R = \frac{x+y}{2},$$
$$\xi = \frac{x-y}{2},$$

respectively. Most noticeably, for small widths, the wave packet gets ripped apart. Classically this is explained by the short interaction time: only instances after the first photon is converted into an atomic excitation the second photon already has passed the atom, making stimulated emission impossible and the excitation must decay by spontaneous emission. This explains the exponential tail of the first graph in Figure 5.1. For larger wave packets there is enough time for stimulated emission. Thus the two-particle wave function mostly keeps its form and stays bonded in the direction of ξ.

By going to even wider wave packets, we find that the form of the outgoing wave function in the direction of the relative coordinate stops to depend on σ. We will later derive in full generality that for N incoming photons the N-particle bound state possesses a universal form in all coordinates, but the centre-of-mass coordinate. The centre-of-mass contribution on the other hand, depends on the initial wave function. We will prove this statement in the last section, after first discussing three-photon scattering. Here, we just want to motivate this result with some examples. Consider the test wave

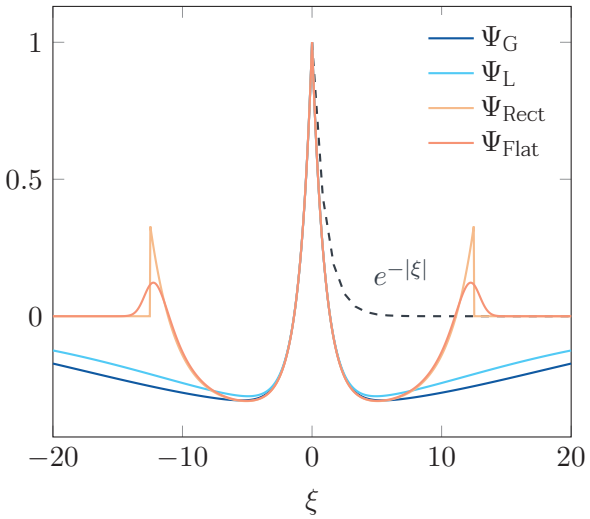

Figure 5.2.
The ξ-dependant part of different wave function at $R = 0$. Around the central peak, the relative part follows a $e^{-|\xi|}$-like distribution. Curves are for $\sigma = 20$ and, for Ψ_{Flat}, we set the parameter $s = 1$.

functions

$$\begin{aligned}
\Psi_{\text{G}}(x) &= e^{-x^2/(2\sigma^2)}, \\
\Psi_{\text{L}}(x) &= \frac{1}{(x/\sigma)^2 + 1}, \\
\Psi_{\text{Rect}}(x) &= \text{rect}(x/\sigma), \\
\Psi_{\text{Flat}}(x) &= \text{erf}(s(x + \sigma/2)) - \text{erf}(s(x - \sigma/2)).
\end{aligned}$$

We dropped the normalisation for every test function, since we will rescale the results for better comparison anyway. Here, $\text{rect}(x) = \Theta(x + \sigma/2) - \Theta(x - \sigma/2)$ denotes the rectangular function.

From all of these test functions, we construct a two-particle product wave function and then compute the outgoing wave function according to Equation (3.15). In Figure 5.2 we compare the different outgoing wave functions along the line $R = 0$. For better comparison, we rescaled all maxima to 1. Apparently, all functions have a generic behaviour around $\xi = 0$. For larger values of ξ, the functions seem to drift apart; especially Ψ_{Rect} and Ψ_{Flat} drop much faster to 0 than the initially Lorentzian and Gaussian shaped wave functions. This behaviour, however, is due to the sharp cut off both functions have at $x = \pm\sigma/2$. This cut off goes to ∞ for increasing values of σ. Thus we recover the universal dynamic in ξ even for these wave functions.

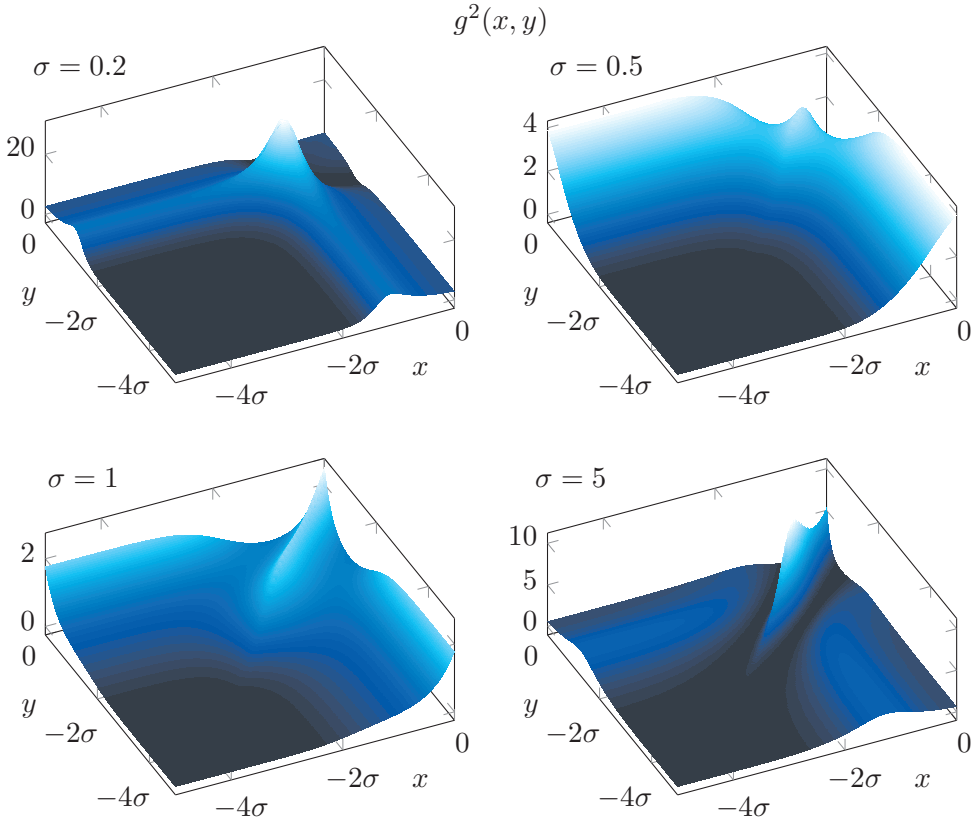

Figure 5.3.
Second order correlation function for a scattered Gaussian wave packet of two photons. For small widths σ of the initial wave function, we find that both photons leave the system uncorrelated. We find the largest correlations when one photon leaves the emitter system with some minor retardation effect,s while the other one remains in an atomic excitation state indefinitely. For growing widths, the spatial correlations between the photon increase and at $\sigma \approx 5$ one finds both photons close together most of the times.

Finally, let us discuss the $g^{(2)}$ correlation function for the stated scattering problem, which we define as

$$g^{(2)}(t,\tau) \equiv \frac{\langle \Psi_0 |\, b^\dagger(x,t) b^\dagger(x,t+\tau) b(x,t+\tau) b(x,t)\, |\Psi_0\rangle}{\langle \Psi_0 | b^\dagger(x,t) b(x,t) |\Psi_0\rangle \langle \Psi_0 | b^\dagger(x,t+\tau) b(x,t+\tau) |\Psi_0\rangle}, \tag{5.1}$$

where Ψ_0 labels the incoming wave function. Now, imagine a physical setup where the Photon detector is so far from the emitter system, that we may assume that every atomic excitation has decayed before the first photon arrives at the detector. Then we can replace $e^{-iHt}\,|\Psi_0\rangle$ by $|\Psi_{\text{out}}\rangle$, the outgoing photonic wave function, which we showed before.

Since we are now dealing with free moving photons, we may use $b(x,\tau) = b(x-\tau) \equiv b(y)$. Altogether we redefine the correlation function as

$$g^{(2)}(x,y) = \frac{\langle \Psi_{\text{out}}|\ b^\dagger(x)b^\dagger(y)b(y)b(x)\ |\Psi_{\text{out}}\rangle}{\langle \Psi_{\text{out}}|b^\dagger(x)b(x)|\Psi_{\text{out}}\rangle\langle \Psi_{\text{out}}|b^\dagger(y)b(y)|\Psi_{\text{out}}\rangle}. \tag{5.2}$$

We picture the correlation function in Figure 5.3. Here we find that for small widths σ both photons leave the emitter system uncorrelated, but with some delay. By increasing the wave function's width, the photons have enough time to interact and leave the emitter together via stimulated emission, thus increasing the amplitude of $g^{(2)}$ along the $x = y$ line. Alongside this line, the amplitude starts to dominate at around $\sigma = 1$, i.e., when the width of the wave packet becomes comparable to the mean storage time. Everything we discussed here goes hand in hand with the previous discussion about outgoing photonic wave function. Thus the $g^{(2)}$ function just gave us a new way to look at the correlation effects.

5.2 Three-Photon Scattering

Now, we turn our attention towards three-photon scattering. Genuine three photon bound states are intrinsically hard to construct and our calculations will show, that a Dicke-like system can in principle build correlations between three photons. Following the example of the last section, we compute the outgoing wave function for a Gaussian wavepacket of three photons. For the explicit solution see Appendix (B.2). The following paragraphs will analyse this scattered three-photon state under variation of the initial width.

Let us start by investigating the wave function itself. We are dealing with three photons now, for which we cannot simply display the wave function as above. However, since we are mainly interested in correlation effects between the photon positions, we transform into Jacobi coordinates

$$\begin{aligned}
\xi &= \frac{x-y}{2}, \\
\eta &= \frac{x+y}{2} - z, \\
R &= \frac{x+y+z}{3}.
\end{aligned}$$

Here ξ and η resemble generalised relative coordinates, while R is the centre-of-mass coordinate. For the forthcoming discussions, we usually set $R = 0$ and display the wave functions dependence on ξ and η along this slice through space. For example, we plotted the outgoing wave function for different initial widths σ in Figure 5.4.

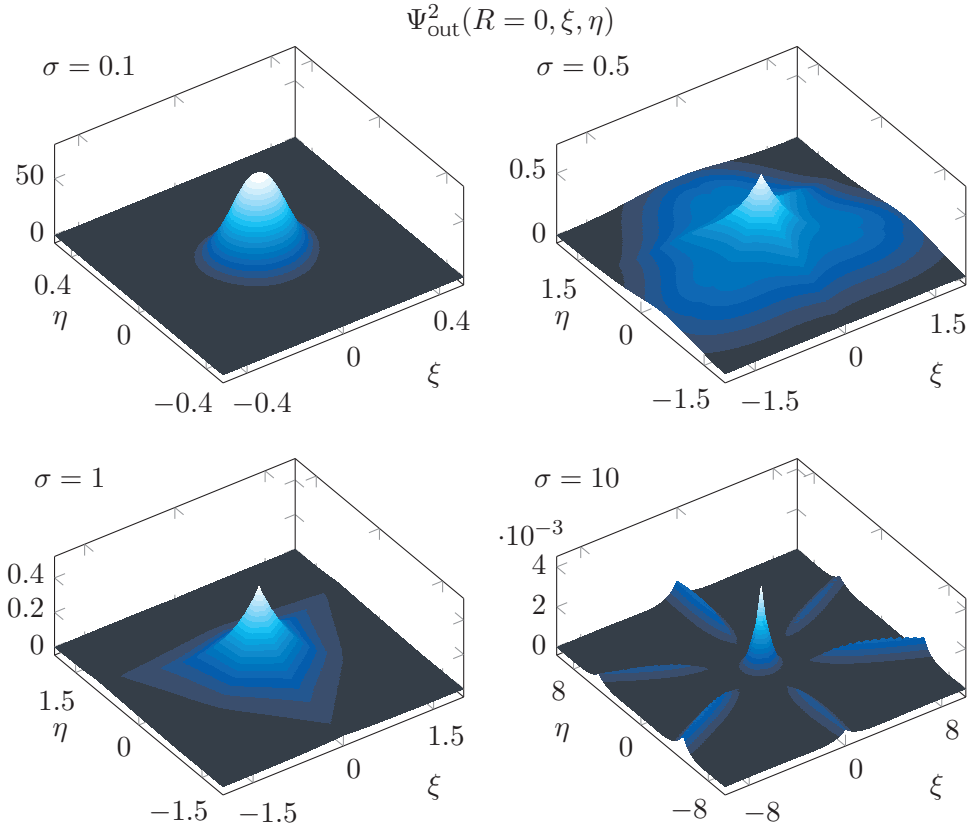

Figure 5.4.
Relative part of the three photon wave function at $R = 0$. For small widths, the relative part obeys a Gaussian form, and it is only weekly distorted by the interaction with the atoms. For wider wave packets, three symmetry lines emerge. These are along $x = y$, $x = z$ and $y = z$, corresponding to two bound photons. For even wider initial photon distributions the symmetry becomes sixfold. Lastly, the central peak emerging here converges to some fixed form. We will later identify it with a three photon bound state.

Roughly speaking, the relative part of the outgoing wave function takes three different forms depending upon the initial width σ. For $\sigma \ll 1$ it approximatively equals a Gaussian and is comparatively similar to the relative part of the incoming wave function. When the width becomes comparable to the decay rate (i.e., $\sigma \approx 1$), a three-fold rotational symmetry emerges along the lines $x = y$, $x = z$ and $y = z$, indicating that two photons enter a bound state. However, in this regime, the wave function strongly depends upon the position of the third photon. It decays much faster in the direction, where the third photon is in front of the two-photon bound state. This dependence on the third photon's position is the reason for the three-fold symmetry.

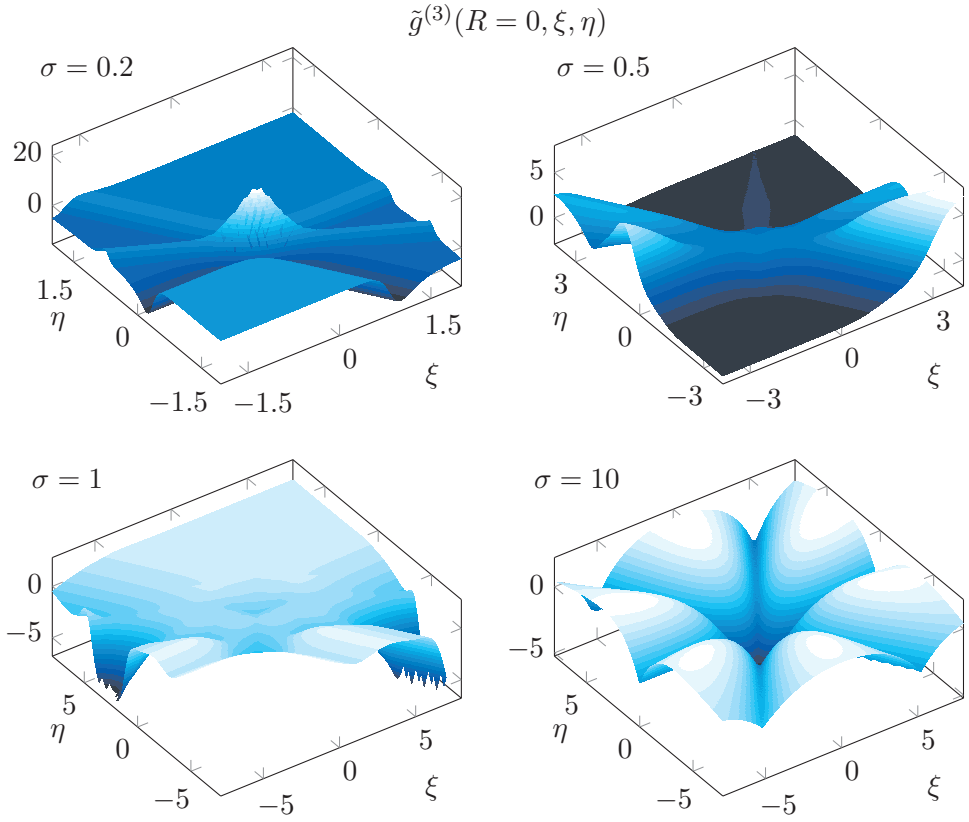

Figure 5.5.
The connected $\tilde{g}^{(3)}$ function in relative coordinates at $R = 0$ for different initial widths σ. For small widths the $g^{(2)}$ contributions cancel most of the pure $g^{(3)}$ parts and only some non-trivial features remain. With increasing width this cancellation first becomes more omnipresent, before at large values the two body correlations $g^{(2)}$ starts to dominate, such that $\tilde{g}^{(3)}$ becomes negative, revealing some non-trivial three photon correlations. The sharp drops in the $\sigma = 1$ figure stem from finite numerical floating point precision. Fixing this issue is possible by increasing the numerical precision. Yet, this makes the computations unnecessarily time expensive.

Lastly, for much larger widths σ the outgoing wave function converges to a six-fold rotational symmetric one; indicating that the position of the third photon becomes independent of the position of the two photon-bound state. Just compare this with the flanks of the last wave function in Figure 5.4. Furthermore, for increasing σ the outgoing wave function develops a central peak of constant width, which converges to some fixed function. We will later see that this peak again has a universal form and stems from the three-photon bound state contribution.

Similarly to the last section, we now want to perform the discussions via correlation

functions. To begin with, we define the three body correlation function similarly to $g^{(2)}$ as

$$g^{(3)}(x,y,z) \equiv \frac{\langle \Psi_{\text{out}}|\ b^\dagger(x)b^\dagger(y)b^\dagger(z)b(z)b(y)b(x)\ |\Psi_{\text{out}}\rangle}{\langle \Psi_{\text{out}}|b^\dagger(x)b(x)|\Psi_{\text{out}}\rangle\langle \Psi_{\text{out}}|b^\dagger(y)b(y)|\Psi_{\text{out}}\rangle\langle \Psi_{\text{out}}|b^\dagger(z)b(z)|\Psi_{\text{out}}\rangle}. \tag{5.3}$$

As we have previously noted, the wave functions appears to show features we can explain by two-particle bound states. These, however, will also yield a contribution to g^3. Thus, we introduce the *connected* correlation function

$$\tilde{g}^{(3)}(x,y,z) \equiv 2 + g^{(3)}(x,y,z) - \Big(g^{(2)}(x,y) + g^{(2)}(x,z) + g^{(2)}(y,z)\Big), \tag{5.4}$$

as in reference [43]. This quantity truly resembles genuine three-body correlations, by subtracting the possible two-body correlations from the total three-body correlation function.

We have no other option than to numerically evaluate this modified three-body correlation function, which, however, is no major hurdle due to the exact wave function (B.2). The numerical computation yields the results as presented in Figure 5.5. The exact form of $\tilde{g}^{(3)}$ appears to be highly involved, yet we can read off some general features. For the beginning, for small σ, notice that the two body contributions seem to cancel the three body effects, except on some small regions. Especially the central peak starts to vanish, indicating that the two-body and three-body effects roughly equal at $x = y = z$. For $\sigma = 1$ the cancellation becomes nearly exact everywhere. The dips in the $\sigma = 1$ figure have numerical nature and stem from the finite numerical precision. They should just be ignored. Increasing σ even further results in the two-body effects overtaking, for which $g^{(3)}$ becomes negative at the centre and along the symmetry lines. Especially the behaviour at the centre indicates that the central peak does not only stem from two body effects, otherwise we would not see any dip here.

In conclusion, we have found that the behaviour at the centre $x = y = z$ for wide initial wave functions stems from two and three photon effects. Especially the three-photon contribution seems not to vanish for large σ, again indicating the emergence of three-photon correlations. One crucial player for these correlations is three-photon bound state. Especially in the wave function picture, we asserted that the central peak partially stems from this bound state. The following and last section will validate these claims.

5.3 Universal Bound State Dynamics in the Dicke Model

For both the two and three photon scattering processes, we stated that the outgoing wave function in the $\sigma \to \infty$ limit decomposes into a relative and a centre-of-mass contribution.

Furthermore, this relative contribution is universal, i.e., it does not depend upon the form of the initial wave packet. In this final section, we want to prove this statement and give an explicit expression for the relative part of the outgoing wave function. Here, we will perform the calculation in the three-photon sector. This simplifies the discussion compared to the general case, without dropping any relevant step needed for an arbitrary number of photons. The results we derive here are readily generalised.

To do all of this, we will compute the projector onto the three-photon bound state subspace. Per definition, we consider a state to be a three-photon bound state if it's built from three-photon strings, i.e., any state of the form

$$|\Psi\rangle = \int \mathrm{d}\Lambda\, c(\Lambda)\, |\Lambda - i/2, \Lambda, \Lambda + i/2\rangle\ . \tag{5.5}$$

Consequently, the projector onto this subspace takes the form

$$P_{\mathrm{B}} = \int \mathrm{d}\Lambda\, |\Lambda - i/2, \Lambda, \Lambda + i/2\rangle\langle\Lambda - i/2, \Lambda, \Lambda + i/2|\ . \tag{5.6}$$

Now we want to explicitly compute projection for an arbitrary state $|\Psi\rangle$.

First and foremost, due to our primary interest in scattered states, we restrict the proof to purely photonic wave functions $|\Psi\rangle$ with support on $x \geq 0$, i.e., $b(y)\,|\Psi\rangle = a\,|\Psi\rangle = 0$ for $y < 0$. This assumption yields

$$\begin{aligned}
\langle\Lambda - i/2, \Lambda, \Lambda + i/2|\Psi\rangle =& \int \mathrm{d}^3y \big[1 - \mathrm{sgn}(y_1 - y_2)\big]\left[1 - \frac{\mathrm{sgn}(y_1 - y_3)}{2}\right]\big[1 - \mathrm{sgn}(y_2 - y_3)\big] \\
&\times \frac{\Lambda + i + i/2\,\mathrm{sgn}\, y_1}{\Lambda + i/2}\frac{\Lambda + i/2\,\mathrm{sgn}\, y_2}{\Lambda - i/2}\frac{\Lambda - i + i/2\,\mathrm{sgn}\, y_3}{\Lambda - 3i/2} \\
&\times e^{y_1 - y_3} e^{-i\Lambda(y_1 + y_2 + y_3)}\Psi(y_1, y_2, y_3) \\
=& 3! \int \mathrm{d}^3y\, \Theta(y_3 \geq y_2 \geq y_1)\frac{\Lambda + 3i/2}{\Lambda - 3i/2} \\
&\times e^{y_1 - y_3} e^{-i\Lambda(y_1 + y_2 + y_3)}\Psi(y_1, y_2, y_3),
\end{aligned}$$

where we used $2\Theta(-x) = 1 - \mathrm{sgn}(x)$, and that $\Psi(y_1, y_2, y_3) = \langle y_1, y_2, y_3|\Psi\rangle$ has its support on $y_i \geq 0$. Additionally, we dropped the normalisation of $|\Lambda - i/2, \Lambda, \Lambda + i/2\rangle$, which is just constant in Λ. Now we turn our attention to the full projection of $|\Psi\rangle$ onto the three-body bound states

$$\begin{aligned}
P_{\mathrm{B}}\,|\Psi\rangle =& 3!^2 \int \mathrm{d}\Lambda \int \mathrm{d}^3x \int \mathrm{d}^3y \Theta(x_3 \geq x_2 \geq x_1)\Theta(y_3 \geq y_2 \geq y_1) \\
&\times \frac{\Lambda - i - i/2\,\mathrm{sgn}\, x_1}{\Lambda - i/2}\frac{\Lambda - i/2\,\mathrm{sgn}\, x_2}{\Lambda + i/2}\frac{\Lambda + i - i/2\,\mathrm{sgn}\, x_3}{\Lambda - 3i/2} \\
&\times e^{x_1 - x_3} e^{y_1 - y_3} e^{3i\Lambda(R_x - R_y)}\Psi(y_1, y_2, y_3)\prod_{\mathrm{i}=1}^{3} r^\dagger(x_{\mathrm{i}}, \Lambda + (\mathrm{i} - 2)i)\,|0\rangle\ .
\end{aligned} \tag{5.7}$$

For brevity, we defined $R_x = (x_1 + x_2 + y_3)/3$ and analogously R_y.

So far, it's hard to read off anything from this projection, thus we will remove unphysical sectors $x_i < 0$ first. We assume $x_1 < 0$, which cancels the $\Lambda = i/2$ singularity. If $x_3 < 0$ then $x_2 < 0$ as well, for which the $\Lambda = -i/2$ singularity gets removed by the second numerator in (5.7). Otherwise, for $x_3 > 0$, the third numerator removes it. Therefore, in the $x_1 < 0$ sector only the $\Lambda = 3i/2$ singularity remains. If we can close the Λ contour below, which is the case for $R_x < R_y$, the integral vanishes trivially. Thus, we find

$$\begin{aligned} P_{\mathrm{B}} \left|\Psi\right\rangle &\propto \Theta(R_x \geq R_y) e^{x_1 - x_3} e^{-9/2(R_x - R_y)} \Psi(y_1, y_2, y_3) \\ &\leq \Theta(R_x \geq R_y) e^{x_1 - x_3} \Psi(y_1, y_2, y_3) \\ &\leq \Theta(R_x \geq R_y) e^{x_1 - 3R_y/2} \Psi(y_1, y_2, y_3). \end{aligned} \tag{5.8}$$

The last inequality stems from $R_x \geq R_y$ and $x_3 \geq x_2$, directly resulting in $x_3 \geq 3R_y/2$ for $x_1 < 0$. Since $\Psi(y_1, y_2, y_3)$ resembles a wave packet of photons, which have passed the emitter system long ago, we may assume R_y to be large in the region where the amplitude of $\left|\Psi\right\rangle$ is not minuscule. Thus, the $x_1 < 0$ region is exponentially suppressed, and we conclude that only the $x_1 > 0$ region yields a relevant contribution. Since $x_3 \geq x_2 \geq x_1$ this implies $x_{\mathrm{i}} > 0$ for all i.

Bringing the results from the previous paragraph together this simplifies the projection (5.7) to

$$\begin{aligned} P_{\mathrm{B}} \left|\Psi\right\rangle =& 3!^2 \int \mathrm{d}\Lambda \int \mathrm{d}^3x \int \mathrm{d}^3y \Theta(x_3 \geq x_2 \geq x_1) \Theta(y_3 \geq y_2 \geq y_1) \\ &\times e^{x_1 - x_3} e^{y_1 - y_3} e^{3i\Lambda(R_x - R_y)} \Psi(y_1, y_2, y_3) \left|x_1, x_2, x_3\right\rangle \\ =& 4\pi \cdot 3! \int \mathrm{d}^3x \int \mathrm{d}^3y \, \Theta(x_3 \geq x_2 \geq x_1) \Theta(y_3 \geq y_2 \geq y_1) \\ &\times e^{x_1 - x_3} e^{y_1 - y_3} \delta(R_x - R_y) \Psi(y_1, y_2, y_3) \left|x_1, x_2, x_3\right\rangle \\ \equiv& \int \mathrm{d}^3x \, \Theta(x_3 \geq x_2 \geq x_1) e^{x_1 - x_3} \tilde{\Psi}(R_x) \left|x_1, x_2, x_3\right\rangle \end{aligned} \tag{5.9}$$

We already see that the projection onto the bound states splits into a part only depending upon the centre-of-mass coordinate R_x and a part which solely depends upon the relative coordinates $x_1 - x_2$ and $x_2 - x_3$. However, the representation (5.9) gives a wave function which is antisymmetric in (x_1, x_2, x_3). Its symmetrised generalisation reads

$$\left|\Psi_{\mathrm{B}}\right\rangle \equiv P_{\mathrm{B}} \left|\Psi\right\rangle = \int \mathrm{d}^3x \, e^{-\Delta(x_1, x_2, x_3)/2} \tilde{\Psi}(R_x) \left|x_1, x_2, x_3\right\rangle , \tag{5.10}$$

where

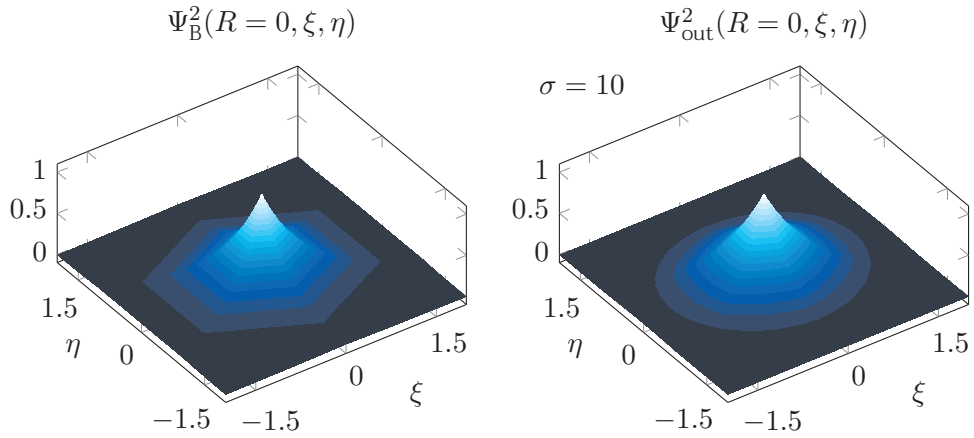

Figure 5.6.
Side by side comparison of the relative part of the generic three body bound state with the central peak of a scattered Gaussian wave packet with initial width $\sigma = 10$. Both figures look similar, however the scattered state does not have the same sharp contours as the universal bound state. This difference is due to contributions from two photon bound states and free photon states.

$$\begin{aligned}\Delta(x_1,x_2,x_3) &\equiv 2\big(\mathrm{Min}(x_1,x_2,x_3) - \mathrm{Max}(x_1,x_2,x_3)\big)\\ &= |x_1-x_2| + |x_2-x_3| + |x_3-x_1|. \end{aligned} \tag{5.11}$$

Obviously, while the last line of (5.11) is specific for three photons, the definition via the Min and Max functions holds for any number of photons. The proof that $\exp(-\Delta(x_1,\ldots,x_N)/2)$ yields the bound state for any number of photons requires exactly the same arguments as before, thus we will accept this as our general result.

We emphasise, the relative part of the bound state wave function is wholly universal and does not depend on any initial parameters. Figure 5.6 compares this bound state with the outgoing wave function of a scattered Gaussian wave packet. Both relative parts look comparable; however, the scattered state has smoother contours along the lines $x = y$, $x = z$ and $y = z$. This fact stems from the remaining two photon bound state contributions and goes hand in hand with the observations from the previous section.

Lastly, so far the argumentation was partly on an empirical level. We claimed that the central peak in the scattered states primarily emerges due to a three-photon bound state contribution. To make this statement more rigorous, we should compute the amplitude of the three-photon bound state part of the outgoing wave function. To do so, we need to compute $\tilde{\Psi}(R_x)$, which depends on the initial state. Notice, since $|\Lambda - i/2, \Lambda, \Lambda + i/2\rangle$ is an eigenstate of H, the projector P_{B} commutes with H. Thus, for any arbitrary initial

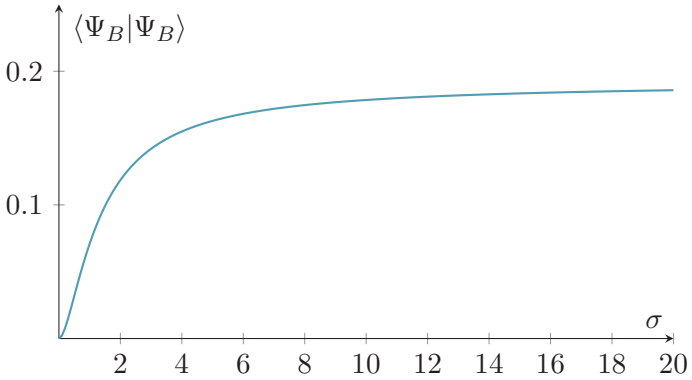

Figure 5.7.
Three body bound state fraction of the total outgoing wave function for different widths σ of the initial wave function. As stated before, the three body bound state part increases with the width and finally converges as $\sigma \to \infty$.

state $|\Psi\rangle$,

$$\begin{aligned}\langle\Psi_B(t)|\Psi_B(t)\rangle &= \left\langle \Psi e^{-iHt} P_{\mathrm{B}} \middle| P_{\mathrm{B}} e^{-iHt}\Psi\right\rangle \\ &= \left\langle \Psi P_{\mathrm{B}} e^{-iHt} \middle| e^{-iHt} P_{\mathrm{B}}\Psi\right\rangle \\ &= \langle \Psi P_{\mathrm{B}} | P_{\mathrm{B}}\Psi\rangle \\ &= \langle\Psi_B|\Psi_B\rangle\,. \end{aligned} \tag{5.12}$$

Hence, we do not need to compute $\tilde{\Psi}(R_x)$ from the outgoing state, but we can use the initial state as well. If the initial wave function has its support on the left side of the emitter then we can show that $\tilde{\Psi}(R_x)$ obeys the representation (5.9) as well.

We now discuss the example of an initially Gaussian wave packet. The emergent integrals are readily solved, and we find

$$\int_{-\infty}^{\infty} \left|\tilde{\Psi}(R_x)\right|^2 \mathrm{d}R_x = \frac{e^{2\sigma^2}}{3\sqrt{3}} \left(\int_0^{\infty} \operatorname{erfc}\left(\frac{\xi + 3\sigma^2}{2\sqrt{3}\sigma}\right) e^{-\frac{(\xi-\sigma^2)^2}{4\sigma^2}} \mathrm{d}\xi \right)^2 . \tag{5.13}$$

The other contribution to (5.12) stems from the integral over $\exp(-\Delta(x_1, x_2, x_3))$, which we separately evaluated in Jacobi coordinates; it yields $3/2$. We cannot solve the last integral in (5.13), for which we proceed with a numerical analysis. The overlap of the outgoing wave function with the three-body bound state for different initial widths σ is plotted in Figure 5.7. We now see that our previous statements were indeed correct; for increasing width of the initial wave function, the overlap with the three-photon bound state sectors starts to increase and finally converges to some value below 0.2. We did not bother to determine this value exactly, but this indicates that other contributions, like from two bonded photons, are important as well.

A Green's function without permutations

Here, we want to prove the theorem 2, which enabled us to derive the generating functional (3.15) for outgoing wave functions in the Dicke model.

Proof For the proof, we use induction in N.

$\boldsymbol{N=2}$ We calculate the right hand side of (3.12), but ignore the z_3 limit for the moment

$$\begin{aligned}
&\prod_{i=1}^{2} \partial_{\alpha_i} e^{-\chi\alpha_i} \Theta(z_i + \alpha_i - y_i)\Theta(y_i + \alpha_i - z_{i+1})\Big|_{\alpha_i=0} \\
&= \prod_{i=1}^{2} \left[-\chi\Theta(z_i - y_i)\Theta(y_i - z_{i+1}) + \delta(z_i - y_i)\Theta(y_i - z_{i+1}) + \Theta(z_i - y_i)\delta(y_i - z_{i+1})\right] \\
&= \prod_{i=1}^{2} \Theta(z_i - y_i)\Theta(y_i - z_{i+1}) \left[-\chi + \delta(z_i - y_i) + \delta(y_i - z_{i+1})\right] \\
&= \Theta(z_3 \le y_2 \le z_2 \le y_1 \le z_1) \prod_{i=1}^{2} \left[-\chi + \delta(z_i - y_i) + \delta(y_i - z_{i+1})\right] \\
&= \Theta(z_3 \le y_2 \le z_2 \le y_1 \le z_1) \\
&\qquad \left[-\chi + \delta(z_1 - y_1) + \delta(y_1 - z_2)\right] \left[-\chi + \delta(z_2 - y_2) + \delta(y_2 - z_3)\right].
\end{aligned}$$

Let us now consider each term separately. First of all, we will ignore every term with $\delta(y_2 - z_3)$, since the limit $z_3 \to \infty$ removes these effectively. We start with the constructive

example of the terms in $\mathcal{O}(\chi^2)$. Here we have

$$\Theta(z_3 \leq y_2 \leq z_2 \leq y_1 \leq z_1)\chi^2 = \Theta(z_3 \leq y_2 \leq z_2 \leq y_1 \leq z_1)\chi^2 \times \left[\Theta(z_1 - y_2)\Theta(z_2 - y_2) + \Theta(z_1 - y_2)\Theta(z_2 - y_1)\right],$$

since $\Theta(z_1 - y_1)\Theta(z_2 - y_2)$ equals one if $\Theta(z_3 \leq y_2 \leq z_2 \leq y_1 \leq z_1) = 1$, while $\Theta(z_1 - y_2)\Theta(z_2 - y_1)$ vanishes under the same condition, but on the zero measure set $\{y_1 = z_2\}$. We repeat this strategy for every other power of χ, i.e., we add Heaviside- and Delta-functions, which are either trivial — due to the $\Theta(z_3 \leq y_2 \leq z_2 \leq y_1 \leq z_1)$ term — or vanish everywhere, except on a set with measure zero.

The terms in power $\mathcal{O}(\chi)$ are

$$\begin{aligned}&\Theta(z_3 \leq y_2 \leq z_2 \leq y_1 \leq z_1)\left[\delta(z_1 - y_1) + \delta(z_2 - y_1) + \delta(z_2 - y_2)\right] \\ &= \Theta(z_3 \leq y_2 \leq z_2 \leq y_1 \leq z_1)\left[\delta(z_1 - y_1)\Theta(z_2 - y_2) + \delta(z_2 - y_1)\Theta(z_1 - y_2)\right. \\ &\quad \left. + \Theta(z_1 - y_1)\delta(z_2 - y_2) + \Theta(z_2 - y_1)\delta(z_1 - y_2)\right].\end{aligned}$$

The first three inserted Heaviside-functions are again trivial, while the last term vanishes except on the set $\{(y_1, y_2)|y_1 = z_2\}$. The remaining terms in $\mathcal{O}(1)$ are

$$\begin{aligned}&\Theta(z_3 \leq y_2 \leq z_2 \leq y_1 \leq z_1)\left[\delta(z_1 - y_1)\delta(z_2 - y_2) + \delta(z_2 - y_1)\delta(z_2 - y_2)\right] \\ &= \Theta(z_3 \leq y_2 \leq z_2 \leq y_1 \leq z_1)\left[\delta(z_1 - y_1)\delta(z_2 - y_2) + \delta(z_2 - y_1)\delta(z_1 - y_2)\right].\end{aligned}$$

We used that the set with $y_1 = y_2$, i.e., where both photons at the same position, has again vanishing measure. The other term $\delta(z_2 - y_1)\delta(z_1 - y_2)$ is zero, since y_2 will never take the value z_1.

In total, we now have

$$\begin{aligned}&\lim_{z_3 \to -\infty} \prod_{\mathrm{i}=1}^{N} \left[-\chi + \delta(z_1 - y_1) + \delta(y_1 - z_2)\right]\left[-\chi + \delta(z_2 - y_2) + \delta(y_2 - z_3)\right] \\ &= \Theta(y_2 \leq z_2 \leq y_1 \leq z_1)\Big\{\chi^2\big[\Theta(z_1 - y_2)\Theta(z_2 - y_2) + \Theta(z_1 - y_2)\Theta(z_2 - y_1)\big] \\ &\qquad -\chi\big[\delta(z_1 - y_1)\Theta(z_2 - y_2) + \delta(z_2 - y_1)\Theta(z_1 - y_2) \\ &\qquad\quad + \Theta(z_1 - y_1)\delta(z_2 - y_2) + \Theta(z_2 - y_1)\delta(z_1 - y_2)\big] \\ &\qquad +\big[\delta(z_1 - y_1)\delta(z_2 - y_2) + \delta(z_2 - y_1)\delta(z_1 - y_2)\big]\Big\} \\ &= \Theta(y_2 \leq z_2 \leq y_1 \leq z_1)\sum_{\sigma \in S_2'} \prod_{\mathrm{i}=1}^{2} \{\delta(z_{\mathrm{i}} - y_{\sigma_{\mathrm{i}}}) - \chi\Theta(z_{\mathrm{i}} - y_{\sigma_{\mathrm{i}}})\},\end{aligned}$$

Bringing us directly to the left hand side of (3.12), which ends the induction basis.

$\boldsymbol{N \to N+1}$ For the induction step, we start with the left-hand side of the equation (3.12). Hold in mind that we sum over a reduced set of permutations $\sigma \in S'_{N+1}$, with the useful property $\sigma_\mathrm{i} \geq \mathrm{i} - 1$. So, for the $(N+1)$-th photon, there are two possible permutations, the identity $(N+1, N+1)$ and the non-trivial permutation $(N+1, N)$, where (a, b) denotes the permutation between elements a and b. Therefore, we rewrite the set of reduced permutations as

$$S'_{N+1} = (N+1, N+1)S'_N \cup (N+1, N)S'_N.$$

With this we can split the summation in (3.12) into two parts and get

$$\begin{aligned}
&\Theta(y_{N+1} \leq z_{N+1} \leq \cdots \leq y_1 \leq z_1) \sum_{\sigma \in S'_{N+1}} \prod_{\mathrm{i}=1}^{N} \{\delta(z_\mathrm{i} - y_{\sigma_\mathrm{i}}) - \chi\Theta(z_\mathrm{i} - y_{\sigma_\mathrm{i}})\} \\
&= \Theta(z_{N+1} - y_{N+1})\Theta(y_N - z_{N+1})\Theta(y_N \leq z_N \leq \cdots \leq y_1 \leq z_1) \\
&\qquad \times [\delta(z_{N+1} - y_{N+1}) - \chi\Theta(z_{N+1} - y_{N+1})] \sum_{\sigma \in S'_N} \prod_{\mathrm{i}=1}^{N} \{\delta(z_\mathrm{i} - y_{\sigma_\mathrm{i}}) - \chi\Theta(z_\mathrm{i} - y_{\sigma_\mathrm{i}})\} \\
&\quad + \Theta(z_N - y_N)\Theta(y_N - z_{N+1})\Theta(y_{N-1} - z_N)\Theta(y_{N+1} \leq z_{N+1} \leq y_{N-1} \leq \cdots \leq y_1 \leq z_1) \\
&\qquad \times [\delta(z_{N+1} - y_N) - \chi\Theta(z_{N+1} - y_N)] \sum_{\sigma \in (N+1,N)S'_N} \prod_{\mathrm{i}=1}^{N} \{\delta(z_\mathrm{i} - y_{\sigma_\mathrm{i}}) - \chi\Theta(z_\mathrm{i} - y_{\sigma_\mathrm{i}})\} \\
&= \Theta(z_{N+1} - y_{N+1})\Theta(y_N - z_{N+1}) \left[\delta(z_{N+1} - y_{N+1}) - \chi\Theta(z_{N+1} - y_{N+1})\right] \\
&\qquad \times \lim_{z'_{N+1} \to \infty} \prod_{\mathrm{i}=1}^{N} \partial_{\alpha_\mathrm{i}} e^{-\chi\alpha_\mathrm{i}} \Theta(z'_\mathrm{i} + \alpha_\mathrm{i} - y_\mathrm{i})\Theta(y_\mathrm{i} + \alpha_\mathrm{i} - z'_{i+1})\Big|_{\alpha_\mathrm{i}=0} \\
&\quad + \Theta(z_N - y_N)\Theta(y_N - z_{N+1}) \left[\delta(z_{N+1} - y_N) - \chi\Theta(z_{N+1} - y_N)\right] \\
&\qquad \times \lim_{z_{N+2} \to \infty} \prod_{\mathrm{i}=1}^{N-1,N+1} \partial_{\alpha_\mathrm{i}} e^{-\chi\alpha_\mathrm{i}} \Theta(z_\mathrm{i} + \alpha_\mathrm{i} - y_\mathrm{i})\Theta(y_\mathrm{i} + \alpha_\mathrm{i} - z_{i+1})\Big|_{\alpha_\mathrm{i}=0}.
\end{aligned}$$

In the second step, we used that no more y_N term appears in the $\sum_{\sigma \in (N+1,N)S'_N}$ sum. Thus, we regrouped this part as a S'_N-like summation, where the N-th particle has the index $N+1$ instead of N. For the notation, we defined products with two upper indices as

$$\prod_{\mathrm{i}=1}^{a,b} f_\mathrm{i} = f_b \cdot \prod_{\mathrm{i}=1}^{a} f_\mathrm{i}.$$

In the last step, we additionally introduced an auxiliary variable in each summand, z'_{N+1} and z_{N+2}, respectively. Furthermore, in the first sum, we added a prime to every variable

z_i, such that the auxiliary variable z'_{N+1} is not mistaken with the actual variable z_{N+1}, appearing in the second sum. In every other case we of course have $z'_\mathrm{i} = z_\mathrm{i}$.

Now we treat the two summands separately. First consider the term

$$\begin{aligned}
&\Theta(z_{N+1} - y_{N+1}) \left[\delta(z_{N+1} - y_{N+1}) - \chi\Theta(z_{N+1} - y_{N+1})\right] \\
&= \delta(z_{N+1} - y_{N+1}) - \chi\Theta(z_{N+1} - y_{N+1}) \\
&= \lim_{z_{N+2}\to\infty} \left[\delta(y_{N+1} - z_{N+2}) + \delta(z_{N+1} - y_{N+1}) - \chi\Theta(z_{N+1} - y_{N+1})\right] \\
&= \lim_{z_{N+2}\to\infty} \partial_{\alpha_{N+1}} e^{-\chi\alpha_{N+1}} \Theta(z_{N+1} + \alpha_{N+1} - y_{N+1})\Theta(y_{N+1} + \alpha_{N+1} - z_{N+2})\Big|_{\alpha_{N+1}=0}.
\end{aligned}$$

For the second summand, it is sufficient to realize that $\Theta(y_N - z_{N+1})\Theta(z_{N+1} - y_N) = 0$, except on a set with measure zero. Taking this together brings us to

$$\begin{aligned}
&\lim_{z'_{N+2}\to\infty} \prod_{\mathrm{i}=1}^{N-1,N+1} \partial_{\alpha_\mathrm{i}} e^{-\chi\alpha_\mathrm{i}} \Theta(z'_\mathrm{i} + \alpha_\mathrm{i} - y_\mathrm{i})\Theta(y_\mathrm{i} + \alpha_\mathrm{i} - z'_{\mathrm{i}+1})\Big|_{\alpha_\mathrm{i}=0} \\
&\quad \Big[\Theta(y_N - z_{N+1}) \lim_{z'_{N+1}\to\infty} \partial_{\alpha_N} e^{-\chi\alpha_N} \Theta(z_N + \alpha_N - y_N)\Theta(y_N + \alpha_N - z'_{N+1}) \\
&\quad + \Theta(z_N - y_N)\Theta(y_N - z_{N+1})\delta(y_N - z_{N+1})\Big]\Big|_{\alpha_N=0}.
\end{aligned}$$

First perform the $z'_{N+1} \to \infty$ limit. Then, it is quite easy to see, that the term inside the brackets is equal to

$$\partial_{\alpha_N} e^{-\chi\alpha_N} \Theta(z_N + \alpha_N - y_N)\Theta(y_N + \alpha_N - z_{N+1})\Big|_{\alpha_N=0}.$$

Consequently, we are allowed to bring it in the prior product. At large, we end up with

$$\lim_{z'_{N+2}\to\infty} \prod_{\mathrm{i}=1}^{N+1} \partial_{\alpha_\mathrm{i}} e^{-\chi\alpha_\mathrm{i}} \Theta(z'_\mathrm{i} + \alpha_\mathrm{i} - y_\mathrm{i})\Theta(y_\mathrm{i} + \alpha_\mathrm{i} - z'_{\mathrm{i}+1})\Big|_{\alpha_\mathrm{i}=0},$$

exactly what we expected. Hence we conclude the proof by induction. ■

Outgoing Wave functions for the Dicke model

We will list here the analytical results for the two and three photon scattering of Gaussian wave packets in the Dicke model, which we used in chapter 5. For this, let us introduce two definitions to shorten the notation, namely

$$\Psi_{\mathrm{G}}(x) \equiv \frac{e^{-x^2/2\sigma^2}}{(\pi\sigma^2)^{1/4}},$$
$$\Psi_{\mathrm{E}}(x) \equiv \left(\frac{\pi\sigma^2}{4}\right)^{1/4} e^{x/2+\sigma^2/8}\mathrm{erfc}\left(\frac{2x+\sigma^2}{2\sqrt{2}\sigma}\right).$$

With this we are prepared to give the outgoing wave functions. For two photons this is

$$\begin{aligned}\Psi(x,y) =&\Psi_{\mathrm{G}}(x)\Psi_{\mathrm{G}}(y)\\ &-\Psi_{\mathrm{E}}(x)\Psi_{\mathrm{G}}(y)-\Psi_{\mathrm{G}}(x)\Psi_{\mathrm{E}}(y)\\ &+\Psi_{\mathrm{E}}(x)\left[\Psi_{\mathrm{E}}(y)-e^{(y-x)/2}\Psi_{\mathrm{E}}(x)\right].\end{aligned} \tag{B.1}$$

The scattered three-photon wave function takes a similar form, more precisely

$$\begin{aligned}\Psi(x,y,z) =&\Psi_{\mathrm{G}}(x)\Psi_{\mathrm{G}}(y)\Psi_{\mathrm{G}}(z)\\ &-\Psi_{\mathrm{E}}(x)\Psi_{\mathrm{G}}(y)\Psi_{\mathrm{G}}(z)-\Psi_{\mathrm{G}}(x)\Psi_{\mathrm{E}}(y)\Psi_{\mathrm{G}}(z)-\Psi_{\mathrm{G}}(x)\Psi_{\mathrm{G}}(y)\Psi_{\mathrm{E}}(z)\\ &-\Psi_{\mathrm{G}}(x)\Psi_{\mathrm{E}}(y)\left[\Psi_{\mathrm{E}}(z)-e^{(z-y)/2}\Psi_{\mathrm{E}}(y)\right]\\ &-\Psi_{\mathrm{G}}(y)\Psi_{\mathrm{E}}(x)\left[\Psi_{\mathrm{E}}(z)-e^{(z-x)/2}\Psi_{\mathrm{E}}(x)\right]\end{aligned}$$

$$
\begin{aligned}
&- \Psi_{\mathrm{G}}(z)\Psi_{\mathrm{E}}(x)\left[\Psi_{\mathrm{E}}(y) - e^{(y-x)/2}\Psi_{\mathrm{E}}(x)\right] \\
&- \Psi_{\mathrm{E}}(x)\left[\Psi_{\mathrm{E}}(y) - e^{(y-x)/2}\Psi_{\mathrm{E}}(x)\right]\left[\Psi_{\mathrm{E}}(z) - e^{(z-y)/2}\Psi_{\mathrm{E}}(y)\right]. \qquad \text{(B.2)}
\end{aligned}
$$

Notice, both the two- and tree-photon wave functions are not symmetric in their arguments. More specifically, since these results are based on our Green's function (3.12) they are only applicable in the sectors $x > y$ and $x > y > z$, respectively.

Statutory Declaration

I hereby declare that I have developed and written the enclosed Master Thesis entirely by myself. I neither used sources nor means without declaration within the text. The Master Thesis was not used in the same or in a similar version to achieve an academic grading or is being published elsewhere. Lastly, I assure that the electronic copy of this Master Thesis is identical in content with the enclosed version.

Stuttgart, 14. November 2017

Acknowledgements

This thesis not only summarises my research over the last year, but it also marks the point where a five year long journey comes to an end. Therefore, this is an excellent moment to take inventory and thank all those people involved in my academic and personal life.

First and foremost I want to thank my supervisor, Professor Hans Peter Büchler. I cannot appreciate enough the amount of useful feedback I got during our talks. Working at his institute was a genuinely pleasant experience and I am looking forward to my Ph.D. at the ITP3.

In the same breath, I obviously want to acknowledge my dear colleagues from the ITP3. Working with them was immensely diverting, and I hope we'll manage to win SCoPE tournament in the coming years. Especially, I want to thank Tobias Ilg. Sharing an office with him was an enriching and entertaining experience.

Beyond the Third Institute for Theoretical Physics, there are so many more people at the university, who deserve being mentioned. Firstly, a big shout-out goes to Johannes Greiner for proofreading my manuscript and for enabling me to conduct my own quantum information exercise class merely one semester after taking the course. This substantiated the notion that you learn something best when you have to explain it to others. Next, I want to thank Michael Bauer for proofreading, and am grateful for the friendship we now have. Furthermore, I want to mention the guys from the Second Institute for Theoretical Physics; especially Patrick Pietzoka, Robert Wulfert and Sebastian Goldt. Even though I found a new "family", I still feel welcome in your midst. Lastly, a special thank you goes to Holger Cartarius. Although I had no affiliations whatsoever with his institute, he always had an open door and two open ears for any physics-related problems. Holger is the best mentor a student can wish for, and I cannot put the help I received from him into words.

Next, I must not undercut the influence of my friends in the last couple of years. I know, they will always drag me out of my office when I reach my physics threshold. I cannot emphasise enough how much they influenced both the last couple of years as well as myself as a person. Even if the list of names is too long to be listed here, know,

that I think of every single one of you.

And finally, with all of my heart, I want to thank my family. They truly accompanied me during every single step of my studies; during rough and easy times. I am indefinitely happy to have them, and I would not be here if it were not for them.

Bibliography

[1] A. Sydorenko, "Evidence for light-by-light scattering in heavy-ion collisions with the atlas detector at the lhc", Technical report, ATL-COM-PHYS-2017-077 (2017).

[2] M. Lukin, "Colloquium: Trapping and manipulating photon states in atomic ensembles", *Reviews of Modern Physics* **75**, 457 (2003).

[3] V. Yudson, "Dynamics of integrable quantum systems", *Zh. Eksp. Teor. Fiz* **88**, 1757 (1985).

[4] T. Rosenband, D. Hume, P. Schmidt, C.-W. Chou, A. Brusch, L. Lorini, W. Oskay, R. E. Drullinger, T. M. Fortier, J. Stalnaker, *et al.*, "Frequency ratio of Al+ and Hg+ single-ion optical clocks; metrology at the 17th decimal place", *Science* **319**, 1808 (2008).

[5] A. D. Ludlow, M. M. Boyd, J. Ye, E. Peik, and P. O. Schmidt, "Optical atomic clocks", *Reviews of Modern Physics* **87**, 637 (2015).

[6] A. Blais, R.-S. Huang, A. Wallraff, S. M. Girvin, and R. J. Schoelkopf, "Cavity quantum electrodynamics for superconducting electrical circuits: An architecture for quantum computation", *Physical Review A* **69**, 062320 (2004).

[7] M. Giustina, A. Mech, S. Ramelow, B. Wittmann, J. Kofler, J. Beyer, A. Lita, B. Calkins, T. Gerrits, S. W. Nam, *et al.*, "Bell violation with entangled photons, free of the fair-sampling assumption", *Nature* **497**, 227 (2013).

[8] J.-Å. Larsson, M. Giustina, J. Kofler, B. Wittmann, R. Ursin, and S. Ramelow, "Bell-inequality violation with entangled photons, free of the coincidence-time loophole", *Physical Review A* **90**, 032107 (2014).

[9] M. Giustina, M. A. Versteegh, S. Wengerowsky, J. Handsteiner, A. Hochrainer, K. Phelan, F. Steinlechner, J. Kofler, J.-Å. Larsson, C. Abellán, *et al.*, "Significant-loophole-

free test of bell's theorem with entangled photons", *Physical review letters* **115**, 250401 (2015).

[10] J. S. Bell, "On the einstein podolsky rosen paradox", *Physics* **1**, 195 (1964).

[11] D. P. DiVincenzo *et al.*, "The physical implementation of quantum computation", *arXiv preprint quant-ph/0002077* (2000).

[12] S. Yang, Y. Wang, D. B. Rao, T. H. Tran, A. S. Momenzadeh, M. Markham, D. Twitchen, P. Wang, W. Yang, R. Stöhr, *et al.*, "High-fidelity transfer and storage of photon states in a single nuclear spin", *Nature Photonics* **10**, nphoton (2016).

[13] D. Chang, V. Gritsev, G. Morigi, V. Vuletic, M. Lukin, and E. Demler, "Crystallization of strongly interacting photons in a nonlinear optical fiber", *arXiv preprint arXiv:0712.1817* (2007).

[14] S. John and J. Wang, "Quantum electrodynamics near a photonic band gap: Photon bound states and dressed atoms", *Physical review letters* **64**, 2418 (1990).

[15] I. Iakoupov, *Enhancement of optical nonlinearities with stationary light*, Ph.D. thesis, FACULTY OF SCIENCE UNIVERSITY OF COPENHAGEN Enhancement of optical nonlinearities with stationary light Ivan Iakoupov PhD thesis Academic advisor: Anders S. Sørensen This thesis has been submitted to the PhD School of The Faculty of Science, University of Copenhagen (2016).

[16] D. Roy, C. Wilson, and O. Firstenberg, "Strongly interacting photons in one-dimensional continuum", *arXiv preprint arXiv:1603.06590* (2016).

[17] J.-T. Shen and S. Fan, "Strongly correlated two-photon transport in a one-dimensional waveguide coupled to a two-level system", *Physical review letters* **98**, 153003 (2007).

[18] M. Ringel, M. Pletyukhov, and V. Gritsev, "Topologically protected strongly correlated states of photons", *New Journal of Physics* **16**, 113030 (2014).

[19] H. Pichler, T. Ramos, A. J. Daley, and P. Zoller, "Quantum optics of chiral spin networks", *Physical Review A* **91**, 042116 (2015).

[20] V. Yudson, "Dynamics of the integrable one-dimensional system "photons+ two-level atoms"", *Physics Letters A* **129**, 17 (1988).

[21] V. Yudson and P. Reineker, "Multiphoton scattering in a one-dimensional waveguide with resonant atoms", *Physical Review A* **78**, 052713 (2008).

[22] J. Petersen, J. Volz, and A. Rauschenbeutel, "Chiral nanophotonic waveguide interface based on spin-orbit interaction of light", *Science* **346**, 67 (2014).

[23] R. H. Dicke, "Coherence in spontaneous radiation processes", *Physical Review* **93**, 99 (1954).

[24] M. Bajcsy, S. Hofferberth, V. Balic, T. Peyronel, M. Hafezi, A. S. Zibrov, V. Vuletic, and M. D. Lukin, "Efficient all-optical switching using slow light within a hollow fiber", *Physical review letters* **102**, 203902 (2009).

[25] A. Akimov, A. Mukherjee, C. Yu, D. Chang, A. Zibrov, P. Hemmer, H. Park, and M. Lukin, "Generation of single optical plasmons in metallic nanowires coupled to quantum dots", *Nature* **450**, 402 (2007).

[26] A. Wallraff, D. I. Schuster, A. Blais, L. Frunzio, R.-S. Huang, J. Majer, S. Kumar, S. M. Girvin, and R. J. Schoelkopf, "Strong coupling of a single photon to a superconducting qubit using circuit quantum electrodynamics", *Nature* **431**, 162 (2004).

[27] O. Astafiev, A. M. Zagoskin, A. Abdumalikov, Y. A. Pashkin, T. Yamamoto, K. Inomata, Y. Nakamura, and J. Tsai, "Resonance fluorescence of a single artificial atom", *Science* **327**, 840 (2010).

[28] D. Roy and N. Bondyopadhaya, "Statistics of scattered photons from a driven three-level emitter in a one-dimensional open space", *Physical Review A* **89**, 043806 (2014).

[29] M. O. Scully and M. S. Zubairy, *Quantum optics*, AAPT (1999).

[30] V. Rupasov and V. Yudson, "Rigorous theory of cooperative spontaneous emission of radiation from a lumped system of two-level atoms: Bethe ansatz method", *Zh. Eksp. Teor. Fiz* **87**, 1617 (1984).

[31] V. Rupasov and V. Yudson, "Exact dicke superradiance theory: Bethe wavefunctions in the discrete atom model", *Zh. Eksp. Teor. Fiz* **86**, 825 (1984).

[32] T. Grass, A. Celi, G. Pagano, and M. Lewenstein, "Chiral spin currents in a trapped-ion quantum simulator using floquet engineering", *arXiv preprint arXiv:1708.01882* (2017).

[33] H. Pichler and P. Zoller, "Photonic circuits with time delays and quantum feedback", *Physical review letters* **116**, 093601 (2016).

[34] P.-O. Guimond, M. Pletyukhov, H. Pichler, and P. Zoller, "Delayed coherent quantum feedback from a scattering theory and a matrix product state perspective", *Quantum Science and Technology* **2**, 044012 (2017).

[35] A. M. Strathearn, B. W. Lovett, and P. Kirton, "Efficient real-time path integrals for non-markovian spin-boson models", *New Journal of Physics* (2017).

[36] T. Shi, D. E. Chang, and J. I. Cirac, "Multiphoton-scattering theory and generalized master equations", *Physical Review A* **92**, 053834 (2015).

[37] T. Caneva, M. T. Manzoni, T. Shi, J. S. Douglas, J. I. Cirac, and D. E. Chang, "Quantum dynamics of propagating photons with strong interactions: a generalized input–output formalism", *New Journal of Physics* **17**, 113001 (2015).

[38] L. Pucci, A. Roy, T. S. d. E. Santo, R. Kaiser, M. Kastner, and R. Bachelard, "Quantum effects in the cooperative scattering of light by atomic clouds", *arXiv preprint arXiv:1701.04061* (2017).

[39] G. Guarnieri, A. Smirne, and B. Vacchini, "Quantum regression theorem and non-markovianity of quantum dynamics", *Physical Review A* **90**, 022110 (2014).

[40] H.-P. Breuer and F. Petruccione, *The theory of open quantum systems*, Oxford University Press on Demand (2002).

[41] C. Gardiner and P. Zoller, *Quantum noise: a handbook of Markovian and non-Markovian quantum stochastic methods with applications to quantum optics*, volume 56, Springer Science & Business Media (2004).

[42] G. J. Milburn, "Quantum optical fredkin gate", *Physical Review Letters* **62**, 2124 (1989).

[43] K. Jachymski, P. Bienias, and H. P. Büchler, "Three-body interaction of rydberg slow-light polaritons", *Physical review letters* **117**, 053601 (2016).